RECONSTITUTION OF CFTR UBIQUITINATION AND ENDOPLASMIC RETICULUM QUALITY CONTROL

by

Samuel Kenneth Estabrooks

B.S. Microbiology, University of Massachusetts Amherst, 2014

Submitted to the Graduate Faculty of

The Kenneth P. Dietrich School of Arts and Sciences in partial fulfillment

of the requirements for the degree of

Doctor of Philosophy

University of Pittsburgh

2020

UNIVERSITY OF PITTSBURGH

KENNETH P. DIETRICH SCHOOL OF ARTS AND SCIENCES

This dissertation was presented

by

Samuel Kenneth Estabrooks

It was defended on

April 8, 2020

and approved by

Dr. Jon P. Boyle, Associate Professor, Department of Biological Sciences

Dr. Deborah L. Chapman, Associate Professor, Department of Biological Sciences

Dr. James M. Pipas, Professor, Department of Biological Sciences

Dr. Jennifer M. Bomberger, Associate Professor, Department of Microbiology and Molecular Genetics

Dissertation Advisor: Dr. Jeffrey L. Brodsky, Professor, Department of Biological Sciences

RECONSTITUTION OF CFTR UBIQUITINATION AND ENDOPLASMIC RETICULUM QUALITY CONTROL

Samuel Kenneth Estabrooks, Ph.D.

University of Pittsburgh, 2020

Upon its identification in 1989, mutations in the gene encoding the cystic fibrosis transmembrane conductance regulator (CFTR) were conclusively linked to cystic fibrosis. Many of the resultant mutant proteins were shown to misfold during synthesis and be selected for degradation by protein quality control machinery. However, small molecule "corrector" compounds help shield some variants from recognition by degradative machinery, improving protein trafficking in cell culture. Although some of these correctors have received FDA approval, their use in patients has had limited and variable efficacy. Based on emerging data, I propose that inhibition of certain E3 ubiquitin ligases— the enzymes ultimately responsible for committing CFTR to degradation— could synergize with corrector treatment to favor enhanced CFTR maturation and function. Specifically, I propose that the ubiquitin ligase CHIP is among the most attractive candidates for chemical inhibition because it is so broadly involved in the triage of misfolded CFTR substrates, contributing to the turnover of CFTR both at the endoplasmic reticulum as it is synthesized and at the cell surface where it functions. As a first step toward this goal, I have developed assays to measure ubiquitin conjugation and CHIP activity in a variety of conditions, and most notably in the presence of misfolded CFTR variants. In this thesis, I present my findings from these assays and discuss how these results further our understanding of the degradation of misfolded, disease-causing CFTR variants.

TABLE OF CONTENTS

LIST OF TABLES

LIST OF FIGURES

LIST OF ABBREVIATIONS

Below is a list of abbreviated terms used throughout this dissertation. Units, chemical formulae, and the most frequently used biological terms (e.g. µM, NaCl, pH, DNA) are omitted from this list.

A_{280}	Absorbance at 280 nm
ABC	ATP-Binding Cassette
ADP	Adenosine Diphosphate
ATP	Adenosine Triphosphate
BCA	Bicinchoninic Acid
CAL	CFTR-Associated Ligand
cAMP	Cyclic Adenosine Monophosphate
CF	Cystic Fibrosis
CFBE	Cystic Fibrosis Bronchial Epithelia
CFLD	Cystic Fibrosis Liver Disease
CFTR	Cystic Fibrosis Transmembrane Conductance Regulator
CFTR2	Clinical and Functional Translation of CFTR (Variant Database)
CHIP/STUB1	C-Terminus of Hsc70 Interacting Protein/ STIP1 Homology and U-Box-Containing Protein 1
CNX	Calnexin
ddH_2O	Double Distilled Water
DNAJ/J-protein	DnaJ Homologue/J-Domain Containing Protein (see Hsp40)
DMEM	Dulbecco's Modified Eagle Medium

DMSO	Dimethyl Sulfoxide
DPBS	Dulbecco's Phosphate Buffered Saline
E1	Ubiquitin Activating Enzyme
E2	Ubiquitin Conjugating Enzyme
E3	Ubiquitin Ligase
EDTA	Ethylenediaminetetraacetic Acid
EGAD	Endosome and Golgi Associated Degradation
ENaC	Epithelial Sodium Channel
ER	Endoplasmic Reticulum
ERAD	Endoplasmic Reticulum Associated Degradation
FDA	United States Food and Drug Administration
FBS	Fetal Bovine Serum
FEV_1	One Second Forced Expiratory Volume
FP	Fluorescence Polarization
gp78/AMFR/RNF45	Glycoprotein of 78 kDa/Autocrine Motility Factor Receptor/ RING Finger Protein 45
GRASP	Golgi Reassembly Stacking Protein
GST	Glutathione S-Transferase
HBE	Human Bronchial Epithelia
HeLa	Henrietta Lacks
HECT	Homologous to E6-AP Carboxyl Terminus
HEK293	Human Embryonic Kidney 293
HEPES	2-[4-(2-Hydroxyethyl)Piperazin-1-yl]Ethanesulfonic Acid
His	6×Histidine
HOP	Hsc70/Hsp90 Organizing Protein
HRP	Horseradish Peroxidase
HSP	Heat Shock Protein
Hsc70	70 kDa Heat Shock Cognate Protein
Hsp40	40 kDa Heat Shock Protein (see DNAJ/J-protein)
Hsp70	70 kDa Heat Shock Protein

Hsp90	90 kDa Heat Shock Protein
IP	Immunoprecipitation
IPTG	Isopropyl β- d-1-Thiogalactopyranoside
LB	Luria Broth
LINCS	NIH Library of Integrated Cellular Signatures
MDS	Molecular Dynamics Simulation
MG-132	Proteasome Inhibitor Carbobenzoxy-Leu-Leu-Leucinal
mRNA	Messenger Ribonucleic Acid
MSD/TMD	Membrane Spanning Domain/Transmembrane Domain
MVB	Multivesicular Body
MWCO	Molecular Weight Cutoff
NBD	Nucleotide Binding Domain
NCL	Native Chemical Ligation
NEM	N-Ethylmaleimide
NIH	United States National Institutes of Health
OD_{600}	Optical Density at 600 nm
P_0	Open Probability
p97/VCP	Valosin Containing Protein
PBS	Phosphate Buffered Saline
PEI	Polyethylenimine
PIC	Roche cOmplete™ EDTA-Free Protease Inhibitor Cocktail
PKA	Protein Kinase A
PMSF	Phenylmethylsulfonyl Fluoride
PMT	Photomultiplier Tube
PQC	Protein Quality Control
RING	Really Interesting New Gene
RFFL	Rififylin
RMA1/RNF5	RING Membrane-Anchor 1/RING Finger Protein 5
RNF185	RING Finger Protein 185

SDS	Sodium Dodecyl Sulfate
SDS-PAGE	Sodium Dodecyl Sulfate Polyacrylamide Gel Electrophoresis
Sec61	Secretory Protein 61
sHSP	Small Heat Shock Protein
siRNA	Small Interfering Ribonucleic Acid
SNO	S-Nitrosothiol
SRP	Signal Recognition Particle
TBE	Tris Boric Acid EDTA
TBS	Tris Buffered Saline
TBST	Tris Buffered Saline + 0.2% Tween 20
TCT	Triple Drug Combination Therapy
TNT	Tris Sodium Chloride Triton X-100
TPR	Tetratricopeptide Repeat
Tris	2-Amino-2-(Hydroxymethyl)Propane-1,3-Diol
Ub	Ubiquitin
Ube1	Ubiquitin Activating Enzyme 1
UbcH5	Ubiquitin Conjugating Enzyme H5
UPS	Ubiquitin Proteasome System
VX-445	Vertex Pharmaceuticals CFTR Corrector 445 (Elexacaftor)
VX-661	Vertex Pharmaceuticals CFTR Corrector 661 (Tezacaftor)
VX-770	Vertex Pharmaceuticals CFTR Potentiator 770 (Ivacaftor)
VX-809	Vertex Pharmaceuticals CFTR Corrector 809 (Lumacaftor)

PREFACE

I was well warned that graduate school is a marathon, not a sprint. In retrospect, I have to say that this advice was spot on. In 2013 I was an undergraduate microbiology student at UMass Amherst, aspiring to continue my studies in a master's program, when my undergraduate research advisor, Dr. Klaus Nüsslein, suggested that perhaps I ought to consider doctoral programs instead. While I didn't realize at the time what I was getting into (even if I thought I did), it would be hard to imagine things turning out any other way. During my time in Pittsburgh, I found what I'd begun to learn at UMass to be true, that a scientist is rarely, if ever, made in isolation. Indeed, while this document serves to summarize my research over the past five years, it truly reflects the broader efforts of a much larger community, to which I owe many thanks.

First and foremost, I wish to thank my family—my parents Leigh and Paul Estabrooks, and my brother Ben Estabrooks—whose unyielding support kept my journey here always moving forward. Picking up everything to start a new life in another state proved challenging in more ways than I expected, yet I could always count on my family for guidance and reassurance. I am especially grateful to my parents for their nightly phone calls, care packages, holiday cards, and the trips they've taken to visit me in Pittsburgh. I am thankful to my brother for our games together online when I needed to put my mind somewhere else, as well as for the times when we could share our mutual enthusiasm for biology, even as we pursue our shared interest in different ways. Additionally, I want to extend my deepest thanks to my grandparents, Pete and Gary

Barrett, and our dearest friends, Donald and Kitty Hooper, who have always been among my most ardent supporters. While Granny Pete and Donald couldn't see this day, they knew it would arrive nonetheless and I know that they would be proud.

Second, I wish to express my profound gratitude for my dissertation advisor, Dr. Jeff Brodsky. When I initially interviewed in Pittsburgh, one professor's passion for research—whether his own or that of an aspiring graduate student—stood out from the rest. Fortunately, I would have the opportunity to study with Jeff myself. Where others had been quick to criticize my work at the bench as "paralytic", Jeff gave me a fair shot and ultimately judged my perceived weaknesses to in fact be among my strengths. Over the years I've come to know Jeff as an able mentor, a reliable source of encouragement, and one who can find the positives in failure. Jeff's mentorship had made much possible for me and indeed I could not imagine conducting my graduate studies with any other advisor.

Third, I wish to thank the many members of the Brodsky Lab who I've come to know over the past few years, for the entirely positive influence they've had upon my experience here. In particular, I would like to thank the lab manager (Jen Goeckeler-Fried), graduate students (Dr. Mike Preston, Dr. Lynley Doonan, Dr. Tim Mackie, Dr. Zhihao Sun, Deepa Kumari, Grant Daskivich, Katie Nguyen, and Morgan Webb), postdoctoral fellows (Dr. Annette Chiang, Dr. Sara Sannino, and Dr. Miguel Betegon), medical fellows (Dr. Brighid O'Donnell and Dr. Aiden Porter) and research professors (Dr. Teresa Buck, Dr. Chris Guerriero, Dr. Patrick Needham, and Dr. Ally O'Donnell) who have made this experience so memorable through their mentorship, good humor, and conversation. The time we've spent together in lab, and out, has been remarkable. I'd also like to thank the slew of undergraduate researchers and lab technicians who have been in and out of the lab during my time, for their diligence preparing reagents and for the

way they livened our lab. I'd especially like to thank undergraduate researcher Jason Li, whom I had the privilege of mentoring as we worked together to advance my project.

Finally, I wish to express my gratitude for all the others who have contributed to this journey at one time or another. To name just a few, I'd like to thank Dr. Bob Duda and Dr. Roger Hendrix for their superb tutelage during my first year in Pittsburgh. I'd also like to thank Dr. Jacob Spiegel for his companionship in the Hendrix Lab and for including me at his wedding and Seders thereafter. I'd also like to thank Dr. Nancy Kaufmann, Dr. Dawn Bisi, and Dr. Ling Xu for the fantastic impact they had upon my teaching experience in Pittsburgh, as well as my dissertation committee (Dr. Jon Boyle, Dr. Debbie Chapman, Dr. Jim Pipas, and Dr. Jen Bomberger) for their invaluable feedback as my project progressed. I'd be remiss if I didn't express my gratitude for my high school biology teacher, Dr. Susan Offner, who (in spite of my passing out during our fetal pig dissection) saw something in me as a young AP student, encouraging me to work on science fair projects and introducing me to the University of Pittsburgh. I would furthermore like to thank Dr. Megan Rokop for her advice on my science fair projects and for giving me the opportunity to conduct a semester-long research project at the Broad Institute of MIT and Harvard as a high school student. Last, I would also like to thank my late friend and undergraduate research partner, Slav Yanyuk, for our time together learning to become researchers. Though brief, his legacy continues to inspire me to make the most of the opportunities I have, however arduous the path forward may be.

1.0 INTRODUCTION

(Significant portions of the following chapter have been separately published as a review article appearing in the *International Journal of Molecular Sciences*.) (Estabrooks and Brodsky, 2020)

Cystic fibrosis (CF) is a genetically inherited disease that negatively impacts the lives of approximately 70,000 patients worldwide. Though most notorious as a condition affecting the respiratory system, CF broadly perturbs the function of mucus-lined and other epithelial tissues found throughout the human body, with symptoms typically appearing at birth (Elborn, 2016). Virtually every CF case is caused by the same underlying genetic determinant: inheritance of dysfunctional variants of a single chloride channel, the cystic fibrosis transmembrane conductance regulator (CFTR). Although disease-causing variants vary in the precise nature of their molecular defect, most frequent are CFTR variants that misfold as they are synthesized in the endoplasmic reticulum (ER) of epithelial cells. Because misfolded CFTR is aggressively targeted by endoplasmic reticulum associated degradation (ERAD), misfolding variants are retained by the ER and directed to the cytosol for ubiquitin-proteasome-dependent proteolysis, precluding their function at the cell surface (Jensen et al., 1995; Ward et al., 1995).

In the following chapter, I explore the pathology of CF, the properties of CFTR, the range of clinical variants, and the multitude of cellular factors that guide CFTR channels toward either maturation or degradation. I also discuss the ongoing development of molecular therapies aimed

at restoring function to otherwise dysfunctional CFTR variants, and propose that ablation of select factors which otherwise promote CFTR degradation could synergize with existing therapies to restore the function of disease-causing CFTR variants.

1.1 CYSTIC FIBROSIS

1.1.1 Pathology

Originally identified as a distinct pathology over eighty years ago, CF was initially defined as a lethal, primarily digestive disorder affecting newborns (Anderson, 1938). Described at the time as “cystic fibrosis of the pancreas”, postmortem observations of infants succumbing to the disease revealed thick, immobile mucus lining the digestive tract, which blocked entry of pancreatic enzymes into the intestine via the pancreatic duct. As a result of severe pancreatic insufficiency, infants with CF tended to exhibit meconium ileus (intestinal obstruction), perforated intestines, abnormal stools, and a failure to thrive, rarely surviving for more than a few months. Fortunately, CF patients today have ready access to pancreatic enzyme replacement therapy (PERT), which along with multivitamins alleviates digestive symptoms and restores typical nutrient absorption (Singh and Schwarzenberg, 2017). With rigorous newborn genetic screening, many CF patients are now diagnosed and prescribed PERT before gastrointestinal symptoms even have the opportunity to develop.

Further clinical characterization led to the observation that CF patients also acquire and die from respiratory infections such as pneumonia and bronchitis, provided that these individuals did not first succumb to intestinal blockage (Anderson and Hodges, 1946). As care improved and

patients gradually lived beyond infancy into childhood, it became clear that pulmonary dysfunction is a hallmark of CF. Just as within the digestive tract, CF causes the layer of mucus coating tissues of the respiratory tract to become dehydrated, immobile, and increasingly acidic (Haq et al., 2016; Verkman et al., 2003). Because mucus fluidity is critical for maintaining the efflux of inhaled microorganisms from the respiratory tract, the lungs of CF patients gradually become infected with pathogenic bacteria and fungi (Frayman et al., 2017). Once these intractable infections are established, they permanently activate an immune response (Cantin et al., 2015), causing persistent inflammation of respiratory tissue that drastically reduces lung function, which is typically measured by forced expiratory volume (FEV) (Szczesniak et al., 2017). Although the makeup of lung flora varies widely by patient, *Pseudomonas aeruginosa*, *Staphylococcus aureus*, and non-Tuberculosis mycobacterial species are among the most common bacterial pathogens that colonize CF lungs (Furukawa and Flume, 2018; Hector et al., 2016). Intriguingly however, it is worth noting that even without bacterial colonization, CF ferrets (an animal model that successfully recapitulates CF respiratory symptoms) still exhibit inflammatory lung disease (Rosen et al., 2018), suggesting that bacterial colonization—while associated with poor prognosis—may not be required to activate an immune response in CF. Regardless, in an effort to dislodge mucus plugs, ease inflammation, and reduce pathogenic burden, CF patients are frequently prescribed mucolytics, corticosteroids, inhaled hypertonic saline, as well as oral or inhaled antibiotics (Mogayzel et al., 2014). Additionally, numerous techniques have been designed to physically clear airways, such as forced expiration, exercise, and the use of a high frequency chest wall oscillation (HFCWO) vest (Grosse-Onnebrink et al., 2017; McIlwaine et al., 2019). Even so, the vast majority of CF patients ultimately endure pulmonary exacerbations, periods of intense pathogenic burden and sharply reduced pulmonary

function requiring hospitalization. Though pulmonary exacerbations are typically the terminal event for CF patients, therapeutic advancements made over the past several decades have steadily slowed the rate of respiratory decline in patients and reduced the frequency of exacerbations, enabling patients to lead longer, healthier lives (see Section 1.3 below). Indeed, only recently did the median age of CF patients surpass 18 years of age for the first time (Cystic Fibrosis Foundation Patient Registry, 2019), shifting how this once pediatric disease is now viewed and treated.

As patients live longer, however, additional complications not originally appreciated as symptoms of CF have begun to emerge. For example, even with prolonged replacement of pancreatic function, ~40% of CF patients are diagnosed with gastroesophageal reflux disease (GERD), for which many individuals additionally take acid blockers or proton pump inhibitors (Maqbool and Pauwels, 2017). Furthermore, almost one-third of adult CF patients exhibit glucose intolerance and have been further diagnosed with CF-related diabetes (CFRD), which requires regular insulin injections (Kelsey et al., 2019; Moheet and Moran, 2018). Although less frequent, some CF patients also display unusual liver function, generally referred to as CF liver disease (Kamal et al., 2018). Moreover, as male fertility also relies on mucus-lined ducts, nearly all male patients have congenital bilateral absence of the vas deferens (CBAVD) and are rendered infertile, a topic of concern as a growing number CF patients survive into adulthood (Bernardino et al., 2013; Chillon et al., 1995). Finally, approximately one-quarter of all CF adults report suffering from depression or anxiety (Quittner et al., 2014; Smith et al., 2016), indicating that this disease not only takes a physical toll upon those afflicted, but a psychological one as well. Overall, how CF affects the health of most tissues throughout the body remains incompletely understood but is of significant concern as the CF population continues to age.

1.1.2 CFTR Structure and Function

Early studies into the epidemiology of CF noted that the disease affects males and females at equal rates, but appeared to be hereditary as it tracked within certain families at a much higher frequency than the general population (Anderson and Hodges, 1946). Decades later, the genetic determinant would be pinpointed to a single locus on chromosome 7, a ~6500 base pair gene thereafter known as the cystic fibrosis transmembrane conductance regulator (CFTR) (Kerem et al., 1990; Riordan et al., 1989).

The CFTR gene encodes a 1480 amino acid, ~168 kDa protein which is classified as a member of the ATP-binding cassette (ABC) transporter superfamily, a set of interrelated transmembrane proteins found in both eukaryotes and prokaryotes that bind ATP and promote substrate transport across cellular membranes. As such, CFTR (alternately known as ABC subfamily C member 7) bears close structural homology to other ABC transporters, including certain bacterial multidrug resistance pumps (Mornon et al., 2008). Like these, CFTR contains two hydrophobic transmembrane domains (TMDs) that anchor the protein in the membrane, as well as two nucleotide binding domains (NBDs) that reside in the cytosol (Figure 1A). Unlike other ABC transporters, CFTR also harbors a regulatory (R) domain between NBD1 and TMD2, which provides an extra layer of control over its activity. Specifically, the R domain must be phosphorylated by Protein Kinase A in a cyclic AMP (cAMP)-dependent manner for CFTR to fully function (Cheng et al., 1991). Phosphorylation displaces the flexible R domain, favors NBD interaction, and exposes the protein's positively charged central pore (Liu et al., 2017; Zhang and Chen, 2016) (Figure 1B). Intimate association between the NBDs allows for two, shared ATP-binding sites to be established at their interface. Notably, each site is composed of the Walker A (GXXGXGKS/T) and Walker B (ΦΦΦΦD, where Φ is hydrophobic) motifs of one domain and

the signature motif (LSGGQ) of the other, which together coordinate the phosphate groups of ATP and bind an associated magnesium ion (Moran, 2014). Only one of these composite sites is active in CFTR however, as the site established by the Walker motifs of NBD1 and the signature motif of NBD2 contains a nonconserved signature motif (LSHGH), causing this site to bind but fail to catalyze ATP. These shared ATP binding sites are required for ATP hydrolysis, and the resulting conformational change transitions CFTR between closed and open states, effecting the movement of substrates through a central pore (Fay et al., 2018; Hwang et al., 1994; Liu et al., 2017; Zhang et al., 2018).

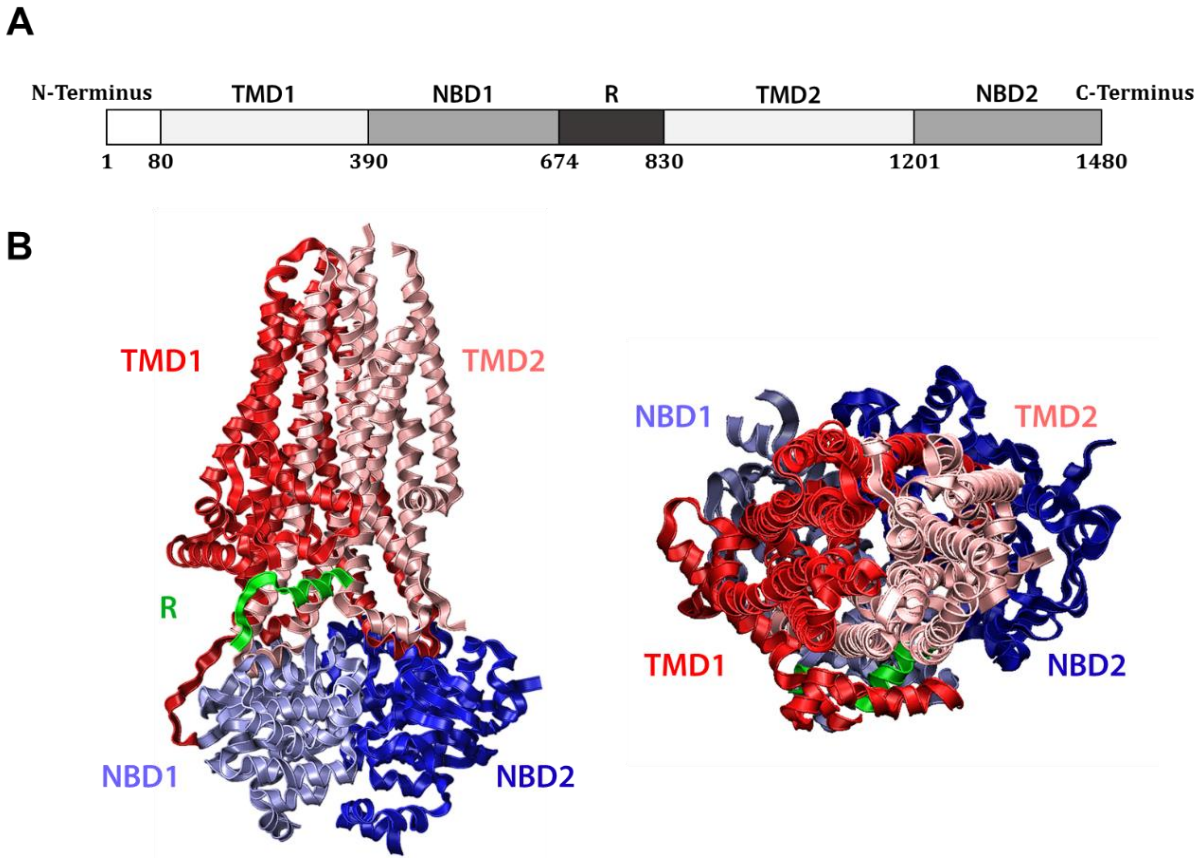

Figure 1. Structure of CFTR.

(A) Linear schematic of CFTR domain organization; (B) Side view (left) and top view (right) depicting the Cryo-EM structure of phosphorylated, ATP-bound CFTR (PDB ID: 6MSM) (Zhang et al., 2018). Note that only part of the R domain is included, as the inherent flexibility of this domain limits its visibility by Cryo-EM.

The pore formed by CFTR also differs from other ABC transporters. Uniquely, CFTR facilitates the movement of anions across a cellular membrane, the only ABC transporter known to do so (Sheppard and Welsh, 1999). Moreover, CFTR functions as a channel rather than as a bona fide transporter. Unlike multidrug resistance pumps, which hydrolyze ATP to actively pump potentially toxic compounds out of cells against a chemical gradient (Locher, 2016), CFTR utilizes ATP to transition between the open and closed states but cannot specify the direction of flow. Therefore, when CFTR opens at the surface of epithelial cells, anions flow passively down their electrochemical gradient. In most epithelial tissues, such as those in the lungs and digestive tract, this corresponds to an efflux of chloride and bicarbonate from within cells into the extracellular space. Chloride release generates a motive force for the concomitant transport of water, thus hydrating the apical surface of these organs. By additionally releasing bicarbonate from cells, CFTR also mitigates acidity in the respiratory tract (Shah et al., 2016). Therefore, when CF patients inherit dysfunctional variants of CFTR, the mucus lining the airways becomes dehydrated and increasingly acidic, providing an ideal environment to support bacterial growth (Pezzulo et al., 2012).

In contrast to pulmonary tissue, the extracellular concentration of chloride is typically higher than the intracellular concentration in sweat ducts (Ram and Kirk, 1989). Consequently, CFTR opening instead triggers a net influx of chloride from the extracellular environment. As a result, electrolytes tend to linger in significantly higher quantities on the skin of CF patients. Though of little pathological consequence, it was the recognition of this trait that brought about sweat chloride testing as the first bioassay used to distinguish CF from other respiratory ailments

(di Sant'Agnese et al., 1953). Measurements of sweat chloride continue to be used as a reliable means of assessing the efficacy of therapeutics that target CFTR (LeGrys et al., 2018).

1.1.3 Inheritance of Dysfunctional CFTR Variants Causes CF

Mutations in CFTR are thought to have been selected for amongst Bronze Age peoples of Western Europe as an adaptation against secretory diarrheal diseases, such as cholera (Farrell et al., 2018; Gabriel et al., 1994). Notably, individuals carrying one defective allele are less prone to severe dehydration. To date, over 300 distinct CFTR mutations have been identified that cause CF (https://cftr2.org). These mutations have been binned into five separate classes based on their molecular defects (Welsh and Smith, 1993).

Class I variants are those which produce either an incomplete CFTR protein or no protein at all. This typically occurs due to a mutation in CFTR that causes translation to prematurely terminate, but can also occur due to the insertion or deletion of base pairs that shift the CFTR reading frame. Class I variants, such as G542X and W1282X CFTR, produce truncated channels and account for around 15% of CFTR variants carried by CF patients in the United States (Cystic Fibrosis Foundation Patient Registry, 2019; Sosnay et al., 2013). Currently, these have proven difficult to "correct" therapeutically (also see Section 3).

Class II variants are full length CFTR channels, but include a mutation which causes domains within the protein to misfold, preventing the channel from trafficking to the cell surface. Class II variants are the most frequently occurring mutations amongst CF patients. Indeed, 86% of American CF patients encode at least one copy of the most prominent Class II variant, F508del CFTR (Cystic Fibrosis Foundation Patient Registry, 2019). The deletion of phenylalanine 508 from NBD1 causes this domain to misfold and compromises interactions both

between NBD1 and NBD2 and between NBD1 and the transmembrane domains (Hoelen et al., 2010; Qu et al., 1997; Sharma et al., 2001; Thomas et al., 1992; Younger et al., 2006; Zhang et al., 1998). Based on its frequency in the population, there has been significant interest in correcting the molecular defects associated with this variant (see Section 3.1). Other more infrequent variants, such as G85E (0.7% of patients) and N1303K (2.4% of patients), also impair CFTR folding but reside within TMD1 and NBD2, respectively.

Both Class III and IV variants instead affect the function of CFTR channels at the cell surface. Class III variants traffic normally to the surface but are gated incorrectly. These variants, which include G551D CFTR (4.5% of patients), cannot open or exhibit reduced open probabilities. As such, Class III variants fail to conduct sufficient chloride and bicarbonate ions across epithelial cell membranes. The activity of some of these mutations is significantly improved by small molecule "potentiator" compounds that are used clinically (Yu et al., 2012) (see Section 3.2). While Class IV variants closely resemble Class III variants in terms of their mitigated function, they instead conduct ion currents weakly due to mutations that misshape or confer an unfavorable electrochemical charge within the channel's central pore.

Finally, Class V variants include those that produce functional CFTR channels but in quantities too small to effectively facilitate anion exchange across cell membranes. For instance, A455E CFTR (0.6% of patients) is as functional as wild-type CFTR, but causes a moderate form of CF due to its inherently lower level of protein synthesis (Sheppard et al., 1995).

While these classifications exist to better guide therapeutic strategies to address the underlying molecular defect of individual variants, it has become increasingly clear that dysfunctional variants can fall into multiple classes (Veit et al., 2016). For instance, F508del CFTR has been characterized as a Class II, Class III, and Class IV variant. In addition to the

misfolding defect of this variant (see above), any F508del channels that do manage to fold and reach the cell surface conduct current across the membrane with reduced efficiency (Dalemans et al., 1991; Hwang et al., 1997; Van Goor et al., 2009). Thus, optimal treatments for individuals carrying the F508del allele require drug combinations that target each of these distinct defects (see Section 3.3).

1.2 CFTR PROTEIN QUALITY CONTROL

Like numerous other cellular proteins that traffic from the endoplasmic reticulum (ER) to the cell surface through the secretory pathway, CFTR is perpetually monitored by protein quality control (PQC) factors. Quality control "decisions" regarding CFTR are generally made at two key points in the cell, either 1) at the ER as CFTR is synthesized, and/or 2) in post-ER compartments after CFTR has folded and trafficked from the ER. How different CFTR variants interact with the PQC machinery at each of these locations has major ramifications for the disease severity associated with distinct variants, as well as the approaches used to therapeutically treat the disease. The PQC machinery, the pathways that lead to the degradation or folding of cellular proteins, and the stress responses that are triggered when misfolded proteins accumulate have collectively been referred to as protein homeostasis, or "proteostasis".

1.2.1 Protein Quality Control at the ER: The Roles of Molecular Chaperones and the Proteostatic Network

As previously noted, CFTR is a relatively large monomeric protein. This is in stark contrast to most other ion channels, which are multimeric. The natively folded state of CFTR channels therefore consists entirely of intramolecular rather than intermolecular interactions. As a single CFTR polypeptide takes approximately 10 min to be fully translated (Ward and Kopito, 1994), folding between domains primarily occurs co-translationally (Kleizen et al., 2005). However, some of the most crucial stabilizing inter-domain interactions, such as those between NBD1 and NBD2, cannot be established until translation is complete (Du and Lukacs, 2009; Rabeh et al., 2012). As a result, CFTR lingers at the ER in a partially folded, energetically unfavorable state, during which it is especially vulnerable to targeting by components of the PQC machinery.

CFTR PQC requires factors that drive the channel toward one of two diametrically opposed cellular fates (Figure 2). Some factors bind to CFTR to promote folding and maturation, whereas other factors recognize unfolded CFTR and instead direct these misfolded, potentially toxic channels for degradation. Though some factors bear both pro-maturative and pro-degradative activities during the biogenesis of proteins at the ER, typically one of these two activities has a greater net effect (Brodsky, 2007).

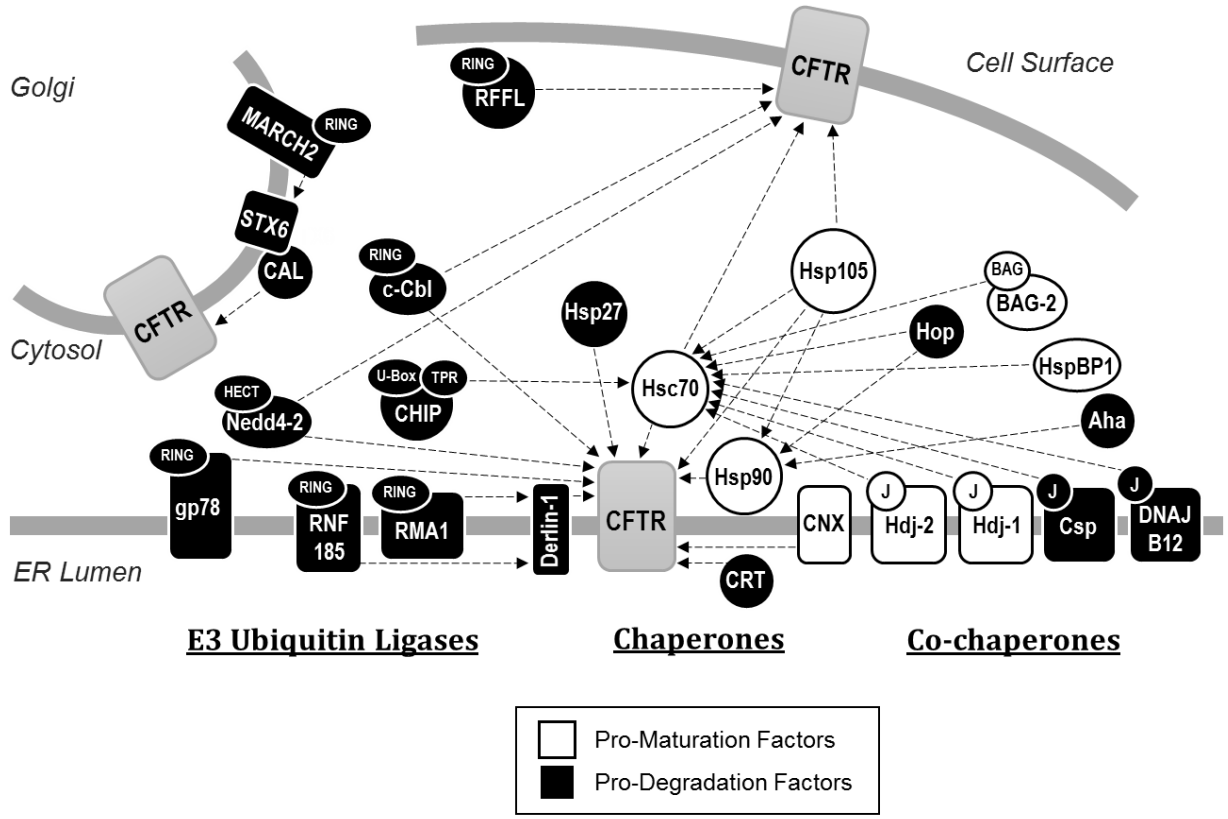

Figure 2. Network of CFTR PQC interactors.

In broad terms, interaction partners sort into one of three groups: chaperones, co-chaperones, and E3 ubiquitin ligases. Each component within the network either enhances maturation of CFTR to the cell surface, or hinders maturation by selecting channels for degradation, although select factors share both pro-maturative and pro-degradative traits. While chaperones and co-chaperones vary widely in their effect, E3 ubiquitin ligases obligately facilitate degradation of CFTR through either the 26S proteasome or lysosome. Factors with an effect reported on either wild-type or F508del CFTR are depicted. Domains required for protein interactions and/or enzymatic activities are additionally depicted. Note that only select interactors are discussed at length.

Molecular chaperones (also known as heat-shock proteins, or Hsps) are among the first components of the cellular PQC machinery to interact with CFTR, frequently acting co-translationally. These include Hsp90 and both the constitutively expressed and stress inducible isoforms of Hsp70, respectively referred to as Hsc70 and Hsp70 (Bagdany et al., 2017; Loo et

al., 1998; Matsumura et al., 2011; Meacham et al., 1999; Scott-Ward and Amaral, 2009). Hsc70, Hsp70, and Hsp90 bind CFTR and support folding through cycles of ATP hydrolysis. Specifically, their ablation in cell culture model systems causes nascent channels to become terminally misfolded and degraded. Although each of these chaperones nominally supports CFTR folding, Hsp70 and Hsp90 recruit numerous other PQC components, many of which antagonize channel folding and maturation. For example, the Hsp70/Hsp90 organizing protein (HOP) has an overall pro-degradative effect upon CFTR by drawing CFTR-bound Hsp90 into interactions with Hsc70 or Hsp70, and in turn with CHIP, an E3 ubiquitin ligase which directs the channel for degradation (see below). These events titrate CFTR off a pro-folding pathway into a pro-degradative pathway. As anticipated, inhibition of HOP favors CFTR maturation (Marozkina et al., 2010b; Zaman et al., 2016). In contrast, HspBP1, a nucleotide exchange factor for Hsc70 and Hsp70, directly inhibits Hsc70 or Hsp70-bound CHIP and helps keep nascent CFTR on the pro-folding pathway (Alberti et al., 2004; Kabani et al., 2002).

Other Hsc70 co-chaperones, chiefly Hsp40 co-chaperones (also known as J-proteins), vary widely in their effects during the early maturation of CFTR. The ER-integral Hsp40 Hdj2 (DNAJA1) was the first member of the Hsp40 family recognized to bind CFTR and support productive folding (Meacham et al., 1999). While Hsc70 was initially observed to independently facilitate NBD1 folding *in vitro* (Strickland et al., 1997), this chaperone was found to utilize both Hdj2 as well as a second Hsp40, Hdj1 (DNAJB1), to effectively rescue ER-retained wild-type, but not F508del CFTR from degradation (Farinha et al., 2002). However, while Hsp40s like Hdj2 or Hdj1 are required for efficient CFTR folding, these co-chaperones can also act as elements of the degradative PQC machinery. For example, in spite of its role in folding CFTR, Hdj2 can sharply increase the ubiquitin ligase activity of the Hsc70/CHIP complexes, as

evidenced upon examination of CFTR sub-domains (Younger et al., 2004). Another Hsp40, cysteine string protein (Csp, DNAJC5) facilitates degradation of CFTR due to its ability to independently recruit CHIP (Schmidt et al., 2009; Zhang et al., 2002; Zhang et al., 2006). Similarly, DNAJB12 stimulates degradation of both immature forms of wild-type and F508del CFTR, but does so by recruiting another E3 ubiquitin ligase, RMA1, to Hsc70 (Grove et al., 2011; Yamamoto et al., 2010). The role of Hsp40s during degradation was also evidenced from studies in model systems. For example, the yeast ER-localized Hsp40 homologues Ydj1 and Hlj1 function redundantly to contribute to the degradation of ectopically expressed CFTR (Youker et al., 2004).

In contrast to the pro-degradative effects of Hsp70 and its broader co-chaperone network (Yang et al., 1993), Hsp90 is an important pro-folding chaperone, as perturbation of its function through either its deletion in the yeast model or its inhibition in human cell culture using small molecules prevents correct assembly of CFTR cytosolic domains and causes the nascent channels to be degraded (Loo et al., 1998; Youker et al., 2004). In contrast, small heat shock proteins (sHsps) play a more complex role during wild-type and F508del CFTR biogenesis. These chaperones, which lack the ATPase domains of their larger counterparts but exhibit potent misfolded protein "holdase" activity (Mogk et al., 2019), were initially implicated in the PQC of CFTR because deletion of the yeast sHsps, Hsp26 and Hsp42, greatly slowed CFTR degradation without altering the attachment of ubiquitin to the ER-retained channel (Ahner et al., 2007) (see below). As expected, overexpression of the human sHsp αA-crystallin (HSPB4) in human cell culture accelerated degradation of F508del CFTR. Later studies indicated that a second human sHsp, Hsp27 (HSPB1), stimulated F508del CFTR degradation but did so by binding to incompletely folded NBD1 and recruiting Ubc9, an enzyme that catalyzes the attachment of

small ubiquitin-like modifier (SUMO) (Ahner et al., 2013; Gong et al., 2016). In some cases, SUMO addition then leads to ubiquitination (Ahner et al., 2013). Consistent with these data, when the folding of NBD1 was improved, there was reduced SUMO addition, suggesting that sHsps primarily target incompletely folded conformations of CFTR.

In parallel, studies by Balch and colleagues used proteomic techniques to elucidate the broader CFTR "interactome", revealing PQC elements that had not been previously revealed (Wang et al., 2006). These included Aha1, a co-chaperone of Hsp90 that enhances the chaperone's ATPase activity and displays an overall pro-degradative effect, perhaps because its action decouples Hsp90 from nascently folded CFTR and leaves the protein in a state where it is more vulnerable to co-translational degradation (Koulov et al., 2010). These studies also revealed the involvement of FKBP8, an ER localized peptidylprolyl isomerase that is specifically upregulated upon expression of F508del CFTR and recruited to chaperone complexes. FKBP8 mediates the *cis-trans* interconversion of proline residues necessary for CFTR to attain a trafficking-competent conformation (Hutt et al., 2012). Yet another CFTR-associated chaperone identified was Hsp105, which is a nucleotide exchange factor for Hsc70 (Bracher and Verghese, 2015). Hsp105 stimulates the co-translational degradation of CFTR while also enhancing its post-translational maturation (Saxena et al., 2012). Together, it is clear that a spectrum of primary and secondary chaperone-associated partners is required to fold CFTR.

In contrast to wild-type CFTR, F508del displays a vastly shifted interactome, characterized by an increase in associated chaperones and co-chaperones, including many that target the channel for degradation (Wang et al., 2006). Remarkably, early data indicated that prolonged hypothermia restores F508del CFTR processing and function (Denning et al., 1992) and does so by remodeling the interaction network to more closely resemble that of wild-type

(Pankow et al., 2015). These data suggested that modifying the interactome, or "proteostatic network", could achieve the same feat.

1.2.2 Targeting of CFTR for Endoplasmic Reticulum Associated Degradation (ERAD)

Like other membrane proteins, CFTR enters the ER and becomes embedded into the ER membrane after entry through the Sec61 protein conducting channel (Bebök et al., 1998; Oberdorf et al., 2005; Pitonzo et al., 2009). More specifically, when polytopic integral membrane proteins such as CFTR enter Sec61, stretches of hydrophobic sequences corresponding to transmembrane spans fail to thread completely into the ER lumen but are instead released through a lateral gate in Sec61 and integrate into the membrane, leaving adjacent hydrophilic domains exposed to either the cytosol or ER lumen (Rapoport et al., 2017). In contrast, as soluble luminal domains of CFTR enter the ER, the protein is N-glycosylated at two asparagine residues (N894 and N900) after synthesis of TMD2 (Cheng et al., 1990). As a result of this modification, CFTR may become subject to PQC decision-making by the lectin-like chaperones calnexin (CNX) and calreticulin (CRT) (Harada et al., 2006; Pind et al., 1994). Though each of these chaperones is involved in the binding and retention of incompletely folded N-linked glycoproteins in the ER, their precise effects upon CFTR differ. CNX, an integral membrane chaperone in the ER, appears to facilitate the correct folding of the TMDs (Rosser et al., 2008). While its prolonged binding impedes maturation of channels from the ER, CNX may also shield incompletely folded forms of CFTR from recognition by pro-degradative PQC elements (Egan et al., 2004; Okiyoneda et al., 2008). Even so, inhibition of CNX heavily favors the trafficking of wild-type CFTR from the ER but provides no benefit to the maturation of F508del CFTR. These results suggest that severely misfolded variants, like F508del, are generally targeted for

degradation prior to the recognition of glycosylated asparagine residues (Farinha and Amaral, 2005). In contrast, CRT, a soluble chaperone in the ER lumen, may facilitate CFTR turnover, perhaps because it extends ER dwell time without actively contributing to domain folding (Harada et al., 2006).

Although the degree of wild-type or F508del protein that folds might be both cell type and species specific (Bebök et al., 2005; Ostedgaard et al., 2007; Varga et al., 2004), it is clear that the complex folding itinerary in the ER results in a significant amount of degradation of even the wild-type form of CFTR. In fact, even with the aid of the many identified pro-folding chaperones, perhaps only one-third of wild-type and virtually no F508del CFTR manages to attain a conformation that can be successfully trafficked from the ER; the remaining protein is instead degraded by the ubiquitin-proteasome system (Cheng et al., 1990; Lukacs et al., 1994; Ward and Kopito, 1994). Why processing of CFTR evolved to be so inherently inefficient is unclear, but might have emerged this way as an overabundance of functioning channels at the cell surface could plausibly cause salt wasting, leading to chronic dehydration. Whatever the reason, these misfolded channels selected for ubiquitin-proteasome-dependent degradation are handled by the ER Associated Degradation (ERAD) pathway. After recognition by pro-degradative chaperones, such as those outlined above, misfolded CFTR in the ER becomes covalently attached to chains of a 76-amino acid polypeptide, known as ubiquitin, which signals CFTR extraction from the ER membrane. The extraction, or "retrotranslocation", of CFTR from the ER membrane requires an AAA-ATPase, known as p97, which then hands the protein off to cytosolic or ER-associated 26S proteasomes (Lukacs et al., 1994; Xiong et al., 1999). It is unclear whether CFTR is directly retrotranslocated from the ER membrane or whether it first enters a putative retrotranslocation channel, although interactions with some of these channels

have been observed (Baldridge and Rapoport, 2016; Ballar et al., 2010; Bebök et al., 1998; Pitonzo et al., 2009; Sun et al., 2006; Wang et al., 2008; Younger et al., 2006). Ultimately, CFTR is hydrolyzed by the proteasome, which contains three unique proteolytic activities. Interestingly, only one of these activities, the chymotrypsin-like activity, is primarily required for CFTR turnover (Oberdorf et al., 2001).

Several enzymes are required for the polyubiquitination of ERAD substrates, such as CFTR (Preston and Brodsky, 2017; Varshavsky, 2012). First an E1 ubiquitin activating enzyme must covalently bind ubiquitin in an ATP-dependent manner before transferring the activated ubiquitin to one of dozens of distinct E2 ubiquitin conjugating enzymes. These E2 enzymes, in turn, act in conjunction with specific E3 ubiquitin ligases to attach the ubiquitin moiety to lysine sidechains on suitable substrate proteins, or onto lysine sidechains of ubiquitin itself to extend the growing polyubiquitin chain. In the case of these isopeptide polyubiquitin linkages, the use of distinct internal lysine residues determines chain topology and cellular function. Canonically, polyubiquitin chains linked through K48 or K11 designate substrate proteins for degradation by the proteasome, whereas K63 linkages typically act as an endocytic signal (Komander and Rape, 2012). While it is unclear exactly which linkage type(s) mark CFTR for ERAD, or whether branched or mixed linkage chains are utilized (which appear to be quite common (Leto et al., 2019)), ubiquitination of certain lysine residues within the channel (specifically K14, K68, and K1218) preferentially selects CFTR for degradation (Lee et al., 2014).

To date, > 600 putative E3 ubiquitin ligases have been identified in the human genome (Li et al., 2008). While some of these enzymes are substrate-specific, most are thought to target multiple substrates, especially during ERAD (Leto et al., 2019). Therefore, each protein can be

ubiquitinated by multiple E3s. Indeed, to date four ubiquitin ligases, RMA1, gp78, CHIP, and RNF185, have been conclusively shown to mediate the ERAD of CFTR.

A significant body of data indicates that RMA1, gp78, CHIP, and RNF185 act at different steps during CFTR biogenesis. Early studies by Kopito and colleagues revealed that CFTR is translated within 30 min but ubiquitination of both wild-type and F508del CFTR begins to appear after only 20 min, indicating that ubiquitination occurs concurrently with translation, at least in an *in vitro* reticulocyte lysate (Sato et al., 1998). Consistent with these data, the earliest acting ubiquitin ligases on CFTR are a pair of ER integral membrane proteins, RMA1 (also known as RNF5) and its highly conserved homologue, RNF185, which target immature or misfolded forms of CFTR immediately after NBD1 translation (El Khouri et al., 2013; Younger et al., 2006). Neither enzyme is capable of binding CFTR directly, but do so through Derlin, an integral membrane adaptor protein that—as noted above—has been suggested to act as a retrotranslocation channel and also assembles multiple components of the ERAD machinery (Carvalho et al., 2010; Claessen et al., 2010; Mehnert et al., 2014; Mehnert et al., 2015; Wahlman et al., 2007). While RMA1 and RNF185 readily target both wild-type and F508del CFTR intermediates for degradation (El Khouri et al., 2013; Younger et al., 2006), RMA1 ablation more prominently improves F508del CFTR maturation and can partially alleviate a CF phenotype in mice, even without additional therapeutic interventions (Tomati et al., 2015). Consistent with data that E3 ubiquitin ligases work with one another (Leto et al., 2019), a third ER-integral E3 ubiquitin ligase, gp78, augments the activity of RMA1 and RNF185 (Morito et al., 2008) by predominantly elongating polyubiquitin chains initiated by either enzyme and contributes to the ERAD of F508del CFTR. In contrast to these early acting E3 ubiquitin ligases, the cytosolic ubiquitin ligase CHIP is most active on fully translated CFTR (Younger et al.,

2006). Like RMA1 and RNF185, CHIP is unable to bind misfolded CFTR channels directly, but in this case it does so by binding Hsc70 (or Hsp70) through an EEVD motif present at the carboxyl terminus of the chaperone. Thus, CHIP co-opts the activity of otherwise pro-folding chaperones to instead trigger ERAD (Ballinger et al., 1999; Meacham et al., 2001). Interestingly, although Hsp90 shares a similar carboxyl-terminal motif, CHIP only stimulates the ERAD of CFTR through its interaction with Hsc70 or Hsp70 (Meacham et al., 2001).

1.2.3 Trafficking of CFTR from the ER

In order to evade ERAD and traffic from the ER, CFTR must pass several of the PQC checkpoints noted above. First, the channels must be sufficiently folded to be released by CNX and CRT. Substrate binding and release of CNX/CRT-substrate complexes depends on the configuration of the glycan, a branched polysaccharide that is gradually trimmed as secretory proteins dwell in the ER (Tannous et al., 2015). CNX and CRT bind glycans with a single terminal glucose but release glycoprotein substrates after this glucose is cleaved by α-glucosidase II. In turn, nascent proteins that have failed to acquire their native conformations can be re-glucosylated by an enzyme that monitors protein conformation. Second, CFTR folding conceals four partially redundant arginine-framed tripeptide (AFT) sequences located within the N-terminus, NBD1, and R domain of CFTR, which facilitate the retention of CFTR in the ER if exposed to the cytosol (Chang et al., 1999). Although mutagenizing these motifs favors F508del CFTR trafficking and function at the cell surface in cell culture, their removal has no discernable impact upon the processing of wild-type CFTR. This result suggests that AFTs alone are not responsible for the retention and degradation of the majority of these channels. Finally, a di-acidic motif (YKDAD) on the surface of NBD1 must be engaged at ER exit sites by two

secretory trafficking components, Sec23/Sec24 (Wang et al., 2004; Yoo et al., 2002), which function as inner coat components of COPII vesicles that mediate ER-to-Golgi transport of secreted cargo proteins (Fromme et al., 2008). Thus, after recognition, properly folded forms of CFTR are sorted into COPII-coated vesicles, which bud from the ER. In the Golgi, CFTR is further modified by *O*-linked glycosylation *en route* to the cell surface (Chang et al., 1994; Cheng et al., 1990).

Studies from the analysis of numerous intragenic suppressor mutations in the gene encoding F508del CFTR led to the concept that more than one mechanism is needed to "fix" the folding defect and allow for ER exit. While misfolding within NBD1 is the primary folding defect caused by the absence of F508 (Hoelen et al., 2010), this mutation also disrupts the interaction between NBD1 and TMD2 at highly conserved residues in intracellular loop 4 (ICL4) (Mendoza et al., 2012; Rabeh et al., 2012). Notably, distinct second-site suppressors could restore favorable folding within NBD1 or interdomain assembly between NBD1 and TMD2. While the presence of either suppressor alone proved insufficient to restore maximal F508del CFTR assembly and function, when these distinct suppressor mutations were combined they acted synergistically to produce CFTR channels that folded, exited the ER, and functioned at the cell surface. This finding signaled that a single compound designed to facilitate the folding of a specific domain in F508del CFTR or other misfolded variants would be unable to fully mend the aberrant channel. The developments leading to subsequent combinatorial therapies are discussed further in Section 3.

In contrast to the forward trafficking pathway, CFTR can also undergo anterograde trafficking through an unconventional pathway when cells are exposed to ER stress, which disrupts ER-to-Golgi transport. During stress, activation of IRE1, which initiates the unfolded

protein response (UPR), increases both the number of ER exit sites and expression of Sec16A, a secretory protein concentrated at these sites that facilitates scaffolding of COPII-coated vesicles (Farhan et al., 2008; Piao et al., 2017). Concurrently, the Golgi-resident protein GRASP55 is phosphorylated, which causes it to dissociate from homodimers into monomers that traffic to the ER where they interact with Sec16A (Kim et al., 2016; Piao et al., 2017). Through a mechanism that remains incompletely understood, GRASP55/Sec16A drives the export of CFTR directly to the cell surface, apparently bypassing the Golgi since CFTR trafficked under these conditions lacks Golgi-associated glycosylation. Fascinatingly, the unconventionally trafficked F508del CFTR protein is sufficiently functional, as transgenic mice expressing GRASP55 lack phenotypes associated with the F508del allele, suggesting that modulation of this pathway could provide therapeutic benefit (Gee et al., 2011). Earlier hints that CFTR bypasses the Golgi apparatus also emerged from work in which the protein was shown to leave the ER even in spite of overexpressed dominant negative versions of required COPII trafficking regulators, yet remained dependent upon fusion with endosomes (Yoo et al., 2002). Which proteins coat CFTR-containing vesicles emerging from ER exit sites and how these vesicles interact with cytoskeletal components in this unconventional pathway remain to be elucidated.

1.2.4 Post-ER Quality Control: Targeting of Plasma Membrane and Endosomal CFTR for Lysosomal Degradation

After its delivery to the cell surface, CFTR acts as an anion channel with a moderate open probability after phosphorylation (wild-type $P_0 \approx 0.4$) (Dalemans et al., 1991; Van Goor et al., 2009). Even after residing in its ultimate site of action, the channel remains acutely sensitive to PQC components. To this end, a tyrosine-based endocytic motif within the C-terminus of CFTR

(YXXΦ) (Collawn et al., 1990; Peter et al., 2002; Weixel and Bradbury, 2002) signals the sorting of CFTR into clathrin-coated pits through direct binding with the adaptor protein AP-2 (Bradbury et al., 1994; Kumari et al., 2017; Weixel and Bradbury, 2000). After subsequent budding from pits into clathrin-coated vesicles, binding between Dab2 and AP-2 links vesicles to myosin IV for transport from the plasma membrane to post-endocytic compartments (Ameen and Apodaca, 2007; Fu et al., 2015; Fu et al., 2012; Swiatecka-Urban et al., 2004). CFTR residing in endosomes is then either transported back to the cell surface via recycling endosomes, or is selected by PQC components for trafficking to the lysosome through late endosomes and multivescicular bodies (MVBs). Similar to ERAD, selection for lysosomal trafficking and degradation is signaled by CFTR polyubiquitination. Interestingly, if F508del CFTR folding is restored (e.g., by low temperature correction; see Section 3.1), which facilitates accumulation of the protein at the cell surface, PQC components recognize the channel more readily than wild-type CFTR (Gentzsch et al., 2004; Okiyoneda et al., 2010). As a result, F508del CFTR is endocytosed faster than the wild-type channel. Interestingly, there is some evidence that folding correctors also stabilize F508del CFTR at the cell surface (Eckford et al., 2014). Regardless, because the mutant channel also exhibits a substantially lower P_0 than the wild-type protein at the cell surface (Dalemans et al., 1991; Van Goor et al., 2009), for clinical benefit small molecule correction of F508del CFTR folding must be accompanied by drugs that also improve channel gating (see below).

Two E3 ubiquitin ligases have been implicated in the ubiquitination of CFTR at the cell periphery. Just as in ERAD, cytosolic CHIP/Hsc70 complexes recognize misfolded F508del CFTR in endosomes and recruit components of the ubiquitination machinery to mark these channels for lysosomal degradation (Okiyoneda et al., 2010). Interestingly, CHIP activity on

CFTR in the late secretory pathway is abrogated by the loss of endocytic factors, such as Dab2, and occurs ~15 min after internalization (Fu et al., 2015). This observation suggests that CHIP acts upon CFTR in endosomes, but not at the cell surface. A second cytosolic E3 ubiquitin ligase, RFFL, is also involved in the turnover of CFTR residing at the cell surface. Unlike CHIP, RFFL is palmitoylated and interacts directly with CFTR, binding through disordered regions independent of molecular chaperones (Okiyoneda et al., 2018). Ablation of RFFL in cell culture has no effect on the turnover of wild-type CFTR at the cell membrane, indicating that the ligase specifically targets mutant CFTR variants at the cell surface.

The C-terminus of CFTR also binds to numerous PDZ proteins, such as NHERF1 (Loureiro et al., 2015), which stabilize and limit the membrane mobility of both wild-type and rescued F508del CFTR at the cell surface (Haggie et al., 2006; Valentine et al., 2012). One notable exception is the CFTR-associated ligand (CAL), which binds peripheral CFTR and targets it for lysosomal degradation by recruiting a SNARE protein, syntaxin 6 (STX6) (Cheng et al., 2010; Cheng and Guggino, 2013; Cheng et al., 2004). Additionally, CAL has been reported to localize to the ER where it contributes to the ERAD of F508del CFTR (Bergbower et al., 2018). In principle, effective modulators that inhibit binding of CAL to CFTR are anticipated to have therapeutic benefits (Wolde et al., 2007), and to this end both peptide and small molecular interventions that block PDZ domain binding have been explored (Wolde et al., 2007; Zhao et al., 2018).

1.3 PHARMACOLOGICAL INTERVENTIONS IN CYSTIC FIBROSIS

As mentioned in Section 1, CF therapies initially focused on alleviating disease symptoms rather than rectifying its core molecular defect: the dysfunction of CFTR channels. However, the discovery of CFTR as the genetic determinant for disease, in conjunction with subsequent elucidation of the proteostatic pathways that regulate the folding, degradation, trafficking, and function of the channel, have led to the development of therapeutics that directly modulate the biogenesis and activity of otherwise defective CFTR variants.

1.3.1 Correction of CFTR Misfolding Promotes Forward Trafficking

Although class II CFTR variants are retained in the ER and targeted for ERAD (see above), simply shifting cells to a lower temperature corrects the misfolding defect for many variants, including F508del, and enables the release of maturely glycosylated, partially functional channels to the cell surface (Denning et al., 1992; Lopes-Pacheco et al., 2017). Though of limited therapeutic benefit, this observation was significant because it implied that if mutant CFTR could be rescued by hypothermia, it might also be rescued by treatment with a compound or set of compounds that successfully recapitulates the effect of low temperature. Welsh and colleagues were the first to provide proof-of-concept for this hypothesis, demonstrating that chemical chaperones, such as glycerol and trimethylamine N-oxide (TMAO), which favor protein folding *in vitro*, restored F508del CFTR processing and activity when added to cultured cells at 37 °C (Brown et al., 1996; Brown et al., 1997; Sato et al., 1996). Over time, other osmolytes and chemical chaperones were identified that conferred similar protective effects (Hanrahan et al., 2019).

Subsequent studies sought compounds that also thermodynamically stabilized F508del CFTR but could be tolerated *in vivo*. One such chemical chaperone, 4-phenylbuterate (4PBA), emerged as an early candidate as it had already received regulatory approval for the treatment of urea cycle disorders. Indeed, high micromolar treatment with 4PBA restored functional maturation of F508del CFTR in cell culture (Rubenstein et al., 1997). Moreover, 4PBA appeared to interfere with the selection of F508del CFTR for degradation by downregulating Hsc70 (Rubenstein and Zeitlin, 2000). While early trials of 4PBA in CF patients showed that it was generally well tolerated and quantifiably stimulated channel activity, it conferred only a slight benefit on respiratory function (Rubenstein and Zeitlin, 1998; Zeitlin et al., 2002). Clearly, more specific modulators would be needed to successfully resolve the misfolding defect caused by F508del and similar malfunctioning alleles.

The advent of massive libraries of drug-like compounds and the development of a fluorescence-based cell culture assay for CFTR activity that was suitable for high throughput screening (HTS) made it possible to query tens of thousands of compounds, leading to the identification of CFTR modulators that exhibited effects at low micromolar concentrations (Ma et al., 2002). These modulators sorted into one of two conceptual classes: "corrector" compounds, which improve CFTR function by augmenting folding and trafficking of the channel, and "potentiator" compounds, which improve the frequency at which the channel gates to conduct anions. Subsequent screening using a modified assay, in which CFTR was rescued by low temperature prior to screening, identified several dozen CFTR potentiators that were structurally unrelated to correctors and previously identified potentiators (Yang et al., 2003).

Ongoing HTS efforts led to the discovery of ever more potent CFTR correctors. One compound was Corr-4a, the first corrector to restore as much F508del CFTR function at 37 °C as

that restored by incubation of untreated cells at 27 °C (Pedemonte et al., 2005). Studies by Vertex Pharmaceuticals then identified VRT-422 and VRT-325, which restored F508del CFTR-mediated chloride current to ~10% of wild-type CFTR current in human bronchial epithelial (HBE) cells, a level associated with a mild CF phenotype (Van Goor et al., 2006). Further medicinal chemistry efforts by the company bore VX-809, which rescued ~30% of F508del CFTR from ERAD and restored ~14% of wild-type chloride secretion; the compound also lacked the off-target effects associated with other compounds (Van Goor et al., 2011). Additional studies indicated that VX-809 interacted directly with nascent channels, most likely by binding at the interface between NBD1 and TMD1 to stabilize early folding intermediates during translation (Loo et al., 2013; Ren et al., 2013). Even so, VX-809 does not correct every misfolding defect associated with F508del as it displays additive effects with Corr-4a, VRT-325, low temperature, and with the introduction of several folding suppressor mutations into F508del CFTR (Farinha et al., 2013).

1.3.2 Potentiation of Channel Conductance

Compounds that potentiate the anion transducing activity of cell surface CFTR channels were well known prior to the identification of folding correctors. One such early potentiator was genistein, a plant product that closely resembles estradiol. When combined with forskolin, a cAMP agonist, enhanced CFTR conductance was observed in cell culture (Illek et al., 1995). Although a portion of this effect was proposed to stem from the action of genistein as a tyrosine kinase inhibitor, possibly preventing CFTR dephosphorylation (Illek et al., 1996), later electrophysiological studies revealed that even in excised cell membrane patches, genistein enhanced conductance of both wild-type and F508del CFTR (Hwang et al., 1997).

Potentiators initially identified through HTS strategies had no effect on the forward trafficking of F508del CFTR but improved gating of low temperature-rescued F508del channels as effectively as genistein, yet with ~10-fold higher affinity (Yang et al., 2003). A subsequent HTS conducted by Vertex Pharmaceuticals led to the identification of VRT-532, a potentiator that also improved F508del CFTR conductance but additively improved conductance when combined with correctors, such as VRT-422 or VRT-325. These data supported the notion that misfolding and inadequate gating arise from distinctly different defects caused by the F508del mutation, and that fixing each defect would require dedicated modulators. Additional examination of VRT-532 indicated that the compound directly bound F508del CFTR channels, as predicted (Wellhauser et al., 2009).

Further efforts to refine the pharmacology of VRT-532 and other hits from earlier potentiator screens resulted in the isolation of VX-770 (Van Goor et al., 2009). Approximately 70 times more potent than genistein, VX-770 acted as a potentiator for CFTR variants regardless of folding propensity, enhancing the open probability of wild-type, F508del, and G551D CFTR channels in excised patches. Additionally, low micromolar quantities of VX-770 increased the height of airway surface liquid in F508del/G551D human bronchial epithelia (HBE) cultures from one-quarter to one-half of that in control HBE. This result signified that the potentiator might meaningfully counteract dehydration of the mucous layer in CF epithelia harboring at least one trafficking-competent CFTR variant. Recent breakthroughs in determining the molecular structure of CFTR channels (Liu et al., 2017; Zhang and Chen, 2016; Zhang et al., 2018) have lent support to the notion that VX-770 mediates channel activity via hydrogen bonding to the transmembrane domains of CFTR, as does an unrelated potentiator developed by Galapagos

Pharmaceuticals. Collectively, it appears that binding to transmembrane domains is a general mechanism of action amongst CFTR potentiators (Kim Chiaw et al., 2011; Liu et al., 2019).

1.3.3 Compounds Currently in Clinical Use

VX-809 and VX-770 (subsequently re-identified as lumacaftor and ivacaftor, respectively) entered clinical trials soon after their isolation. Trials with VX-770 concluded that the potentiator provided substantial benefit to respiratory function and overall quality of life among CF patients 12 years and older with at least one G551D CFTR allele, a classical class III variant (Ramsey et al., 2011). VX-770 received FDA approval in 2012 and was then marketed as Kalydeco™, the first small molecule modulator designed to directly address an underlying molecular defect in CF. Studies published soon after indicated that VX-770 similarly improved the *in vitro* conductance of a broad range of class III and class IV CFTR variants, opening the door for VX-770 to be tested in patients bearing these alleles as well (Yu et al., 2012). VX-770 furthermore improved conductance of a number of class II variants, beyond F508del (Van Goor et al., 2014). However, in spite of its functional benefit in various cell culture models, treatment with VX-770 alone proved ineffective in patients homozygous for F508del (Flume et al., 2012), confirming that a corrector/potentiator combination therapy would be needed to address the unique challenges presented by class II mutations.

Upon subsequent clinical testing, a VX-809/VX-770 combination, marketed as Orkambi™, received FDA approval in 2015, making CFTR modulator therapy available to a broader cross-section of CF patients. However, the benefit that this drug cocktail provided patients with F508del mutations paled in contrast to that which VX-770 provided to G551D patients. While Kalydeco™ appeared to deliver a “functional cure” for patients encoding even a

single gating mutation, Orkambi™ provided F508del homozygous patients only a 4% enhancement on average of one second forced expiratory volume (FEV_1) (Wainwright et al., 2015). Even so, the number of pulmonary exacerbations in those taking Orkambi™ fell from ~1.1 to ~0.8 over a 48 week time frame. This relatively modest benefit, combined with the fact that VX-809 and VX-770 exhibited antagonistic effects (Cholon et al., 2014; Veit et al., 2014), highlighted the need for additional therapies to successfully modulate CFTR in most patients.

Continued adjustment of corrector therapies led to the development of two next generation CFTR correctors: VX-661 (tezacaftor, a VX-809 mimic with an improved pharmacological profile) and VX-445 (elexacaftor), the latter of which corrects F508del CFTR via a mechanism of action that is distinct from VX-809 and VX-661. Although VX-770 continued to diminish the quantity of mature CFTR rescued by treatment with these correctors and needs to be taken twice daily, the VX-445/VX-661/VX-770 corrector/potentiator combination considerably improved patients' wellbeing, especially when compared to Orkambi™ (Keating et al., 2018). In an early clinical trial of patients with either one or two copies of F508del CFTR, CF patients treated with this triple drug combination displayed a 10% improvement in FEV_1 on average, along with a sharp, concomitant drop in sweat chloride and a significantly reduced frequency of pulmonary exacerbations. Subsequent phase III trials examining the effect of this drug combination on both F508del homozygous and heterozygous patients confirmed the substantial improvements seen in this cohort of CF patients (Heijerman et al., 2019; Middleton et al., 2019). Ultimately, the VX-445/VX-661/VX-770 combination received FDA approval for both patient groups in late 2019 and is now marketed as Trikafta™, replacing Orkambi™ as the gold standard for treatment of severely misfolded CFTR variants.

Perhaps most importantly, Trikafta™ and Kalydeco™ provide benefits for >90% of the CF patient community.

1.3.4 The Path Forward in Cystic Fibrosis

Looking forward, there are several significant considerations for the future of CFTR modulator therapies. First, it appears increasingly important that patients with variants known to respond well to current therapies have access to these treatments from as young an age as possible. Modulation will clearly provide the greatest benefit if started before lung tissue becomes permanently damaged. To this end, therapies initially approved for patients 12 years of age or older have since been tested in younger children. Typically, these patients show similar responses to the drugs as when older patients are treated (Davies et al., 2013; Ratjen et al., 2017).

Second, while I estimate that disease-causing alleles currently approved for treatment with Kalydeco™ or Trikafta™ together encompass 70–80% of CF patients in the United States, Canada, and Europe (https://cftr2.org), patients who encode other variants continue to be left with therapies that alleviate only the symptoms of CF, but not the cause. Therefore it remains vital to continue to "theratype" rare alleles according to their pharmaceutical responses (Clancy et al., 2019). This is especially important for variants that may all appear to exhibit similar defects but may differ radically in the way they interact with correctors and potentiators. For example, F508del, E92K, and G85E CFTR are all class II variants that exhibit severe misfolding defects (Figure 3), yet only F508del and E92K are approved for treatment. In contrast, G85E is completely intractable to correction, whether by low temperature or by treatment with small molecules (Lopes-Pacheco et al., 2017). The nature of this phenomenon remains mysterious. Of particular concern are the CFTR truncation mutations or splice site variants, which can produce

catastrophically altered/misfolded channels, or at best might be partially rescued, as observed with the W1282X allele (Haggie et al., 2016). Ongoing efforts have been dedicated to the identification and clinical evaluation of compounds that promote translational read-through or genetic strategies that silent aberrantly spliced products (Joshi et al., 2019).

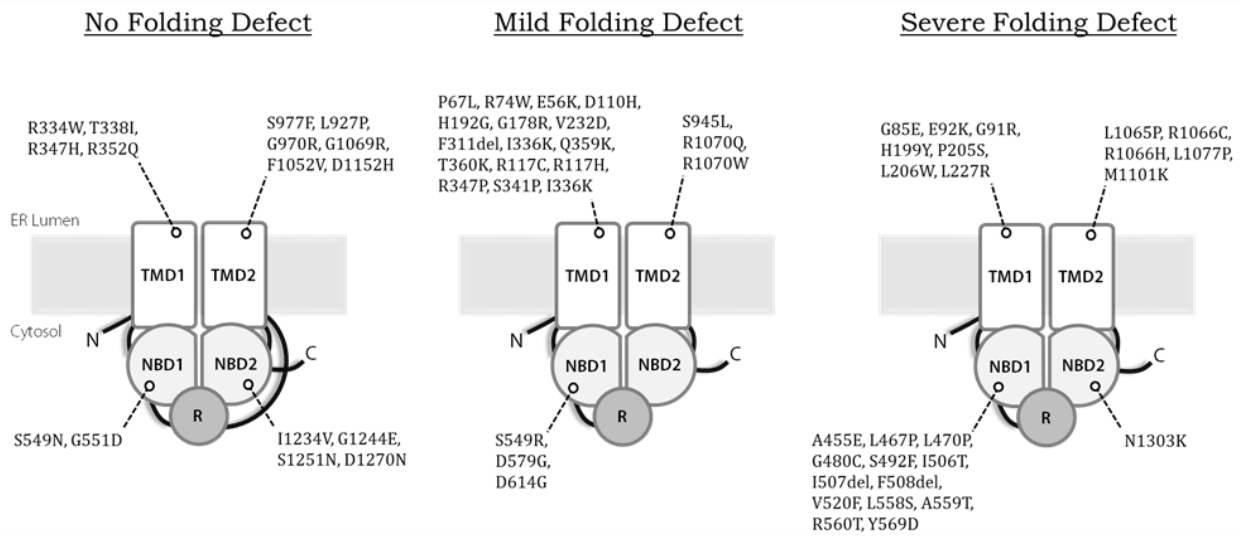

Figure 3. Disease-causing variants of CFTR by channel folding severity.

While severely misfolding variants such as F508del are classified as class II mutations with additional gating and/or conductance defects and are associated with severe CF phenotypes, function of many of these channels could be restored with currently available triple drug combination therapies. Illustration is not intended to depict structures of individual variants.

Third, the long term efficacy of pharmacological correctors and potentiators remains unknown. While current therapies remain relatively new, data for Kalydeco™ have already emerged indicating that VX-770 slows the rate of respiratory decline, but fails to prevent it (Sawicki et al., 2015). Whether the same is true for Trikafta™ remains to be seen. In addition, the current annual price for Trikafta™ is > $300,000. One hopes that the development and approval

of other drug combinations that provide patient benefits will lead to a reduction in the cost of CF therapeutics, improving the availability of these therapies worldwide. Moreover, because VX-445 (elexacaftor) has been tested in patients for a significantly shorter time compared to the other drugs in the cocktail, its long-term effects and any potential negative drug-drug interactions are unknown. Finally, it is unfortunate that not every symptom associated with CF will necessarily be cured by modulator combinations. Ultimately, techniques that edit or replace dysfunctional CFTR genes could provide a permanent cure for all CF patients regardless of allelic combination, bypassing the need for pharmacological modulators altogether.

Until gene editing becomes common, however, it remains imperative that a continued analysis of the proteostatic pathways to which CFTR and disease-causing alleles are subject is continued. In support of this view, studies on the rules governing the identification and disposal of CFTR alleles have yielded surprises. In addition to the non-classical secretion mechanisms noted in the text, some disease-causing alleles appear to be disposed of by the autophagy pathway (Fu and Sztul, 2009; Liu et al., 2018b), and defects in this alternate degradation pathway have been linked to the expression of CF-associated alleles (Luciani et al., 2010). In addition, modulation of the proteostatic pathways that impact CFTR folding, stability, degradation, and trafficking might yield new therapeutic opportunities. Notably, if ERAD of CFTR is slowed through the use of a small molecular inhibitor of the ubiquitin pathway, synergistic effects on F508del maturation and activity are evident when lung epithelial cells are treated with a corrector (Chung et al., 2016). A better understanding of the proteostatic pathways in CF are warranted because small molecule modulators of these pathways are actively being identified and characterized (Kelly, 2019; Labbadia and Morimoto, 2015).

1.4 PROSPECTS FOR INHIBITION OF ERAD TO FAVOR MATURATION AND FUNCTION OF MISFOLDING CFTR VARIANTS

While current development of CF therapeutics primarily focuses on modulation of dysfunctional CFTR channels to restore folding and function (see sections 1.3.1 and 1.3.2), these approaches might additionally benefit from small molecules that manipulate the broader CFTR interactome (Wang et al., 2006). In the following section, I explore the possibility that inhibition of key pro-degradative PQC factors could also support the maturation of otherwise disease-causing CFTR variants.

1.4.1 Inhibition of the Proteasome

Corrector compounds such as VX-809 and VX-661 rescue a subset of defective F508del CFTR channels by favoring folding, which reduces ERAD and provides a significant, albeit limited, benefit to patient condition when combined with potentiators (Heijerman et al., 2019; Middleton et al., 2019; Wainwright et al., 2015). As this therapeutic strategy is intended to solely reduce the predisposition of these channels to misfold, it therefore stands to reason that corrector-based therapies would likely synergize with compounds that directly limit ERAD. To this end, early efforts to inhibit pro-degradative PQC components asked if inhibition of the 26S proteasome would enhance CFTR folding, as activity of this complex is required for CFTR and F508del CFTR degradation via ERAD (Jensen et al., 1995; Ward et al., 1995).

One way to globally attenuate the ERAD of secretory proteins is through proteasomal inhibition. Notably, proteasome inhibitors are effective and generally well-tolerated for the treatment of multiple myeloma (Richardson et al., 2005). Indeed, the proteasome inhibitor

bortezomib has proven to be so effective at reducing the viability of myeloma cells that it and subsequent derivatives remain a first-line treatment for this type of cancer (Okazuka and Ishida, 2018). Given that possibility that proteasomal inhibitors could treat human disease, Kopito and colleagues tested if select proteasome inhibitors would also improve processing of F508del CFTR. While cells treated with the proteasome inhibitor ALLN contained vast quantities of F508del CFTR after 16 hr, this pool of CFTR appeared to be primarily localized to detergent-insoluble peri-nuclear aggregates (Johnston et al., 1998). Moreover, CFTR in these aggregates (termed "aggresomes") was extensively ubiquitinated. Therefore, it appeared that merely ablating the endpoint of ERAD, i.e., degradation, did not prevent CFTR channels from being ubiquitinated and retrotranslocated and led to the formation of potentially toxic aggregates. As this pool of membrane-extracted CFTR would be impossible to rescue, any strategy to improve the processing of CFTR by modulating PQC must therefore focus on quality control events upstream of proteasome action.

1.4.2 Inhibition of E1 Ubiquitin Activating Enzyme

Based on these data, we predicted that inhibiting events upstream of the protein retrotranslocation step might lead to synergy with a chemical corrector of F508del CFTR. To this end, we tested if treatment with PYR-41, a cell-permeant inhibitor of the E1 ubiquitin activating enzyme, Ube1 (Yang et al., 2007), would enhance F508del CFTR expression by globally reducing ubiquitination. As anticipated, E1 inhibition reliably increased levels of immature CFTR, though this did not translate to an increased population of functional, maturely CFTR channels (Chung et al., 2016). However, additionally treating cells with C18 (also known as VRT-534), a CFTR corrector structurally related to the FDA-approved corrector VX-809

(Eckford et al., 2014; Van Goor et al., 2011), synergistically improved both conversion of channels into the mature species, as well as channel conductance. These data provided a convincing proof-of-principle that tuning the activity of the ubiquitination machinery could augment the efficiency of rescue provided by current modulator therapies.

1.4.3 Could Attenuation of E3 Ubiquitin Ligases Enhance Rescue with Corrector Compounds?

E1 inhibition could plausibly provide some benefit to CF patients, but its effects would be global and thus potentially toxic. While the compound might potentially be titrated such that the benefits associated with partial inhibition of ubiquitination are properly balanced with the risks, the range of cellular drug concentrations required to achieve therapeutic benefit without broadly disturbing proteostasis could be narrow or perhaps even nonexistent. Therefore, a more tolerable approach might focus rather on inhibiting select E3 ubiquitin ligases. As mentioned in section 1.2.2, the human genome encodes hundreds of E3 ubiquitin ligases (Li et al., 2008), each with its own select set of target substrates. Moreover, unlike E1 ubiquitin activating enzyme inhibition, the inhibition of any single ubiquitin ligase is less likely to cause widespread proteotoxic stress.

Of the E3 ubiquitin ligases described to act upon misfolded or partially folded CFTR channels (see Section 1.2.2, (Estabrooks and Brodsky, 2020)), the prospect of inhibiting CHIP (Figure 4A,B) is particularly interesting. Due to the cytosolic localization of this enzyme, CHIP inhibition could reduce the turnover of both nascent CFTR channels through ERAD as well as degradation of endocytosed CFTR channels at the cell periphery (Meacham et al., 2001; Okiyoneda et al., 2010; Younger et al., 2004). Thus, the impact of inhibiting CHIP might be

multifaceted. In addition, deactivation of CHIP might reduce both the turnover and recruitment of Hsc70 as pro-degradative PQC components, thereby enhancing the pool of molecular chaperones available to productively facilitate CFTR biogenesis instead. Indeed, cell culture models have already been used to demonstrate the potential benefit of CHIP inhibition upon CFTR levels. For example, F508del CFTR accumulates upon inactivation of CHIP or its primary upstream E2 ubiquitin conjugating enzyme, UbcH5 (Younger et al., 2004). However, unlike the aggregated cytoplasmic pool of F508del CFTR that accumulates upon proteasomal inhibition, this protein pool remains soluble and is capable of forward trafficking. Similar to E1 inhibition, knockdown of CHIP also synergizes with corrector treatment (Grove et al., 2009) and boosts retention of F508del CFTR at the cell surface, as anticipated (Fu et al., 2015; Okiyoneda et al., 2010).

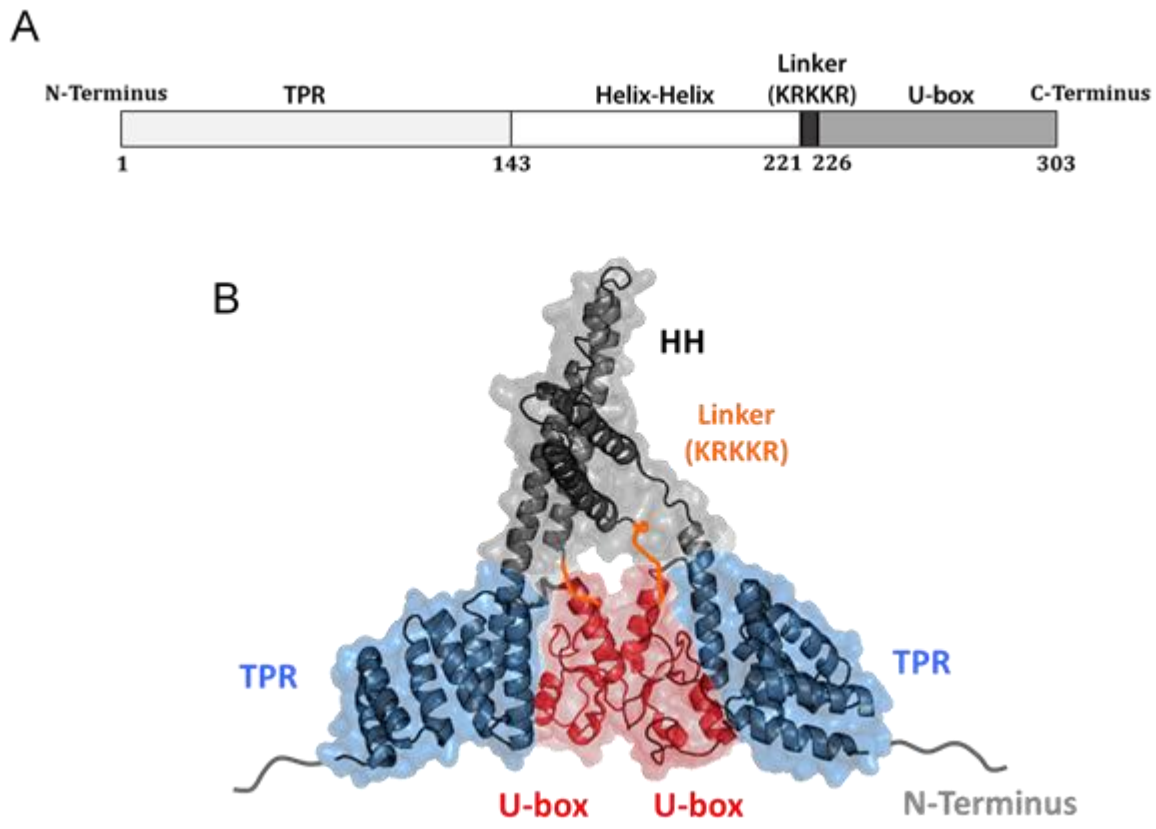

Figure 4. Structure of the E3 ubiquitin ligase CHIP.

(A) Linear schematic of CHIP domain organization. **(B)** Crystal structure of the asymmetric human CHIP homodimer. Figure reproduced with adaptation from Figure 1 in (Ye et al., 2017); also see Appendix A.

Specific inhibition of CHIP is likely to be well tolerated, as evinced by a rare neurodevelopmental disorder. STUB1 (CHIP)-related ataxias are a set of ultra-rare ataxias that cause widespread systemic neurodegeneration that are characterized by wasting of the cerebellum and the pyramidal tract (Bettencourt et al., 2015; Cordoba et al., 2014; Depondt et al., 2014; Hayer et al., 2017; Heimdal et al., 2014; Madrigal et al., 2019; Shi et al., 2014; Shi et al., 2013; Synofzik et al., 2014) (Table 1). While this disease presents with a range of secondary symptoms and bears a highly variable age of onset, every case observed to date can be traced to the inheritance of two dysfunctional CHIP alleles. In contrast, carriers for STUB1-related ataxia— heterozygous parents and unaffected siblings of patients— display neither symptoms of the disease nor an accelerated rate of cognitive decline. Because CHIP is homodimeric (Nikolay et al., 2004), carriers may produce as little as one-quarter the typical number of active CHIP dimers, assuming that dimers containing at least one mutated CHIP variant are inactive. It is worth noting however that it as the number of recognized CHIP heterozygotes observed through these studies remains low, it is unclear whether such reduced CHIP activity leads to other secondary effects, such as a predisposition to various cancers (Liu et al., 2018a; Luan et al., 2018; Shang et al., 2017; Sun et al., 2015; Tang et al., 2019; Wang et al., 2014). Even so, one can extrapolate that the activity of CHIP in CF patients could possibly be inhibited so that only 25% of wild type activity remains without ill effects. Should corrector-based therapies provide only modest benefits to certain patient groups (Wainwright et al., 2015), or benefits that dissipate beyond the short term (Sawicki et al., 2015), inhibition of CHIP is one avenue that could be explored in order to enhance the efficacy of these therapies. Therefore, one of the goals of my work— which is to better define how this enzyme folds and ubiquitinates CFTR— may have future clinical applications.

CHIP Genotype	Subjects	Sex	Age	Age of Onset	National Origin	Study
L165F/L165F	4	F, F, F, M	34-42	14-19	China	Shi et al. 2013
N130I/W147C	1	M	23	20		
Y207X/S236T	1	F	25	16		
T246M/T246M	2	F, F	19-22	17-19		Shi et al. 2014
L275V/‡	1	M	23	15	Argentina	Cordoba et al. 2014
L123V/L123V	1	M	16	2	Germany	Synofzik et al. 2014
M240T/M240T	1	F	21	16	Turkey	
A79T/A79D	2	M, M	46-50	29-49	Saudi Arabia	
N65S/N65S	3	M, M, F	20-30	0-2	Middle East	Heimdal et al. 2014
E28K/K114X	1	F	45	33	Sri Lanka	
K145Q/Y230CfsX8	2	M, M	30-32	23-25	Belgium	Depondt et al. 2014
M221I/G238X	2	F, M	†	20s	Spain	Bettencourt et al. 2015
R119X/I294F	1	M	34	1	Germany	Hayer et al. 2017
K145Q/P243L	2	F, M	45, †	11-12	Belgium	

Table 1. CHIP genotypes causing STUB1-related ataxias.

Summary of patients reported globally with CHIP (STUB1) mutations causing STUB1-related ataxia, alternately known as spinocerebellar ataxia autosomal recessive 16 (SCAR16). Age indicates patient age at time of investigation; "†" denotes that patient was deceased at time of study. M: male; F; female. "‡" denotes a splicing mutation, c.612+1G>C.

1.5 THESIS OBJECTIVES

The underlying motive for my dissertation research is to better understand the function of protein quality control factors that selectively drive misfolded, disease-causing forms of CFTR towards protein degradation pathways. This goal was realized through the development and application of new *in vitro* assays in which early steps during the ERAD of CFTR could be recapitulated. I first established a CHIP *in vitro* ubiquitination assay in order to better examine the activity of this E3 ubiquitin ligase. To this end, I initially utilized this assay to evaluate a unique model for activation of CHIP that had been predicted by molecular dynamics simulations (Ye et al., 2017). I then used this assay to test if putative small molecular inhibitors of CHIP in fact reduced the activity of this enzyme (Pabon et al., 2018; Zaman et al., 2019) . Finally, I tested partially unnatural ubiquitin variants in this assay in order to determine if these could be appended to substrates like wild-type ubiquitin (Werner et al., 2019). In parallel, I also developed a microsomal *in vitro* ubiquitination assay, with which I could assay ubiquitination of CFTR variants. Specifically, I used this assay to test if a set of disease-causing CFTR variants exhibited variable susceptibility to E3 ubiquitin ligases such as CHIP, anticipating that different variants bear distinct folding defects, and thus would be targeted differently by components of protein quality control machinery.

2.0 DEVELOPMENT OF *IN VITRO* UBIQUITINATION ASSAYS TO QUANTIFIABLY MEASURE CHIP ACTIVITY

2.1 INTRODUCTION

Eukaryotic cells utilize a combination of distinct pathways to ensure that misfolded proteins are eliminated before they accumulate and become toxic. These pathways, collectively referred to as protein quality control (PQC), act upon proteins localized to a variety of cellular compartments. As an estimated 30% of eukaryotic proteomes are comprised of secretory proteins (Ghaemmaghami et al., 2003; Venter et al., 2001), PQC is particularly active in the endoplasmic reticulum (ER), where these secreted and integral membrane proteins are synthesized and packaged into vesicles for trafficking to the Golgi, the lysosome (or vacuole in yeast), the plasma membrane, or for soluble proteins, to the extracellular environment. However, when secretory proteins fail to fold correctly, they are instead retained and targeted for ER associated degradation (ERAD). During ERAD, a small polypeptide known as ubiquitin is appended onto lysine sidechains of substrates, ultimately creating polyubiquitin chains that act as potent signals for degradation (Komander and Rape, 2012; Ruggiano et al., 2014). Once marked in this way, substrates are retrotranslocated to the cytosol by an AAA+ ATPase (p97 in humans; Cdc48 in budding yeast) and targeted to the 26S proteasome to be proteolyzed (Richly et al., 2005).

While PQC pathways such as ERAD primarily exist to protect cells from proteotoxic stress arising from misfolded proteins, these same pathways can cause human diseases when substrates containing subtle defects are targeted too aggressively (Houck and Cyr, 2012; Needham et al., 2019; Ruggiano et al., 2014; Welch, 2004). Solute conducting channel and transport proteins are especially vulnerable to overzealous quality control because the folding of these proteins is particularly complex. Specifically, nearly all integral membrane solute channels and transporters contain several transmembrane segments (Hessa et al., 2005a; Hessa et al., 2007), which have to be translated and properly inserted into the ER membrane before the entire structure can stably fold (Buck et al., 2007; Chen and Zhang, 1999; Hessa et al., 2005b; Shurtleff et al., 2018). Compared to other integral membrane proteins, the assembly of these proteins is additionally problematic because the insertion of individual transmembrane helices is not necessarily an energetically favorable process and may require other helices to be synthesized in order to cooperatively improve insertion (Hessa et al., 2007; Ojemalm et al., 2012; Zhang et al., 2007). Channels also have cytosolic domains that fold and assemble independently of membrane-spanning domains, as well as domains that ultimately reside in the extracellular space but initially fold within the ER. The coordinated assembly of a protein that resides in any of these three unique chemical environments is essential in order to avoid selection by the PQC machinery (Buck and Skach, 2005; Fisher et al., 2008; O'Donnell et al., 2017; Qu et al., 1997; Qu et al., 1996; Staub et al., 1997; Zhou et al., 1998). Due to these challenges, it is no wonder that mutations that disrupt this process can dramatically shift the precarious balance between folding and degradation in favor of the latter.

The cystic fibrosis transmembrane conductance regulator (CFTR) is a chloride channel expressed in epithelia throughout the human body that epitomizes this balance. CFTR is a large

monomeric chloride channel that takes ~10 min to translate and an additional 20 min to reach a trafficking-competent state (Cheng et al., 1990; Ward and Kopito, 1994). During that time, it is vulnerable to targeting for ERAD simply due to its intrinsically delayed folding kinetics and thermodynamic instability (Jensen et al., 1995; Sato et al., 1998; Ward et al., 1995). As a result, ~70% of otherwise functional wild-type channels are ubiquitinated and destroyed by ERAD (Lukacs et al., 1994). Mutations that further destabilize CFTR, such as the predominant cystic fibrosis (CF)-causing allele F508del—which compromises the folding of the cytosolic first nucleotide binding domain (NBD1) and attenuates the interaction of this domain with the second nucleotide binding domain (NBD2) and first membrane spanning domain (MSD1) (Hoelen et al., 2010; Mendoza et al., 2012; Rabeh et al., 2012)—cause virtually all channels to be eliminated by ERAD, precluding function at the plasma membrane (Cheng et al., 1990; Lukacs et al., 1993). Furthermore, F508del CFTR channels which manage to escape ERAD, whether through hypothermic incubation in cell culture or by treatment with corrector compounds, are rapidly endocytosed and targeted to the lysosome for degradation (Lukacs et al., 1993; Lukacs et al., 1997; Okiyoneda et al., 2010; Sharma et al., 2001). Remarkably, F508del CFTR retains ~50% of the function of the wild-type channel (Dalemans et al., 1991; Wang et al., 2011), which can be augmented by "potentiator" compounds that restore wild-type conductance (Van Goor et al., 2009; Yang et al., 2003). Because F508del CFTR and similarly misfolded variants might therefore be coerced to function like wild-type channels, considerable effort has been made to elucidate which PQC factors drive the folding and degradation of these channels in the hope of developing therapeutics. These efforts have led the identification of corrector compounds that partially reduce the susceptibility of F508del CFTR to these pro-degradative factors, improving

maturation of this disease-causing CFTR variant (Loo et al., 2013; Lopes-Pacheco et al., 2016; Okiyoneda et al., 2013; Pedemonte et al., 2005).

To date, approximately two dozen factors have been reported to either promote the maturation of CFTR in the ER or catalyze its degradation through the ERAD pathway (Estabrooks and Brodsky, 2020). Folding is initially supported by molecular chaperones, such as Hsc70 and Hsp90, which hydrolyze ATP to actively fold CFTR (Bagdany et al., 2017; Loo et al., 1998; Strickland et al., 1997; Youker et al., 2004). The action of these chaperones is further modulated by a wide variety of co-chaperones, some of which support productive CFTR folding by enhancing the activity of Hsc70 (Farinha et al., 2002; Meacham et al., 1999; Zhang et al., 2006). These factors include DNAJA1 and DNAJA2, which like Hsc70 bind to "hotspots" on the cytosolic surface of CFTR to coordinate folding (Baaklini et al., 2020). Other factors guide channels toward ERAD by recruiting additional pro-degradative PQC factors (Grove et al., 2011; Schmidt et al., 2009). These recruited factors include several E3 ubiquitin ligases, which are ultimately responsible for the attachment of polyubiquitin onto incompletely folded CFTR channels. The integral membrane ubiquitin ligases RMA1 and its close homologue RNF185 are the first to act upon CFTR in the ER, ubiquitinating channels after translation of MSD1 and NBD1 (El Khouri et al., 2013; Tomati et al., 2015; Younger et al., 2006). A similar ligase, gp78, also ubiquitinates CFTR co-translationally, though is thought to primarily extend chains initiated by RMA1 or RNF185 (Morito et al., 2008). In contrast, a cytosolic ubiquitin ligase known as CHIP may have the greatest effect upon fully translated CFTR and is thus a major driver of channel degradation during the ~20 min dwell time prior to the transport of CFTR from the ER to the Golgi (Meacham et al., 2001; Younger et al., 2006; Younger et al., 2004). CHIP is unable to interact directly with CFTR, but does so by way of binding to Hsc70, effectively converting

this pro-folding chaperone into an element of the degradative machinery (Ballinger et al., 1999; Meacham et al., 2001). CHIP can additionally target CFTR for lysosomal degradation after the protein has been endocytosed (Fu et al., 2015; Fu et al., 2012; Younger et al., 2006).

In this chapter, I present a pair of ubiquitination assays that I have developed. Using the first assay, I sought to better understand how CHIP affects CFTR polyubiquitination by employing purified enzymes and model substrates. I then used this assay to better characterize the unique manner in which CHIP is activated and to identify CHIP inhibitors. In the second assay, I reconstituted an early step during the PQC of CFTR by combining enzymes required for polyubiquitination with ER-enriched microsomes prepared from CFTR-expressing human cell cultures. Based on the degree to which a CFTR channel is misfolded, I hypothesized that the recognition of unique CFTR variants to the ubiquitination machinery would differ. Therefore, I compared a range of disease-causing variants using this assay and determined that some variants are indeed ubiquitinated to a greater extent than others. Addition of purified CHIP to these reactions also produced a modest but reproducible enhancement in the ubiquitination of most variants tested. These data highlight the subtle differences in the way in which CFTR variants are recognized by cellular PQC pathways. These differences might also influence how aggressively each variant is targeted for degradation, or perhaps even determine how a variant is targeted for degradation.

2.2 MATERIALS AND METHODS

2.2.1 Cloning TPR-less CHIP for Bacterial Expression and Purification

The pET151/D-TOPO vector containing CHIP (Page et al., 2012; Xu et al., 2008; Zhang et al., 2015) was used to create an inactive CHIP mutant by overlap extension polymerase chain reaction (PCR) (Forloni et al., 2018) in order to omit the N-terminal TPR domain of CHIP, similar to CHIPΔTPR vectors others have previously designed (Meacham et al., 2001). Briefly, custom 30-mer and 40-mer DNA oligonucleotide primer pairs were designed with homology for pET151/D-TOPO $CHIP_{1\text{-}303}$, which was provided as a gift from Dr. Saurav Misra at Kansas State University. Primer pair F1 and R1 (see Table 2) was designed to amplify a 5' section of the CHIP gene encoding an upstream NdeI restriction site, the ATG start (M), a His tag (HHHHHH), the V5 tag (GKPIPNPLLGLDST), a TEV protease cleavage site (ENLYFQGIDPFT), and the first residue of CHIP (M). Primer pair F2 and R2 was designed to amplify a 3' section of the same gene encoding CHIP residues 134-303, the TGA stop codon TGA, and a downstream EcoRI restriction site. Primers F2 and R1 were designed as reverse compliments and each had partial homology for the 3' section comprising the first CHIP codon and the upstream TEV protease cleavage site, as well as partial homology for CHIP from codon 134 onward.

Initial PCR reactions with Phusion® polymerase (Thermo Scientific #F-530) and the pET151/D-TOPO template were conducted over 26 cycles (98°C denaturation for 10 s, 55°C annealing for 25 s, 72°C polymerization for 1 min) to generate CHIP fragments F1-R1 and F2-R2, which omit CHIP residues 2-133. After confirming successful amplification of gene sections by 0.5% TBE/agarose gel electrophoresis, aliquots of each initial reaction were combined and polymerized by Phusion® for 4 cycles without primers, then for 21 additional cycles with

addition of primers F1 and R2 to produce CHIP fragment F1-R2. Reaction products were restriction digested by Nde1 and EcoRI, resolved by gel electrophoresis, gel extracted, and ligated by the Quick Ligation™ Kit (New England Biolabs #M2200) into pET151/D-TOPO that had separately been linearized after treatment with NdeI and EcoRI. After transformation of ligated plasmids into NEB5α High Efficiency competent *E. coli* cells (New England Biolabs #C2987U), subsequent plasmid preparation (Thermo Scientific #K0503) and Sanger sequencing verification (GENEWIZ), pET151/D-TOPO $CHIP_{134\text{-}303}$ was transformed into BL21 (DE3) competent *E. coli* (New England Biolabs #C2527I) and used to subsequently express and purify His-$CHIP_{134\text{-}303}$.

Primer	Sequence
F1	5’- GGA GAT ATA CAT ATG CAT CAT CAC CAT CAC CAT GGT AAG C -3’
F2	5’- GAA TTG ATC CCT TCA CCA TGG ACA TCC CCA GCG CTC TTC G -3’
R1	5’- CGA AGA GCG CTG GGG ATG TCC ATG GTG AAG GGA TCA ATT C -3’
R2	5’- ACC GGA ATT CCT ATC AGT AGT CCT CCA CCC -3’

Table 2. PCR primers for the cloning of a plasmid encoding TPR-less CHIP.

Forward (F) and reverse (R) DNA oligonucleotides used in the construction of an N-terminally tagged CHIP gene lacking codons 2-133, corresponding to a deletion of the majority of the CHIP TPR domain.

2.2.2 Cloning CFTR2 Variants for Expression in Human Cell Culture

pcDNA5/FRT human cell expression vectors for CFTR variants were initially obtained from the Sorscher lab at Emory University (Han et al., 2018) and sequence verified through Sanger sequencing (GENEWIZ). In order to enhance the expression of certain disease-causing CFTR variants (P67L, G85E, E92K, W1282X, N1303K) with various levels of misfolding (Estabrooks and Brodsky, 2020), inserts containing the CFTR genes were removed by restriction digest with ApaI, NotI, and SacII restriction endonucleases (Thermo Fisher #FD1414, New England Biolabs #R3189, New England Biolabs #R0157) and resolved by 0.5% TBE/agarose gel electrophoresis. The excised ~4.5 kb CFTR gene inserts were collected by gel extraction (Thermo Scientific #K0692). In parallel, the pcDNA3.1(+) was obtained from the Kleyman lab at the University of Pittsburgh, digested with ApaI and NotI restriction endonucleases, resolved by gel electrophoresis, and ~5.4 kb linear vectors were collected by gel extraction.

Ligations were conducted in a 3:1 molar ratio by the Quick Ligation™ Kit (New England Biolabs #M2200) and transformed into NEB5α High Efficiency competent *E. coli* cells (New England Biolabs #C2987U). Clones containing the ligation products were isolated, and the

plasmids were extracted (Thermo Scientific #K0503) and then screened by digestion with EcoRI restriction endonuclease (Thermo Fisher #FD0274). Plasmids matching the digestion pattern of pcDNA3.1(+) wild-type CFTR control were verified by GENEWIZ Sanger sequencing.

2.2.3 Isolation and Enrichment of His-Ube1

The pET21d His-Ube1 expression vector was a gift from Dr. Cynthia Wolberger at Johns Hopkins University (Addgene plasmid #34965). After transformation into a BL21(DE3) *E. coli* strain for bacterial expression, the cells were cultured overnight in Luria Broth (LB) containing 100 µg/mL Ampicillin (LB + Amp) at 37°C. The saturated overnight culture was used to inoculate a 0.5 L LB + Amp culture to initial optical density at 600 nm (OD_{600}) of 0.05, which was then incubated at 37°C with shaking at 200 rpm. After reaching an OD_{600} of 0.3, 250 µL of 1 M IPTG was added (500 µM final IPTG) to induce expression of His-Ube1 and the culture was incubated at 18°C at 200 rpm overnight, as induction at low temperature had been previously found to be necessary for efficient expression of Ube1 (Carvalho et al., 2012). After overnight incubation, the culture was centrifuged at 5000 rpm (~3600×g) for 10 min at 4 °C, the supernatant was removed, and cell pellets were stored at -80°C.

Pellets were subsequently thawed on ice with 25 mL of Lysis Buffer (2.6 mM NaH_2PO_4, 47.4 mM $Na_2H_2PO_4$, pH 8.0, 300 mM NaCl, 10 mM imidazole, 1% PMSF, 0.2% Leupeptin, 0.1% Pepstatin A, 5 mM 2-mercaptoethanol, 0.25% Triton X-100, 2 mg/mL lysozyme) supplemented with 2 Roche cOmplete™ EDTA-free protease inhibitor cocktail tablets (hereafter referred as “PIC”; Millipore Sigma #11873580001) and incubated for at least 30 min with occasional agitation by hand. After no clumps were visible and the lysate appeared mucoid, it was transferred to an SS34 Sorvall™ tube and sonicated in 30 sec bursts followed by 30 sec on

ice until it reverted to a thin fluid. The lysate was then centrifuged at 10000 rpm (~12000×g) for 10 min at 4°C. A 15 µL aliquot of cleared lysate was collected in 15 µL 2X SDS Sample Buffer (125 mM Tris pH 6.8, 125 mM NaCl, 4% SDS, 20% glycerol, 10% 2-mercaptoethanol, 0.004% bromophenol blue) as a diagnostic sample, while a small scoop of the lysate pellet was also collected and emulsified in 2X SDS Sample Buffer. The remainder of the cleared lysate was then applied to a chromatography column that had previously been packed with 3 mL of Ni-NTA resin (Qiagen #30210), washed with ddH_2O, and equilibrated with 10 mM imidazole buffer. Lysate was flowed across the resin at the slowest possible drip rate and a diagnostic sample of the flow-through was collected. The column was washed with 25 mL of 10 mM Imidazole Wash buffer (2.6 mM NaH_2PO_4, 47.4 mM $Na_2H_2PO_4$, pH 8.0, 300 mM NaCl, 10 mM imidazole, 1% PMSF, 0.2% Leupeptin, 0.1% Pepstatin A) and then with 25 mL 30 mM Imidazole Wash (2.6 mM NaH_2PO_4, 47.4 mM $Na_2H_2PO_4$ pH 8.0, 300 mM NaCl, 30 mM imidazole, 1% PMSF, 0.2% Leupeptin, 0.1% Pepstatin A). His-Ube1 was eluted with a 30 mL 200 mM Imidazole Elution buffer (2.6 mM NaH_2PO_4, 47.4 mM $Na_2H_2PO_4$ pH 8.0, 300 mM NaCl, 200 mM imidazole, 1% PMSF, 0.2% Leupeptin, 0.1% Pepstatin A) + 1 PIC, which was collected in six 5 mL fractions. Washes and elutions were stored on ice at 4°C overnight, and diagnostic samples were collected in 2X SDS Sample Buffer and stored at -20°C.

Next, the diagnostic samples were thawed and resolved across a 10% polyacrylamide/SDS gel by SDS-PAGE, then stained with Coomassie Brilliant Blue stain and destained with Coomassie Destain (50% methanol, 10% acetic acid) to identify peak fractions containing His-Ube1. These fractions were pooled, dialyzed in 20 mM HEPES, pH 7.4, 20 mM NaCl for 4 hr at 4°C, and His-Ube1 was applied to a previously prepared 3 mL column packed with DEAE-Sepharose® Fast Flow resin (GE Healthcate #17-0709-01) that had been equilibrated

in 20 mM HEPES, pH 7.4, 20 mM NaCl. The column was then washed with 20 mL of 20 mM HEPES, pH 7.4, 50 mM NaCl, and His-Ube1 was eluted with 18 mL of 20 mM HEPES, pH 7.4, 150 mM NaCl, followed by 9 ml of 20 mM HEPES, pH 7.4, 200 mM NaCl, followed by 9 ml of 20 mM HEPES, pH 7.4, 300 mM NaCl, all of which were collected in 3 mL fractions. All washes and elutions were stored on ice at 4°C overnight, and diagnostic samples in 2X SDS Sample Buffer were collected for each wash and the elution and stored at 20°C.

The diagnostic samples from this column were subsequently resolved by SDS-PAGE and Coomassie stained as described above, and fractions that were enriched for intact His-Ube1 were again identified. These fractions were pooled, applied to an Amcon® Ultra-15 30000 MWCO centrifugal filter that had previously been equilibrated with 50 mM HEPES, pH 7.5, 0.2% Tween 20, and centrifuged at 3333 rpm (2000×g) 4°C until less than 1 mL remained. His-Ube1 was then diluted into 20 mL 50 mM HEPES, pH 7.5, and recentrifuged until less than 1 mL remained. Concentrated His-Ube1 was next transferred to a new microcentrifuge tube and stored on ice. Diagnostic samples in 2X SDS Sample buffer taken before and after protein concentration were examined by SDS-PAGE and Coomassie stained as described above to determine what proportion of concentrated protein was intact His-Ube1. Finally, 10 µL aliquots were flash frozen in liquid nitrogen and stored at -80°C.

2.2.4 Isolation and Enrichment of Substrates for *in Vitro* Ubiquitination

The pGST||2 $Hsc70_{395\text{-}646}$ was a gift from Dr. Saurav Misra at Kansas State University (Zhang et al., 2015), while pGEX6p1 AT-3 JD was a gift from Dr. Matthew Scaglione at Duke University (Faggiano et al., 2013; Todi et al., 2010). Transformed *E. coli* cultures in LB + Ampicillin were grown to saturation and used to inoculate new 0.5 L cultures with an initial

OD_{600} of 0.05 (see 2.2.1 above). After reaching an OD_{600} of 0.3, protein expression was induced with 500 µM IPTG and the cultures were incubated overnight at 15°C with shaking at 200 rpm. After overnight incubation, the cells were centrifuged at 5000 rpm (~3600×g) for 10 min at 4 °C, the supernatant was removed, and cell pellets were stored at -80°C.

The cell pellets were later thawed on ice and mixed with 25 mL of Lysis Buffer (50 mM Tris, pH 7.5, 150 mM NaCl, 1% PMSF, 0.2% Leupeptin, 0.1% Pepstatin A, 5 mM 2-mercaptoethanol, 0.25% Triton X-100, 2 mg/ml lysozyme) + PIC. After incubation for 30 min with occasional agitation, each lysate was transferred to an SS34 Sorvall™ tube, sonicated, and centrifuged as above. Diagnostic samples were collected for each cleared lysate and lysate pellet. The lysate was then applied to 5 mL of glutathione-agarose resin (Sigma-Aldrich #G4510), which had been washed with ddH_2O and equilibrated with 50 mM Tris, pH 7.5, 150 mM NaCl. Columns were set to drip at as slow a rate as possible and a diagnostic sample of each flow-through was collected. Each column was then washed with 30 mL of Wash Buffer (50 mM Tris pH 7.5, 150 mM NaCl), which was collected in three 10 mL fractions, and then the protein was eluted with 15 mL of Elution Buffer (50 mM Tris pH 7.5, 150 mM NaCl, 6.8 mg/ml reduced glutathione) in five 3 mL fractions. All washes and elutions were stored on ice at 4°C overnight. Diagnostic samples in 2X SDS Sample Buffer and all washes and elutions were stored at -20°C.

Diagnostic samples were thawed, resolved by SDS-PAGE, and Coomassie stained as described above to identify peak fractions containing GST-tagged protein. The corresponding fractions were thawed, pooled, dialyzed into 50 mM HEPES, pH 7.0, 50 mM NaCl for 4 hr at 4°C, and then transferred to fresh tubes on ice. Each substrate was subsequently aliquoted, flash frozen in liquid nitrogen, and stored at -80°C.

2.2.5 Isolation and Enrichment of His-CHIP

The pET151/D-TOPO CHIP and pET151/D-TOPO CHIP$_{134-303}$ vectors were transformed into Rosetta2(DE3) and BL21(DE3) *E. coli*, respectively. Transformed *E. coli* cultures were grown and induced with IPTG, as above, incubated overnight at 18°C with shaking at 200 rpm, and harvested. The lysis and purification of His-CHIP from cell pellets generally followed the procedure used to purify His-Ube1 (see section 2.2.3). In brief, cell pellets were thawed, lysed with buffer containing 10 mM imidazole and protease inhibitors, and after the lysates were cleared by centrifugation, applied to a chromatography column packed with Ni-NTA resin previously washed and equilibrated with 10 mM imidazole. Bound His-CHIP was washed with 10 mM and 30 mM imidazole, though protease inhibitors were not required for efficient purification of His-CHIP, which was more protease-resistant. His-CHIP was eluted in fractions with 200 mM imidazole elution buffer and stored on ice at 4°C. Diagnostic samples were collected at all steps, resolved by SDS-PAGE, and Coomassie stained to indicate peak fractions. These fractions were pooled and dialyzed into 50 mM HEPES, pH7.0, 50 mM NaCl at 4° overnight.

After dialysis, solutions containing both full length His-CHIP and His-CHIP$_{134-303}$ appeared cloudy, indicating precipitation of CHIP due to reduced solubility in the dialyzed buffer. The supersaturated CHIP solution was transferred to microcentrifuge tubes and centrifuged at 13000 rpm (~15900 ×g) for 5 min at 4°C to remove insoluble CHIP, and the supernatant was transferred to fresh tubes on ice and monitored for further precipitation. After none was observed, full length His-CHIP was diluted 1:1 in 50 mM HEPES pH 7.0, 50 mM NaCl, 20% glycerol to maintain solubility. Fractions were aliquoted, flash frozen in liquid nitrogen, and stored at -80°C.

2.2.6 Protein Concentration Determination

Aliquots of isolated, enriched protein were dispensed into wells of a clear, flat-bottomed 96 well plate alongside 10 µL BSA standards (ranging from 0-2000 µg/mL) in 50 mM HEPES pH 7.5 in 50 mM HEPES pH 7.5 and quantified by Pierce™ BCA protein concentration assay (Thermo Fisher Scientific #23225). Where indicated, the effective molarity of the protein was determined by calculating the fractional purity of each sample by densitometry observed by Coomassie staining and the total protein concentration determined by the BCA protein concentration assay.

2.2.7 CHIP *in Vitro* Ubiquitination Assay

In vitro ubiquitination assays containing CHIP were based upon procedures published previously (Zhang et al., 2015). In summary, enzymes were thawed and a master mix was prepared containing the indicated concentrations (see below) of His-Ube1, UbcH5b (Boston Biochem #E2-622), human recombinant ubiquitin (Boston Biochem #U-100H), and ATP Reaction Buffer (50 mM HEPES, pH 7.0, 50 mM NaCl, 20 mM ATP, 40 mM $MgCl_2$, 0.5 mM DTT), which was then incubated at 37°C for 30 min. Meanwhile, reaction tubes were set up on ice containing the indicated concentrations (see below) of His-CHIP, the GST-tagged substrate protein (either GST-$Hsc70_{395-646}$ or GST-AT3 JD), and buffer (50 mM HEPES pH 7.0, 50 mM NaCl). CHIP and substrate proteins were incubated for at least 15 min at 4°C. The pre-incubated Ube1/HbcH5b/ubiquitin/ATP master mix was then dispensed to all reactions and incubated at 37°C for 30 min. Final 20 µL reactions typically contained 0.125 µM His-Ube1, 1 µM UbcH5b, 200 µM ubiquitin, 3 µM His-CHIP, 10 µM GST-tagged substrate, and 2 mM ATP. Reactions

were quenched by the addition of 20 µL 2X SDS Sample Buffer, and 5 µL of each reaction was resolved across duplicate sets of 5% polyacrylamide/SDS gels by SDS-PAGE and transferred to nitrocellulose membranes overnight.

After transfer, one set of membranes was blocked with milk/TBST (50 mM Tris pH 7.4, 150 mM NaCl, 0.1% Tween 20, evaporated milk) for 1 hr at ambient temperature with rocking, then treated with 1:1000 rabbit anti-GST-HRP (Abcam #ab3416) in milk/TBST with rocking at 4°C overnight. The other set of membranes was immersed in boiling ddH_20 for 45 min, blocked in the milk/TBST solution, and treated with 1:250 mouse anti-ubiquitin (P4D1) (Santa Cruz #sc-8017) in milk/TBST at 4°C overnight. The blots were next washed with TBST three times for 5 min and treated with 1:1000 horse anti-mouse-HRP secondary antibody (Cell Signaling Technology #7076) in TBST for 4 hr at ambient temperature. Both sets of blots were subsequently washed with TBST as above and developed with SuperSignal™ West Pico Chemiluminescent Substrate (Thermo Fisher Scientific #34078). Chemiluminescence indicating substrate ubiquitination (anti-GST blot) and total ubiquitination (anti-ubiquitin blot) was imaged using a Bio-Rad ChemiDoc™ XRS+ Imager.

2.2.8 Human Cell Culture

HEK293 cell cultures were maintained in Falcon® 10 cm sterilized polystyrene dishes (Corning #353003) with 10 mL DMEM (Sigma-Aldrich #D6429) containing 10% FBS (Hyclone #SH30071) at 37°C in a 5% CO_2 humidified atmosphere. Upon reaching confluency, cells were passaged by aspirating media and detached by addition of 2 mL Gibco® TrypLE™ per plate (Thermo Fisher Scientific #12604-021) followed by incubation at ambient temperature for 3 min. Trypsinized cells were then transferred to a sterile conical tube containing 8 mL DMEM and

centrifuged at 1500 rpm (405xg) in a clinical centrifuge for 3 min. After centrifugation, the supernatant was aspirated and the cells were resuspended in at least 3 mL DMEM + 10% FBS, of which 100 µL was dispensed to a 10 cm plate along with 10 mL DMEM + 10% FBS and returned to 37°C. For procedures requiring a precise number of cells (e.g., for transfection), 20 µL of the cell suspension was diluted 1:3 in Trypan Blue Stain (Life Technologies #15250-061), of which 10 µL was examined in a hemocytometer to calculate cell density. Cell cultures were passaged at most five times before they were either discarded or stored in glycerol at -80°C (i.e., resuspended instead in 1–3 mL of 90% FBS, 10% DMSO, aliquoted into 1 mL cryovials, and stored in polystyrene foam racks at -80°C). Frozen cultures were revived by thawing and dispensing into 10 cm plates containing 20 mL DMEM + 10% FBS, which was replaced with 10 mL of fresh DMEM + 10% FBS after overnight incubation, after which cells were passaged normally. Cultures were not used in any experiment until they had been passaged at least once. All cell culture procedures were conducted within a 1300 Series A2 biosafety cabinet (Thermo Fisher Scientific).

To compare microsomes between CFTR-containing HEK293 cells and those prepared from HeLa and CFBE cell cultures, HeLa cells were propagated identically to HEK293 cells, but required 15 min at 37°C to lift from plates with TrypLE. CFBE cells were cultured in MEM with Earle's salts (Thermo Fisher Scientific #11095-080) + 2 mM L-glutamine + 50 U/mL Gibco® penicillin/streptomycin (Fisher Scientific #15140148) + 2 µg/mL puromycin.

2.2.9 Plasmid Transfection into Human Tissue Culture Cells

Plasmids encoding CFTR (pcDNA3.1, pcDNA5/FRT, or pBI-CMV2) were purified from transformed, saturated DH5α or NEB5α *E. coli* cultures grown in LB + 100 µg/mL ampicillin

using either a QIAGEN® Plasmid Maxi Kit (Qiagen #12163) for initial experiments or a higher-yielding ZymoPURE™ II Plasmid Maxiprep Kit (Zymo Research #D4203) for subsequent experiments.

Prior to transfection, 0.6×10^6 HEK293 cells were plated either into wells of a 6 well plate with 2 mL DMEM + 10% FBS per well to test transfection conditions, or into 10 cm plates with 10 mL DMEM + 10% FBS to prepare microsomes. The cultures were incubated for at least 24 hr at 37°C 5% CO_2 before transfection. When cultures reached 50% or higher confluency (ideally 70%), cells were transfected using either Lipofectmine™ 2000 or PEI transfection reagents. For Lipofectmine™ 2000 (Thermo Fisher Scientific #11668) transfection, 6 well plate cultures were transfected with 4 ng plasmid and 10 µL Lipofectmine™ 2000 per well by incubating each reagent alone in Gibco® Opti-MEM® (Thermo Fisher Scientific #31985) for 5 min at ambient temperature before the plasmid and reagent were combined for 20 min and added to cells. Cultures were returned to 37°C for 6 hr, after which the media was aspirated and replaced with 2 mL of new DMEM + 10% FBS. For transfection of 10 cm plate cultures, plasmids and transfection reagents were scaled up 6.6-fold to account for the increased surface area. Transfected cultures were incubated overnight at 37°C 5% CO_2 prior to any subsequent experiment.

For PEI transfection (Polysciences Inc. #23966-1), a 1 mg/mL solution of MW 25000 PEI in ddH_2O was prepared immediately before transfection, which was dissolved by a 5 min incubation at 95°C. Six well plate cultures were transfected with 2 ng plasmid and 20 µL of 1 mg/mL PEI per well. Each reagent was incubated alone in 1X DPBS (Thermo Fisher # 14190-144) for 5 min at ambient temperature before they were combined for 20 min, and the mixture was diluted 1:2 with Opti-MEM® and added to cells. The cultures were then incubated at 37° for

4 hr after which the media was replaced with 2 mL DMEM + 10% FBS per well. As above, reagents were scaled-up when 10 cm plates were used, and cultures incubated overnight at 37°C prior to subsequent experiments. Due to its cost-effectiveness and similar performance to Lipofectmine™ 2000, transfection by PEI was the preferred method for later procedures requiring large numbers of transfected cells (e.g., for the preparation of microsomes).

2.2.10 siRNA Transfection into Human Tissue Culture Cells

Dharmacon™ siGENOME SMARTpool siRNAs (Horizon Discovery #M-007201-02) targeting CHIP transcripts were purchased, reconstituted at 10 µM in RNase-free H_2O, aliquoted, and stored at -80°C. No aliquot of siRNA was thawed and refrozen more than twice. To prepare for transfection, 0.6×10^6 HEK293 cells were plated either to wells of a 6 well plate with 2 mL DMEM + 10% FBS per well to test transfection conditions, or to 10 cm plates with 10 mL DMEM + 10% FBS for microsome preparations (see section 2.2.13). Cultures were incubated for at least one day at 37°C before transfection. When cultures reached at least 30% confluency, cells were transfected using RNAiMAX (Thermo Fisher Scientific #13778). For 6 well plates, at least 10 nM CHIP siRNA and 6 µL RNAiMAX were used per well, and as above each reagent was first incubated alone in 250 µL Gibco® Opti-MEM® (Thermo Fisher Scientific #31985) for 5 min at ambient temperature before the reagents were combined for 20 min and added to cells. Cultures were returned to 37° and incubated overnight, and 72 hr after transfection the cells were lysed and knockdown efficiency determined by western blotting (see below). When 10 cm plates were used, 10 nM CHIP siRNA and 40 µL RNAiMAX were incubated alone in 1.5 mL Gibco® Opti-MEM® and then together as above. In this case, cultures were incubated for 48 hr, then

transfected with pcDNA3.1 CFTR expression plasmids using PEI (see section 2.2.9 above). After an additional ~18 hr at 37°C, microsomes were prepared (see section 2.2.13 below).

2.2.11 Cell Lysis and CFTR Detection

After transfection to transiently express CFTR or knockdown CHIP (see sections 2.2.9 and 2.2.10), transfection efficiency was assessed by preparing cellular lysates for western blots. First, the media was aspirated and replaced with 300 µL (for a 6 well dish) of TNT Buffer (50 mM Tris pH 7.2, 150 mM NaCl, 1% Triton X-100) + 1 PIC. Plates were incubated on ice for 30 min with occasional agitation by hand before centrifugation at 13000 rpm (~16000×g) for 15 min at 4°C. The total protein concentration of cleared lysates was determined as stated previously. Each cleared lysate was diluted into SDS Sample Buffer (see above) and volumes corresponding to 30 µg total protein were resolved by 5% polyacrylamide/SDS gels and SDS-PAGE. To assess CFTR expression, blots were treated with 1:2500 mouse anti-CFTR (antibody 217 from the Cystic Fibrosis Foundation Therapeutics antibody distribution program, University of North Carolina at Chapel Hill). To assess CHIP knockdown, blots were treated with 1:2500 rabbit anti-CHIP (Sigma-Aldrich #PLA0196). All blots were washed with TBST as described above and then treated with either 1:5000 horse anti-mouse-HRP secondary antibody in TBST (Cell Signaling Technology #7076) or 1:5000 goat anti-rabbit-HRP (Cell Signaling Technology #7074) for 4 hr with ambient rocking. After secondary antibody treatment, the blots were again washed, developed with SuperSignal™ West Pico Chemiluminescent Substrate, and imaged using a Bio-Rad ChemiDoc™ XRS+ Imager.

2.2.12 Immunoprecipitation and Detection of Ubiquitinated CFTR

To isolate ubiquitinated CFTR proteins from HEK293 cells, cells in 10 cm plates were transfected with either pcDNA3.1(+) encoding wild-type CFTR, pcDNA3.1(+) encoding F508del CFTR, or pBI-CMV2 encoding N1303K CFTR using PEI as described above. The cells were simultaneously transfected with an equal quantity of pcDNA3.1(+) encoding HA-tagged ubiquitin. After overnight incubation, the media was aspirated and replaced with 10 mL DMEM + 10% FBS +10 µM MG132 (Selleck Chemicals #S2619). Cultures were returned to 37°C for 1 hr before the media was aspirated, the cells were trypsinized with TrypLE™ for 3 min at ambient temperature, and then transferred to conical tubes containing 6 mL DMEM + 10% FBS. The mixture was centrifuged at 1500 rpm for 3 min, and the cell pellets were lysed with 500 µL TNT Buffer + PIC + 25 µM MG132 + 5 mM NEM on ice for 30 min with occasional agitation by hand. After centrifugation at 13000 rpm (~1600×g) for 15 min at 4°C, 750 µg of total protein, 850 µL of TBS + 0.14% Triton X-100 + 25 µM MG132 + 5 mM NEM + 1 PIC, 60 µL of a 1:1 slurry of ProteinA Sepharose™ CL-4B (GE Healthcare #71-7090-00 AF) in TBS, and 3 µL of mouse anti-CFTR antibody (1:1 mix of CFFT antibodies 217 and 596) were combined and incubated on a rotator at 4°C overnight to immunoprecipitate CFTR. The next morning, the tubes were retrieved and centrifuged at 2000 rpm (380×g) for 2 min at 4°C, the pelleted beads were resuspended in IP Wash Buffer (50 mM Tris pH 7.4, 150 mM NaCl, 1% Triton X-100, 0.2% SDS, 5 mM EDTA), and washed three time before the beads were finally resuspended in SDS Sample Buffer, incubated at 37°C for 15 min, and resolved through duplicate 5% polyacrylamide/SDS gels. After proteins were transferred, one set of blots was probed for CFTR as described (see section 2.2.11) while the other set was treated with 1:2000 mouse anti-HA-HRP (3F10) (Millipore Sigma #12013819001), and 1:2000 mouse anti-ubiquitin (P4D1) (Santa

Cruz #sc-8017) antibodies before being subsequently probed with 1:2500 horse anti-mouse-HRP secondary antibody in TBST. Both sets of blots were washed, treated with chemilumenescent substrate, and imaged as described.

2.2.13 ER-Enriched Microsome Preparations from Human Tissue Culture Cells

Human cell cultures were at least 50% confluent at the time of microsome preparation and had been incubated for ~18 hr after prior transfections with CFTR-encoding plasmids (section 2.2.9). Microsomes were prepared using no fewer than three 10 cm plates of cells.

To prepare microsomes, the media was aspirated and cells were suspended by treatment with TrypLE™ for 3 min at ambient temperature. When HeLa cells were used, the cultures were suspended by treatment with TrypLE™ for 15 min at 37°C and the cells were then diluted 1:2 with DMEM + 10% FBS and centrifuged at 1500 rpm (405 ×g) for 3 min at 4°C. After centrifugation, the supernatant was aspirated from the cell pellet, and cells were resuspended in 1X DPBS that had been chilled on ice. After re-centrifugation and aspiration of the supernatant, the cells were resuspended in 10 mL Homogenization Buffer (0.5 M sorbitol, 20 mM HEPES pH 7.4, + 2 PIC) and placed on ice. The cell suspension was then applied to a stainless steel syringe homogenizer fitted with a tungsten carbide ball bearing (Isobiotec), which was 7.980 mm in diameter and allowed for 20 µm clearance, and two 10 mL Luer-Lok™ disposable syringes (Becton Dickinson #309604). The solution was passed from side-to-side for 14 cycles. To prepare microsomes from HEK293 or CFBE cells, a 7.976 mm ball bearing was used, allowing for 24 µm cell clearance. After homogenization, lysed cells were diluted 1:2 with Homogenization Buffer, then centrifuged at 720 rpm (93×g) for 5 min at 4°C in a clinical centrifuge to remove nuclei. The supernatant was then collected into a new SS34 Sorvall™ tube

to which 10 mL of KOAc Buffer (210 mM potassium acetate, 3 mM magnesium acetate, 20 mM HEPES, pH 7.4, + 1 PIC) was added before centrifugation at 10000 rpm (~12000×g) for 10 min at 4°C. The supernatant was removed and the pelleted microsomes were resuspended in 20 mL of Transport Buffer (250 mM sorbitol, 70 mM potassium acetate, 1 mM magnesium acetate, 20 mM HEPES pH 7.4, + 1 PIC) and re-centrifuged. Microsomes were then resuspended in 150-350 µL Transport Buffer as judged by the size of the microsomal pellet. These resuspended microsomes were aliquoted and stored at -80°C. To quantify the relative amounts of microsomes, 1:200 dilutions of each microsome preparation in 2% SDS were prepared and the mean absorbance of each preparation at 280 nm (A_{280}) was calculated. After resuspension, the microsomes typically possessed an A_{280} of 0.10-0.25.

Before using microsomes for *in vitro* ubiquitination assays, expression of CFTR was confirmed by treating microsomes with 1 U RQ1 RNase-free DNase for 20 min on ice (Promega #M6101). The microsomes were then transferred to fresh microcentrifuge tubes, pelleted at 13000 rpm for 5 min at 4°C, and then resuspended with 2X SDS Sample Buffer such that each sample would have a final microsomal A_{280} of 0.125 in a 20 µL volume. A total of 5 µL of each sample was resolved by 10% polyacrylamide/SDS gel electrophoresis and CFTR was detected by western blot as described above (see section 2.2.11).

2.2.14 Radiolabeling of Ubiquitin with Iodine-125

One day prior to labeling, two 2 mL 7K MWCO Zeba™ Spin Desalting Columns (Thermo Fisher Scientific #89889) were vertically clamped, uncapped, filled with freshly mixed 1X DPBS + 1% BSA, and allowed to drain by gravity flow at ambient temperature. Columns

were pre-equilibrated with DPBS/BSA over three washes. After the third wash, the columns were capped, sealed at the ends with Parafilm®, and stored at 4°C overnight.

On the following day, the columns were washed a fourth time with DPBS + 1% BSA, and transferred to a chemical fume hood (Thermo Scientific) equipped with an air pump and air filters for radiological monitoring. Tubes stored at -80°C containing 1 M Tris pH 8.0, 2 M NaCl, 5 mg/mL NaI in 1% BSA, and 33 mM ICl in ddH_2O were thawed. ICl was a gift from Dr. Gerry Apodaca at the University of Pittsburgh. One 1.5 mL microfuge tube was set up for each of two separate iodination reactions, and 100 µl of 1 M Tris pH 8.0 was added to each reaction tube, followed by 20 µL of 1:50 ICl (prepared by diluting 2 µL ICl into 98 µL 2 M NaCl). Next, 4 µL of ^{125}I radionuclide (Perkin Elmer #NEZ033L005MC) was added to each reaction tube on ice and incubated for 1 min, after which 10 µL of thawed 10 mg/mL recombinant human ubiquitin (Boston Biochem #U-100H) in DPBS was added to each reaction and incubated for an additional 10 min. The reactions were quenched by the addition of 100 µL 33 mM NaI, then transferred to pre-equilibrated desalting columns (1 column per reaction) and allowed to drip by gravity flow into microcentrifuge tubes. After the columns drained, 300 µL of DPBS + 1% BSA was added to each column, which was also collected. This flow through was discarded and 600 µL of additional DPBS + 1% BSA was added to each column. Eluted ^{125}I-ubiquitin was collected in collection tubes and the product (2×10^5 - 6×10^5 cpm per µL) was subsequently aliquoted and stored at -80°C.

2.2.15 Microsomal CFTR *in Vitro* Ubiquitination Assay

In vitro ubiquitination assays with human cell-derived ER-enriched microsomes containing CFTR were conducted by preparing 30 µL reactions on ice with Buffer 88 (20 mM

HEPES pH 6.8, 250 mM sorbitol, 150 mM potassium acetate, 5 mM magnesium acetate) + PIC, diluted His-Ube1 (1:2 in Buffer 88 + PIC), diluted UbcH5b (Boston Biochem #E2-622; 1:5 in Buffer 88 + PIC), the indicated concentration of His-CHIP, a 10X ATP Regenerating System (10 mM ATP, 400 µM creatine phosphate, 2 mg/mL creatine phosphokinase in Buffer 88), and 1 U RQ1 RNase-free DNase. The microsomes (prepared as described in section 2.2.13) were thawed and either a fixed quantity of microsomes was added to reactions, regardless of the relative levels of CFTR (such that all reactions contained microsomes with a corresponding A_{280} of 0.02, i.e., 6 µL of microsomes with an A_{280} of 0.15 added to a 30 µL reaction), or the quantities of microsomes added to assays were adjusted such that approximately equal amounts of CFTR were added to all reactions. Microsomes were thus diluted or concentrated to prepare working stocks in Buffer 88 + PIC with an A_{280} of 0.1, 0.3, or 0.5, depending on CFTR levels. Equal volumes of these working stocks were then added to reactions. After the addition of microsomes, reactions were removed from ice and 5 µL of ^{125}I-ubiquitin was added to each reaction and mixed briefly by hand. The reactions were then incubated for 45 min at ambient temperature and typically contained 0.15 µM His-Ube1, 0.25 µM UbcH5b, and 2 µM CHIP (where indicated). Reactions testing the ubiquitination of microsomal CFTR variants prepared from HEK293 cells after CHIP knockdown were conducted with 3 µL of ubiquitin for 30 min to reduce the accumulation of non-CFTR polyubiquitinated species.

After incubation, reactions were quenched by the addition of 70 µL TBS/SDS (50 mM Tris, pH 7.4, 150 mM NaCl, 14% SDS, 1 PIC) and incubated at 37°C for 15 min. Quenched reactions were then supplemented with 900 µL TBS/Triton (50 mM Tris pH 7.4, 150 mM NaCl, 0.24% Triton X-100, 25 µM MG132, 5 mM NEM, 1 PIC), 45 µL of a 1:1 slurry of ProteinA Sepharose™ CL-4B in 1X TBS, and 1.5 µL Mouse anti-CFTR antibody (1:1 mix of CFFT

antibodies 217 and 596), which was then incubated on a rotator at 4°C for 3 hr to immunoprecipitate CFTR. The mixture was centrifuged at 2000 rpm (376×g) for 2 min at ambient temperature to pellet the beads, which were then washed two more times in 500 µL IP Wash Buffer + PIC. Finally, the immunoprecipitated CFTR was resuspended in 50 µL 2X SDS Sample Buffer, incubated at 37°C for 10 min, and stored at -20°C.

To quantify the amounts of precipitated CFTR and ubiquitinated proteins, the precipitates were incubated at 37°C for 10 min and 20 µL was loaded to duplicate sets of 5% polyacrylamide/SDS gels and resolved by SDS-PAGE. One set of gels were treated with SDS-PAGE Fixing Buffer (25% isopropanol, 10% acetic acid) for 30 min with agitation, then dried onto Whatman® filter paper with a dry ice-cooled vacuum pump gel drier for 1.75 hr. Dried gels were then exposed to a blanked phosphorimager screen overnight. After a minimum of three days, the screen was scanned using either a Typhoon™ FLA 7000 or Amersham™ Typhoon™ phosphorimager (GE Healthcare). Sixteen-bit depth phosphorimages were collected at a 50 µm pixel size using an upper PMT voltage of 800 V. The other set of gels was transferred overnight onto nitrocellulose membranes, which were blocked for 30 min in milk/TBST and treated with primary antibodies. Initial experiments were western blotted with 1:2500 mouse anti-CFTR (CFFT antibody 217) and 1:2500 horse anti-mouse-HRP as described (see section 2.2.11). Later experiments were treated similarly, but used 1:5000 rabbit anti-CFTR (D6W6L) (Cell Signaling Technology #78335) and 1:5000 goat anti-rabbit-HRP (Cell Signaling Technology #7074). In both cases, the blots were washed with TBST, developed with either SuperSignal™ West Pico Chemiluminescent Substrate or ProSignal® Pico ECL Reagent (Genesee Scientific #20-300B) and visualized on a Bio-Rad ChemiDoc™ XRS+ Imager.

2.2.16 Ubiquitination of Enriched CFTR

Highly enriched wild-type CFTR was isolated from stably expressing HEK293 cell lines and provided in a HEPES, pH 7.5, 150 mM NaCl, 10 mM magnesium ATP, 0.2 mM TSEP, 0.06% digitonin, 10% glycerol buffer by Dr. Zhengrong Yang and Dr. John Kappes of the Cystic Fibrosis Foundation Protein Production Core at the University of Alabama (Hildebrandt et al., 2015). *In vitro* ubiquitination reactions containing purified CFTR generally followed the same procedure described for the *in vitro* ubiquitination of microsomal CFTR (see above). In brief, reactions contained Buffer 88 + PIC, the ATP Regenerating System, His-Ube1, UbcH5b, and CHIP, where indicated. DNase was omitted, and where noted, 2 µM of human Hsp70 (provided by Dr. Patrick Needham, University of Pittsburgh) was also added (Chiang et al., 2009). A total of 3 µL (~0.1 µM) purified CFTR was added to reactions along with 3 µL of ^{125}I-ubiquitin. After 30 min at ambient temperature, reactions were quenched and incubated with TBS/Triton, ProteinA Sepharose™, and a 1:1 mix of CFTR antibodies 217 and 596. Quenched reactions were incubated at 4°C for 3 hr, washed, and resuspended in 2X SDS Sample Buffer before incubation at 37°C for 10 min. Samples were then stored at -20°C. Once thawed, they were again incubated at 37°C for 10 min and then resolved on duplicate sets of 5% polyacrylamide/SDS gels by SDS-PAGE. One set was fixed, dried, placed on a blanked phosphorimaging screen, and imaged using an Amersham™ Typhoon™ phosphorimager as described (see section 2.2.15 above). The other set was transferred to nitrocellulose, blocked, probed with 1:5000 rabbit anti-CFTR (D6W6L), followed by 1:5000 goat anti-rabbit-HRP, developed with chemiluminescent substrate, and imaged as described (see sections 2.2.11 and 2.2.15).

2.2.17 Image and Statistical Analysis

All western blots and radiographs were collected as unsaturated grayscale images and quantified as either 8-bit or 16-bit TIFFs, respectively. All blot and radiograph densitometry was performed in ImageJ (NIH). Raw integrated densities were exported to Microsoft Excel for basic quantification. For further statistical analysis, Student's two-tailed T-tests were performed with Minitab 19 Statistical Software. Unless otherwise noted, a 0.05 confidence interval was used to evaluate significant differences between samples. Separately conducted *in vitro* ubiquitination assays were treated as independent biological replicates.

2.3 RESULTS

2.3.1 Development of a CHIP *in Vitro* Ubiquitination Assay Using Purified Components

To begin examining the activity of E3 ubiquitin ligases involved in CFTR PQC, I initially adopted and modified a CHIP *in vitro* ubiquitination assay (Zhang et al., 2015). To this end, I obtained bacterial expression vectors to express and enrich His-tagged E1 (His-Ube1), ubiquitin activating enzymes, and an E3 ubiquitin ligase (His-CHIP) to use for *in vitro* assays (Figure 5, Figure 6A-C). While His-CHIP was purified to a high purity, His-Ube1 was degradation-prone during lysis and subsequent purification by Ni-NTA (Figure 6A), resulting in a product that was only ~15% intact. Nevertheless, the protein was viable for this assay since it derived from *E. coli*, which lacks contaminants that support or interfere with crude ubiquitination assays (Rosenbaum et al., 2011). Additionally, I obtained vectors for and purified two distinct GST-tagged *in vitro* CHIP substrates, GST-Hsc70$_{395-646}$ (Figure 7A, 7C) and GST-AT3 JD (Figure 7B, 7D). While the former contains the substrate binding domain of Hsc70 and thus reflects a "canonical" CHIP substrate (Zhang et al., 2015), the latter contains the Josephin domain of ataxin-3, a "non-canonical" substrate of CHIP which binds independently of Hsp70 and Hsc70 (Scaglione et al., 2011; Todi et al., 2009).

After reagent purification, I conducted CHIP *in vitro* ubiquitination with GST-Hsc70$_{395-646}$ by preparing reactions with enriched His-Ube1, UbcH5b (E2), ubiquitin, an ATP-containing reaction buffer, His-CHIP, and the GST-Hsc70$_{395-646}$ substrate (Figure 8A). First, I sought to verify that my purified His-Ube1 could activate ubiquitin for reactions as well as commercially

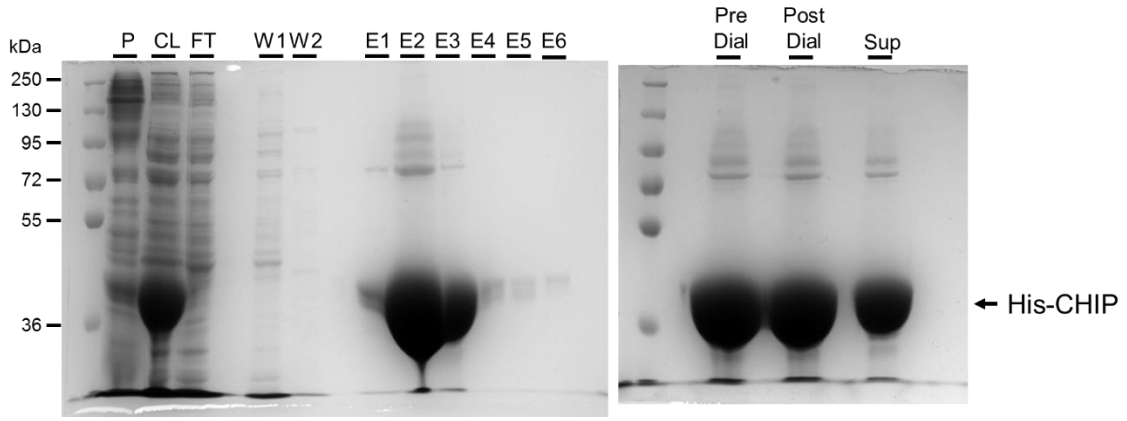

Figure 5. Enrichment of His-CHIP.

SDS-polyacrylamide gels were stained with Coomassie Brilliant Blue to depict distinct steps during the purification of His-CHIP. This included Ni-NTA affinity chromatography (left), followed by subsequent dialysis (right). P: lysed cell pellet; CL: cleared cellular lysate; FT: initial flow-through; W1: 10 mM imidazole wash; W2: 30 mM imidazole wash; E1-E6: 200 mM imidazole elutions; Pre Dial: pre-dialysis; Post-Dial: post-dialysis. During dialysis, His-CHIP partially precipitated. Centrifuging the insoluble protein yielded a final supernatant (Sup) used in *in vitro* ubiquitination assays.

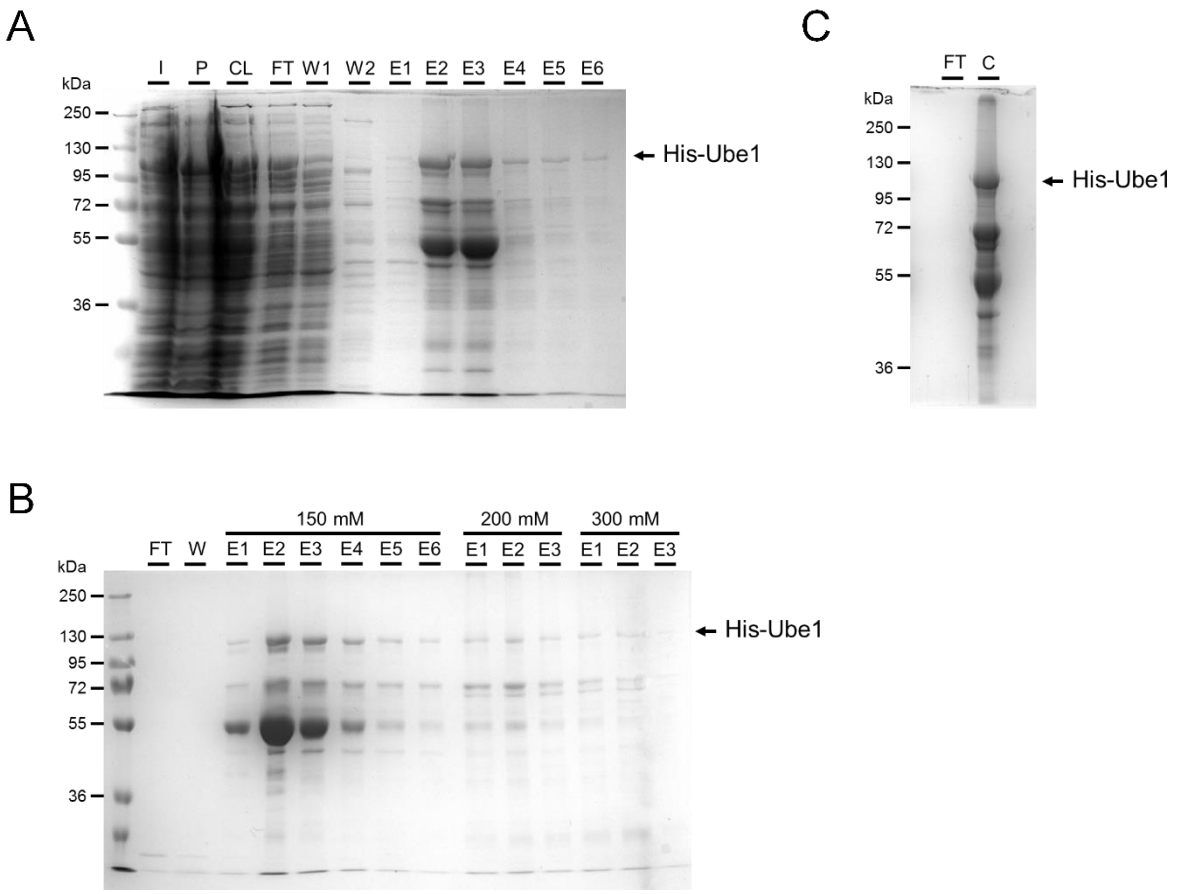

Figure 6. Enrichment of His-Ube1.

(A) SDS-polyacrylamide gels were stained with Coomassie Brilliant Blue to depict the isolation of His-Ube1. His-Ube1 was purified as His-CHIP, but with the addition of protease inhibitors in all wash and elution buffers. Nevertheless, His-Ube1 is rapidly degraded during purification. I: cell pellet prior to lysis; all other abbreviations are as defined in Figure 5. **(B)** Coomassie gel depicting enrichment of His-Ube1 by DEAE. FT: flow-through of pooled fractions from Ni-NTA purification; W: 50 mM NaCl wash; 150 mM E1-E6: 150 mM NaCl elutions; 200 mM E1-E3: 200 mM NaCl elutions; 300 mM E1-E3: 300 mM NaCl elutions. After elution, 150 mM fractions E4-E6, 200 mM fractions, and 300 mM fractions were pooled. The migration of His-Ube1 is depicted. **(C)** A Coomassie-stained SDS-polyacrylamide gel depicting the final fraction of concentrated (C) His-Ube1. FT: concentration column flow-through.

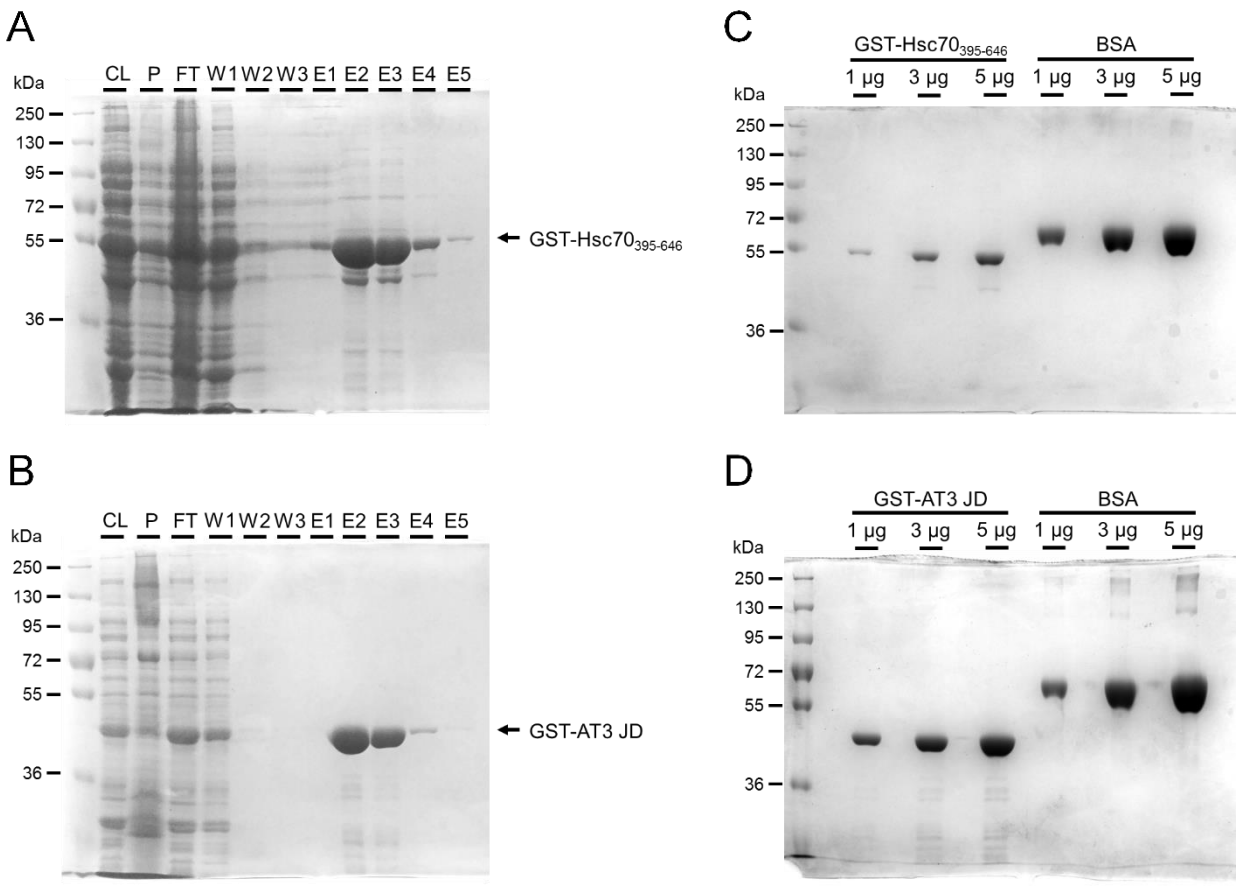

Figure 7. Enrichment of CHIP-dependent ubiquitination substrates.

(A) SDS-polyacrylamide gels were stained with Coomassie Brilliant Blue to depict the isolation of GST-Hsc70$_{395-646}$ from glutathione-agarose resin. CL: cleared cellular lysate; P: lysed cell pellet; FT: initial flow-through; W1-W3: washes; E1-E5: elution with reduced glutathione. Elution fractions E2 and E3 were subsequently pooled and dialyzed. **(B)** SDS-polyacrylamide gels were stained with Coomassie Brilliant Blue to depict the isolation of GST-AT3 JD by glutathione-agarose resin as described in (A). **(C)** After dialysis and quantification, purified GST-Hsc70$_{395-646}$ was resolved by SDS-PAGE alongside a standard curve of known BSA quantities to verify protein concentration. **(D)** As in (C), but with GST-AT3 JD.

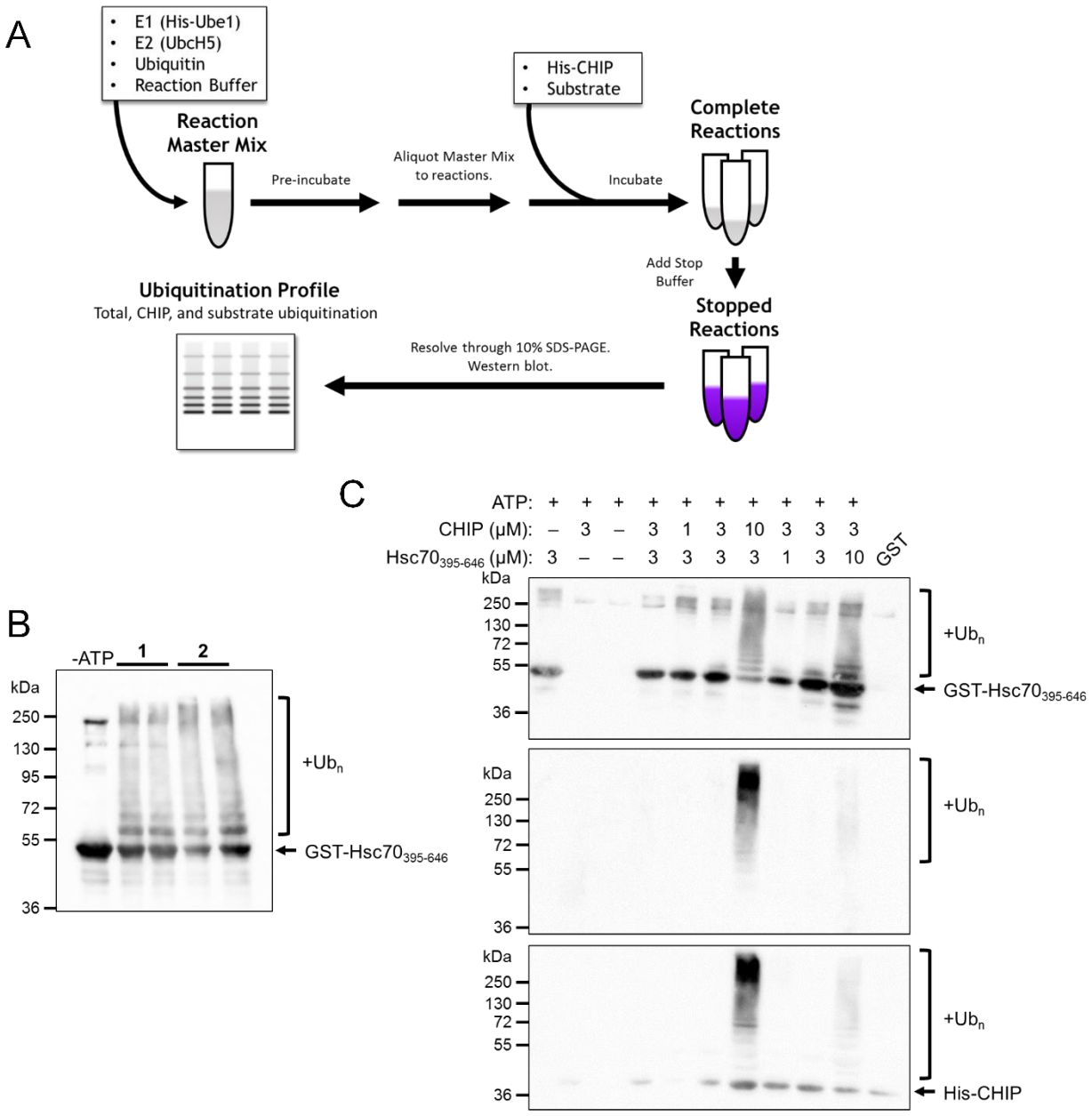

Figure 8. CHIP-dependent ubiquitination of a model substrate in a reconstituted system.

(A) Schematic depicting the procedure used for CHIP-dependent *in vitro* ubiquitination assays. **(B)** Anti-GST western blot indicating *in vitro* ubiquitination by CHIP of GST-Hsc70$_{395-646}$ in reactions containing either commercially purchased Ube1 (1) or partially purified His-Ube1 (2). Two technical replicates are shown for each. –ATP: reaction without ATP. **(C)** Anti-GST (top), anti-ubiquitin (middle), and anti-His (bottom) western blots depicting the products of *in vitro* ubiquitination reactions conducted with purified components. Reactions contained either 0, 1, 3, or 10 μM His-CHIP and the GST-Hsc70$_{395-646}$ substrate, in either the presence or absence of added

ATP. Reactions containing 10 μM His-CHIP and 3 μM GST-Hsc70$_{395-646}$ were most active, producing high molecular weight ubiquitinated species observable by both anti-GST and anti-ubiquitin western blots. A western blot for 6xHis revealed that the majority of the high molecular weight species represented CHIP autoubiquitination. Reaction labeled "GST" indicates a reaction identical to that shown in lane 4, but in which GST-Hsc70$_{395-646}$ was replaced by GST.

purchased Ube1. Fortunately, while reactions without ATP failed to ubiquitinate GST-Hsc70$_{395-646}$, reactions with ATP and either commercially sourced Ube1 or partially purified His-Ube1 ubiquitinated substrates equally well (Figure 8B). I next sought to optimize the levels of His-CHIP and the GST-Hsc70$_{395-646}$ substrate for robust ubiquitination efficiency (Figure 8C). As anticipated, substrate ubiquitination required ATP, His-CHIP, and substrate. In addition, reactions containing 10 μM CHIP and 3 μM substrate produced both the greatest degree of substrate ubiquitination (observed by anti-GST western blotting) and total ubiquitination (observed by anti-ubiquitin western blotting). Interestingly, western blotting for CHIP revealed that the vast majority of polyubiquitinated species produced under these conditions are high molecular weight autoubiquitinated CHIP species. Later experiments indicated that ubiquitination occurred optimally after 30 min, with the majority of ubiquitin conjugates appearing within 15 min (data not shown). I subsequently used these conditions to query CHIP activity by 1) seeking to validate an *in silico* model for its unique mode of activation, 2) seeking to identify novel inhibitors of its activity, and 3) seeking to determine if CHIP could function with unnatural ubiquitin variants as well as it does with wild-type ubiquitin. Each of these projects is described in Appendices A-D.

2.3.2 CHIP Enhances CFTR Ubiquitination in a Cell-Free Assay

To measure the magnitude of CHIP-dependent ubiquitination of CFTR, I designed a second *in vitro* ubiquitination assay which utilized membranes prepared from cells expressing CFTR. Using a protocol similar to those described previously in which yeast lysate is combined with either yeast (Nakatsukasa and Brodsky, 2010) or human (Nakasone et al., 2017) ER-derived microsomes, I combined microsomes prepared from HEK293 cells transiently expressing F508del CFTR with the purified enzymes required for substrate ubiqutination (see Figures 7-8), an ATP regenerating system, and I-125 radiolabeled ubiquitin (Figure 9A). As observed in control reactions containing yeast cytosol (Nakasone et al., 2017), reactions with purified E1 and E2 enzymes efficiently ubiquitinated F508del CFTR (Figure 9B). Of note, addition of purified CHIP was unnecessary to support F508del CFTR ubiquitination, most likely because of the presence of endogenous ubiquitin ligases in or on microsomal membranes (see section 1.2.2) (Estabrooks and Brodsky, 2020). However, addition of His-CHIP enhanced F508del CFTR ubiquitination two-fold (2.00±0.03; n=2) relative to reactions lacking added CHIP (compare lanes 4 and 5). In contrast, addition of an inactive CHIP mutant, $CHIP_{1-297}$ (Ye et al., 2017), failed to enhance ubiquitination (compare lanes 4 and 6). Other reactions testing reduced combinations of components revealed that only the addition of UbcH5b was necessary to support F508del CFTR ubiquitination, indicating that E2 ubiquitin conjugating enzymes are limiting on the surface of the HEK293 cell-derived microsomes (compare lanes 4 and 9). This result further implies that microsomes contain endogenous Ube1 on their surface, since the addition of the E1 was unnecessary. Other cytosolic PQC factors almost certainly adhere to the microsome membrane as well. Finally, a ubiquitination time course with reactions containing F508del CFTR microsomes indicated that ubiquitinated CFTR accumulates at a linear rate (Figure 9C). CHIP

further increased the rate of CFTR ubiquitination by approximately two-fold when added to the reaction, consistent with the data shown in Figure 9B. As the difference in signal between reactions with CHIP and reactions without CHIP was evident after a 45 min incubation time, I conducted all subsequent microsomal *in vitro* ubiquitination assays for this duration, except where otherwise noted.

After determining that F508del CFTR ubiquitination could be recapitulated *in vitro*, I next sought to establish which human cultured cells would synthesize the greatest amount of CFTR and thus maximize the signal for ubiquitinated CFTR. I therefore compared F508del CFTR levels between transiently transfected HEK293 and HeLa cells, and CFBE cells, which endogenously express the protein. The level of expression in HEK293 cells was remarkably greater than that observed in either HeLa or CFBE cells (Figure 10A). Consistent with this result, *in vitro* ubiquitination of F508del CFTR was substantially greater with microsomes prepared from HEK293 cells than with either other cell type (Figure 10B). I therefore prepared microsomes from HEK293 cells transiently expressing CFTR in subsequent experiments.

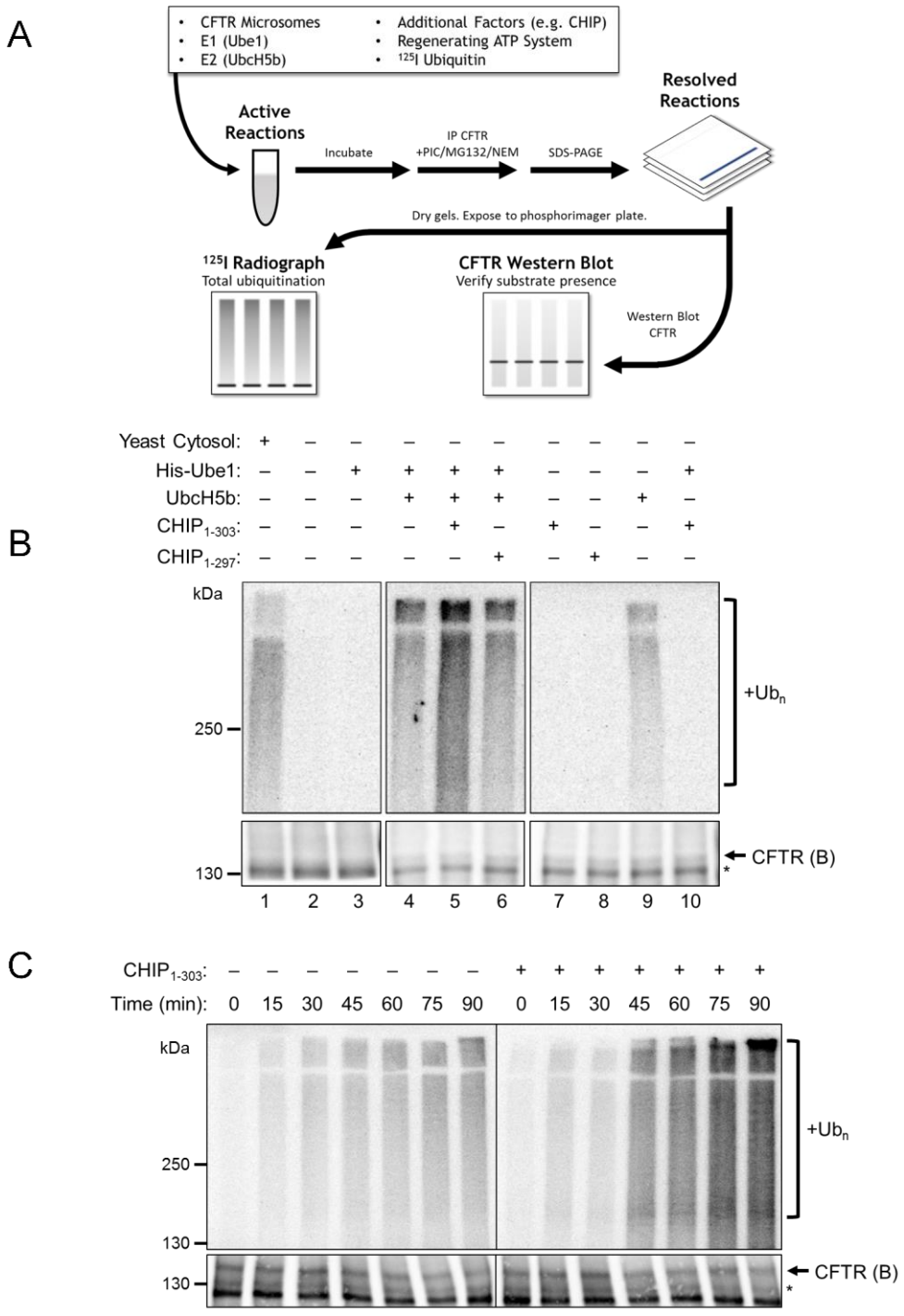

Figure 9. CHIP enhances the *in vitro* ubiquitination of F508del CFTR.

(A) Schematic depicting the procedure used to ubiquitinate microsomal CFTR *in vitro*. **(B)** I-125 radiograph (top) and anti-CFTR western blot (bottom) depicting *in vitro* ubiquitination of F508del-CFTR. Microsomes were prepared from transiently transfected HEK293 cells in culture and assayed with either yeast cytosol, or purified Ube1 (E1),

UbcH5b (E2), and/or CHIP (E3). Either full length CHIP ($CHIP_{1-303}$) or C-terminally truncated CHIP ($CHIP_{1-297}$) was added to reactions as indicated. "B" denotes immaturely glycosylated F508del CFTR. "*" denotes a non-specific antibody band observed by CFTR western blot. **(C)** I-125 radiograph (top) and anti-CFTR western blot (bottom) depicting a time course of *in vitro* ubiquitination with F508del CFTR HEK293 microsomes, and the E1 and E2 enzymes, conducted either in the absence or presence of full length His-CHIP.

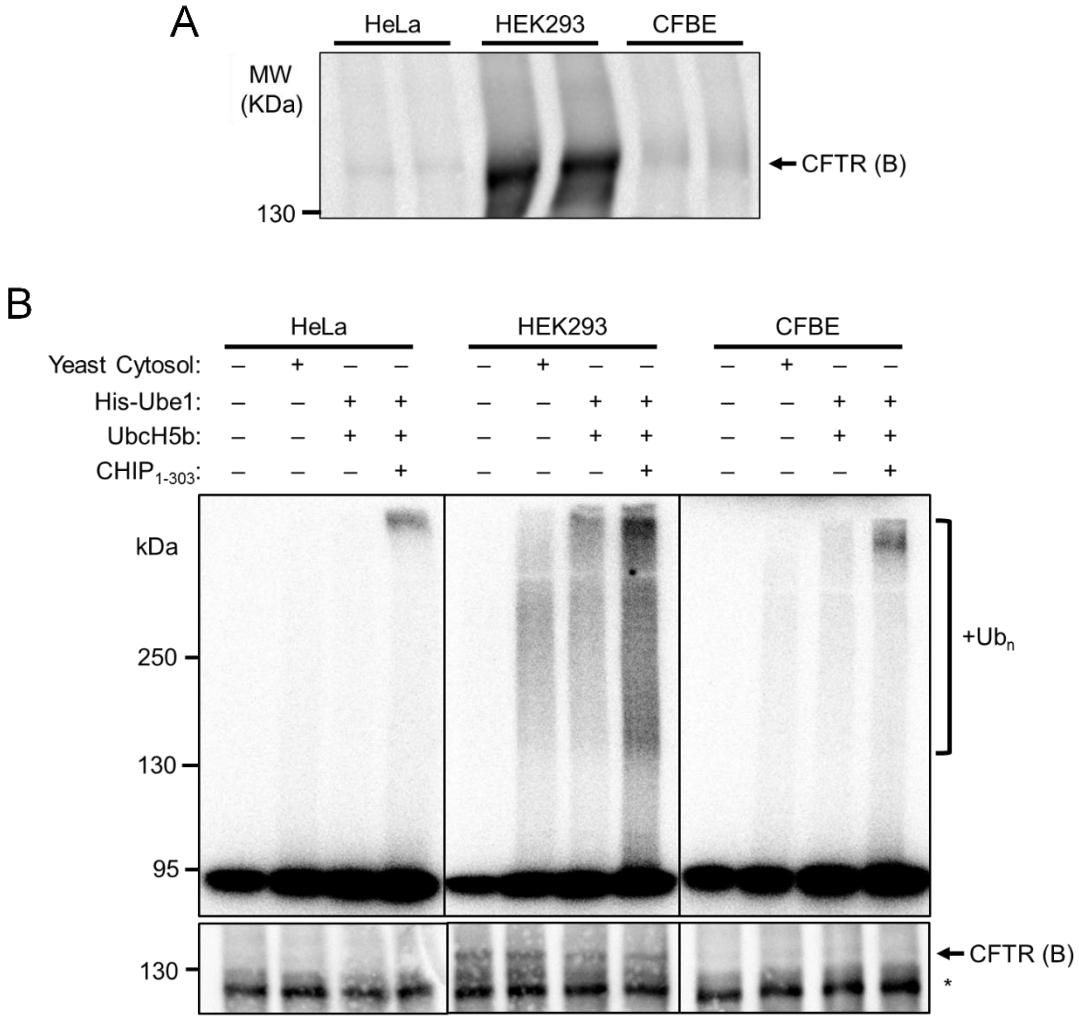

Figure 10. Microsomes from HEK293 cells contain the greatest levels of F508del CFTR for subsequent *in vitro* ubiquitination assays.

(A) Anti-CFTR western blot depicting cell lysates from HeLa, HEK293, and CFBE cell cultures. HeLa and HEK293 cells were transiently transfected with pCDNA3.1 F508del CFTR. CFBE cells endogenously express F508del

CFTR. Protein lysates were quantified by BSA protein concentration assay and equal amounts of total protein were resolved. Two independent replicates are shown for each cell type. **(B)** I-125 radiograph (top) and anti-CFTR western blot (bottom) depicting the *in vitro* ubiquitination of F508del-CFTR-containing microsomes from the cell types shown in (A).

2.3.3 Disease-Causing CFTR Variants are Differentially Ubiquitinated by E3 Ubiquitin Ligases *in Vitro*

I next endeavored to use this assay to compare ubiquitination profiles between different CFTR variants. While ~70% of CF patients encode at least one copy of F508del CFTR, over 300 annotated variants are known to cause cystic fibrosis (https://cftr2.org). These variants sort into five non-mutually exclusive classes, a significant portion of which are categorized at least in part as class II mutations, characterized by impaired folding and maturation from the ER (Veit et al., 2016; Welsh and Smith, 1993). As a result of these mutations, the pool of functional CFTR is lost due to ER retention and subsequent degradation. While the disease-causing mutation in F508del CFTR resides within NBD1, several disease-causing variants display similar processing defects because of mutations in other domains of the channel, such as MSD1 and NBD2 (Van Goor et al., 2014). Mutations in these other domains could cause distinct misfolded conformations, which may be detected and ubiquitinated by a different group or subgroup of PQC factors. To test this hypothesis, I selected a subset of disease-causing CFTR variants which are prone to misfolding for further study (Table 3). These variants include three variants with mutations in MSD1 (P67L, G85E, and E92K), and two variants with mutations in NBD2 (W1282X and N1303K). Wild-type and F508del CFTR were included for a comparison. These variants also differ widely in their ability to be corrected by small molecules. While P67L CFTR

Variant	% of Patients (U.S.)	CFTR2 Allele		Mutant Domain	Disease Severity	Pharmacological Correctability
		Occurrences	Frequency			
WT	—	—	—	—	None	—
F508del	86.4	99061	0.69744	NBD1	Severe	Moderate
N1303K	2.4	2246	0.01581	NBD2	Severe	Moderate
W1282X	2.3	1726	0.01215	NBD2	Severe	Moderate
G85E	0.6	616	0.00434	MSD1	Severe	Low
E92K	<0.5	49	0.00027	MSD1	Severe	Moderate
P67L	<0.5	239	0.00168	MSD1	Mild	High

Table 3. Select CFTR variants representing a range of CF phenotypes and mutant domains.

CFTR variant information from The Clinical and Functional Translation of CFTR (CFTR2); available at https://cftr2.org. ©Copyright 2011 Cystic Fibrosis Foundation, Johns Hopkins University, The Hospital for Sick Children.

causes a relatively mild form of disease and is easily correctable (Gilfillan et al., 1998; Sabusap et al., 2016), G85E is intractable to correction by either hypothermic incubation or corrector compounds (Lopes-Pacheco et al., 2017), despite the remarkably close residence of these mutations in the protein's linear sequence. I estimate that approximately three-quarters of patients globally encode at least one of the disease-causing variants examined in this analysis.

To begin to compare these variants, I first sought to test if differences would emerge between a narrower subset of variants. To this end, I prepared microsomes from HEK293 cells either lacking CFTR or transiently expressing wild-type CFTR, F508del CFTR, and N1303K CFTR and conducted *in vitro* ubiquitination reactions as described above. I first found that F508del CFTR was ubiquitinated to a greater degree than wild-type CFTR, despite being expressed at a lower level (Figure 11A). Based on quantification of the relative amount of ubiquitination when taking into account the amount of protein precipitated, I found that in

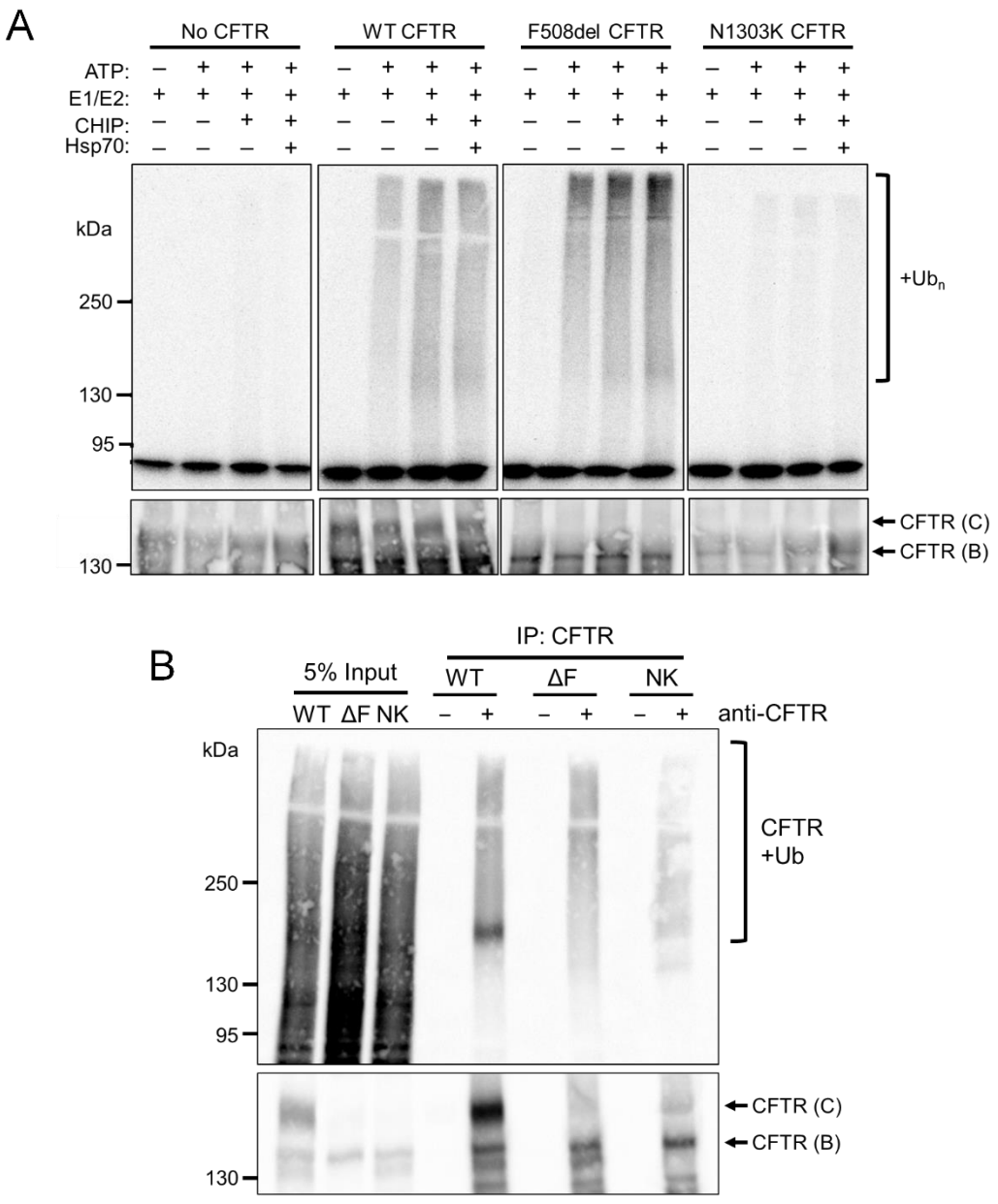

Figure 11. CHIP enhances F508del CFTR ubiquitination to a greater extent than wild-type CFTR.

(A) Representative I-125 radiograph (top) and anti-CFTR western blot (bottom) comparing ubiquitination of wild-type (WT) CFTR, F508del CFTR, and N1303K CFTR in microsomes prepared from HEK293 cells. Cells either lacked a transfected plasmid or were transfected with pcDNA3.1 WT CFTR, pcDNA3.1 F508del CFTR, or pBI-CMV2 N1303K CFTR prior to microsome preparation. Reactions contained ATP, His-Ube1 (E1), UbcH5b (E2), CHIP, and/or Hsp70 as indicated. While no ubiquitination was observed in reactions lacking CFTR, polyubiquitinated CFTR was observed in reactions with either WT or F508del CFTR. Addition of Hsp70 to

reactions with CHIP did not enhance ubiquitination further. In contrast, only trace ubiquitination of CFTR was observed in reactions with N1303K CFTR. **(B)** Anti-ubiquitin/anti-HA western blot (top) and anti-CFTR western blot of lysates from HEK293 cells transfected with WT, F508del CFTR (ΔF)-, or N1303K CFTR (NK)-expressing plasmids as in (A) prior to treatment with MG132 for 1 hr. Polyubiquitination of CFTR was observed in immunoprecipitations of each variant with anti-CFTR antibody, as indicated.

reactions containing Ube1, UbcH5b, and CHIP, F508del CFTR was ubiquitinated approximately two-fold more than the wild-type protein (1.84±0.13; n=2). These data indicate, as anticipated, that the PQC machinery preferentially selects F508del CFTR over wild-type CFTR for degradation. Second, I found that only trace ubiquitination was detected in reactions monitoring N1303K CFTR ubiquitination. This result was unexpected, but might reflect the fact that this allele has been suggested to be targeted for degradation in a distinct manner compared to F508del CFTR (Liu et al., 2018b). As a control for this experiment, no ubiquitination was observed in reactions with microsomes lacking CFTR, and interestingly addition of purified Hsp70 to reactions failed to enhance ubiquitination, suggesting that there is an overabundance of Hsc70 and perhaps Hsp70 on the microsome surface. Indeed, subsequent western blotting of microsomal membranes with an antibody that detects both Hsp70 isoforms confirmed that HEK293 cell membranes contain abundant Hsp70 (data not shown).

To determine whether N1303K CFTR is also ubiquitinated poorly in cells, I next expressed wild-type, F508del CFTR, and N1303K CFTR in HEK293 cells, treated the cells with MG132 for 1 hr to inhibit the proteasome and accumulate any ubiquitinated CFTR, and immunoprecipitated CFTR from cell lysates. Contrary to my findings *in vitro*, each of the three variants were ubiquitinated (Figure 11B). Therefore, N1303K CFTR ubiquitination *in vitro* must be undetectable for another reason. One possibility is the very low level of expression which

might be below the threshold for efficient *in vitro* ubiquitination. Of note, in this experiment different expression vectors were used to transfect HEK293 cells prior to microsome preparation. While wild-type and F508del CFTR were expressed from pcDNA3.1, N1303K CFTR was expressed from pBI-CMV2. Due to the bidirectional nature of this plasmid's promotor, N1303K CFTR might be expressed more weakly, as pcDNA3.1 contains a unidirectional promotor.

To rectify differences in expression level, I next obtained a set of pcDNA5/FRT plasmids encoding each of the CFTR variants listed in Table 3 and prepared fresh HEK293 microsomes. When testing CFTR ubiquitination expressed from this vector, I observed ubiquitination profiles that were markedly different from those observed above. While formerly "smears" of ubiquitinated CFTR had appeared only at and above the expected molecular mass of CFTR (168 kDa), ubiquitinated species instead appeared at lower molecular masses (Figure 12A). Perhaps more disturbingly, similar degrees of ubiquitination were observed in reactions containing or lacking CFTR, a phenomenon that still required the addition of an ATP regenerating system. The identity of these low molecular weight ubiquitinated species was subsequently determined by conducting minimal *in vitro* ubiquitination assays which lacked microsomes: Only the addition of CHIP was necessary to generate these low molecular weight ubiquitinated species (Figure 12B). Thus, CHIP had become autoubiquitinated under these conditions, which is consistent with the native molecular mass of the enzyme (33 kDa) (Ballinger et al., 1999).

To remove CHIP or otherwise prevent it from appearing in CFTR radiographs, I tested the effects of: (1) preclearance with ProteinA Sepharose beads prior to CFTR immunoprecipitation, (2) blocking beads with milk/TBST prior to immunoprecipitation, (3) immunoprecipitation with ProteinG Sepharose beads instead of ProteinA Sepharose, and (4) washing beads containing immunoprecipitated CFTR with chaotropic salt (KI). No condition

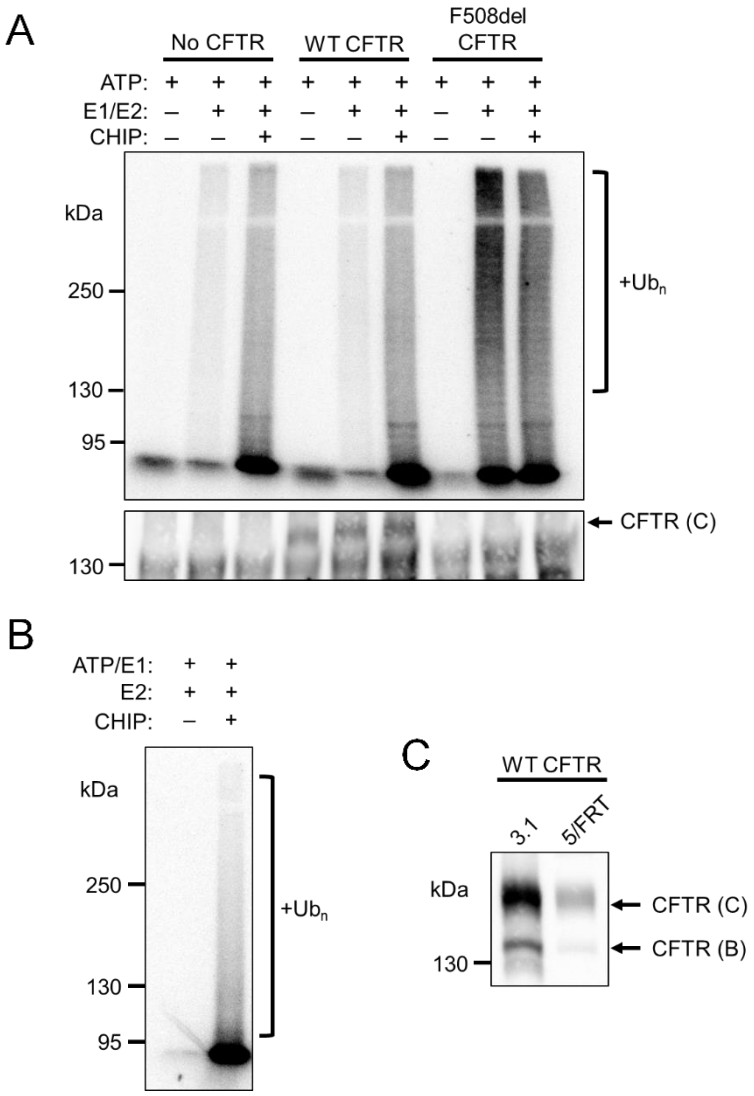

Figure 12. CHIP autoubiquitination obscures CFTR ubiquitination when the protein is expressed from pcDNA5/FRT.

(A) Representative I-125 radiograph (top) and anti-CFTR western blot (bottom) of reactions with CFTR-containing HEK293 cell microsomes from mock-transfected cells and those transfected with pcDNA5/FRT wild-type (WT) CFTR or pcDNA5/FRT F508del CFTR. Reactions contained His-Ube1 (E1), UbcH5b, ATP, and/or CHIP as indicated. For all reactions with ATP, including those without CFTR, I-125 polyubiquitination was observed. **(B)** I-125 radiograph of reactions performed as in (A), but in the complete absence of microsomes. While no ubiquitination was observed in reactions without added CHIP, a polyubiquitin smear was observed with CHIP. **(C)**

Anti-CFTR western blot comparing HEK293 cell lysates of cells transfected with either pCDNA3.1 WT CFTR or pCDNA5/FRT WT CFTR. Total protein concentrations of lysates were determined by the BCA protein concentration assay and equal amounts of total protein were resolved by SDS-PAGE.

could successfully remove autoubiquitinated CHIP (data not shown). When comparing reactions with microsomes prepared from cells transfected with pcDNA5/FRT CFTR versus those transfected with pcDNA3.1 CFTR, I therefore predicted that the expression level from pcDNA5/FRT might be lower, causing a population of autoubiquitinated CHIP species to appear that had previously gone unobserved. Indeed, directly comparing the expression of WT CFTR from each of these plasmids revealed that pcDNA5/FRT expresses CFTR at lower levels than pcDNA3.1, despite both plasmids sharing the same promotor sequence (Figure 12C). The basis for this effect is mysterious.

To restore microsomal CFTR levels to those previously observed, I therefore cloned the CFTR gene for each variant from pcDNA5/FRT and ligated these into a linearized pcDNA3.1 vector (Figures 13A-C). After confirming the identity of these new expression vectors and preparing new microsomes from HEK293 cells, I assayed CFTR ubiquitination *in vitro* either in the presence or absence of added CHIP. First, consistent with my previous findings (Figure 11A), F508del CFTR was ubiquitinated two-fold or even higher than wild-type CFTR (2.42±0.07; N=6) (Figure 14A,B). These data confirm that the *in vitro* assay faithfully recapitulates a cellular PQC check-point. Second, the other variants were ubiquitinated to very different degrees, even when CHIP was added. In this experiment, N1303K was now ubiquitinated in a similar manner as the wild-type protein. A model to explain this result is provided in the discussion below (see section 2.4). Third, even though the variants exhibit different degrees of misfolding and ER retention (Table 3) (Haggie et al., 2016; Lopes-Pacheco

et al., 2017; Rapino et al., 2015; Sabusap et al., 2016), CHIP modestly enhanced ubiquitination of each variant (Figure 14C). Importantly, CHIP-dependent enhancement of ubiquitination required binding to Hsc70 or Hsp70, as addition of a CHIP mutant lacking its N-terminal TPR domain ($CHIP_{134-303}$), which is required for Hsp70/Hsc70 binding (Ballinger et al., 1999), failed to enhance CFTR ubiquitination (Figure 14D).

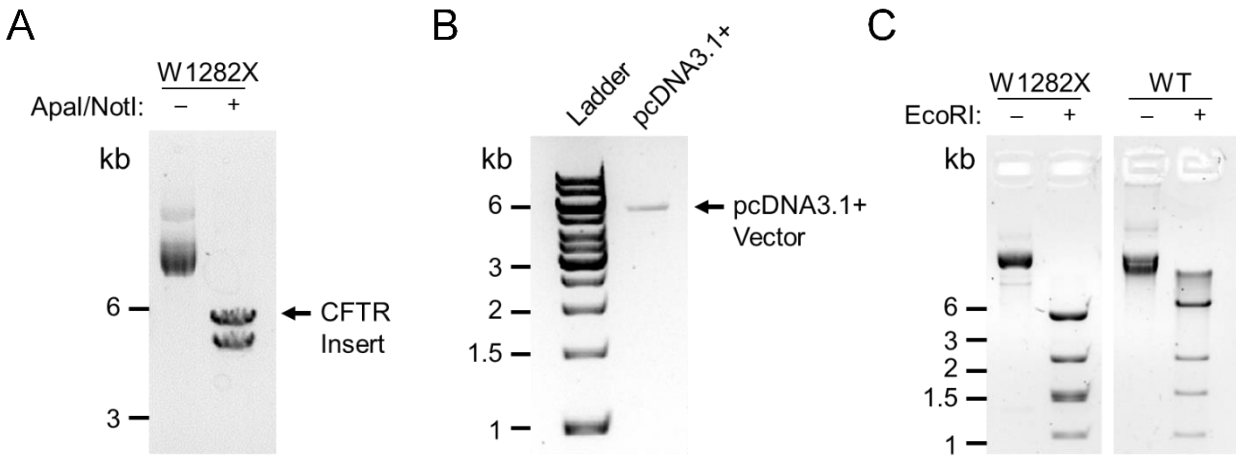

Figure 13. Cloning of CFTR variants for expression from pcDNA3.1.

(A) Ethidium bromide stain of pcDNA5/FRT W1282X CFTR with or without digestion by ApaI and NotI. After digestion, the CFTR gene inserts were gel purified. Digestion of W1282X CFTR is representative for digestion of all variants. **(B)** Ethidium bromide stain of pcDNA3.1+ after digestion with ApaI and NotI. The linearized vector was subsequently gel purified. **(C)** Ethidium bromide stain of EcoRI digested pcDNA3.1 W1282X CFTR after ligating the inserts and vectors, *E. coli* transformation, and purification of the ligated plasmids. The digestion profile of pcDNA3.1 W1282X CFTR is representative of all variants ligated into linear pcDNA3.1, and matches that of control pcDNA3.1 wild-type (WT) CFTR plasmid. Ligated plasmids matching the WT profile were subsequently verified by Sanger sequencing.

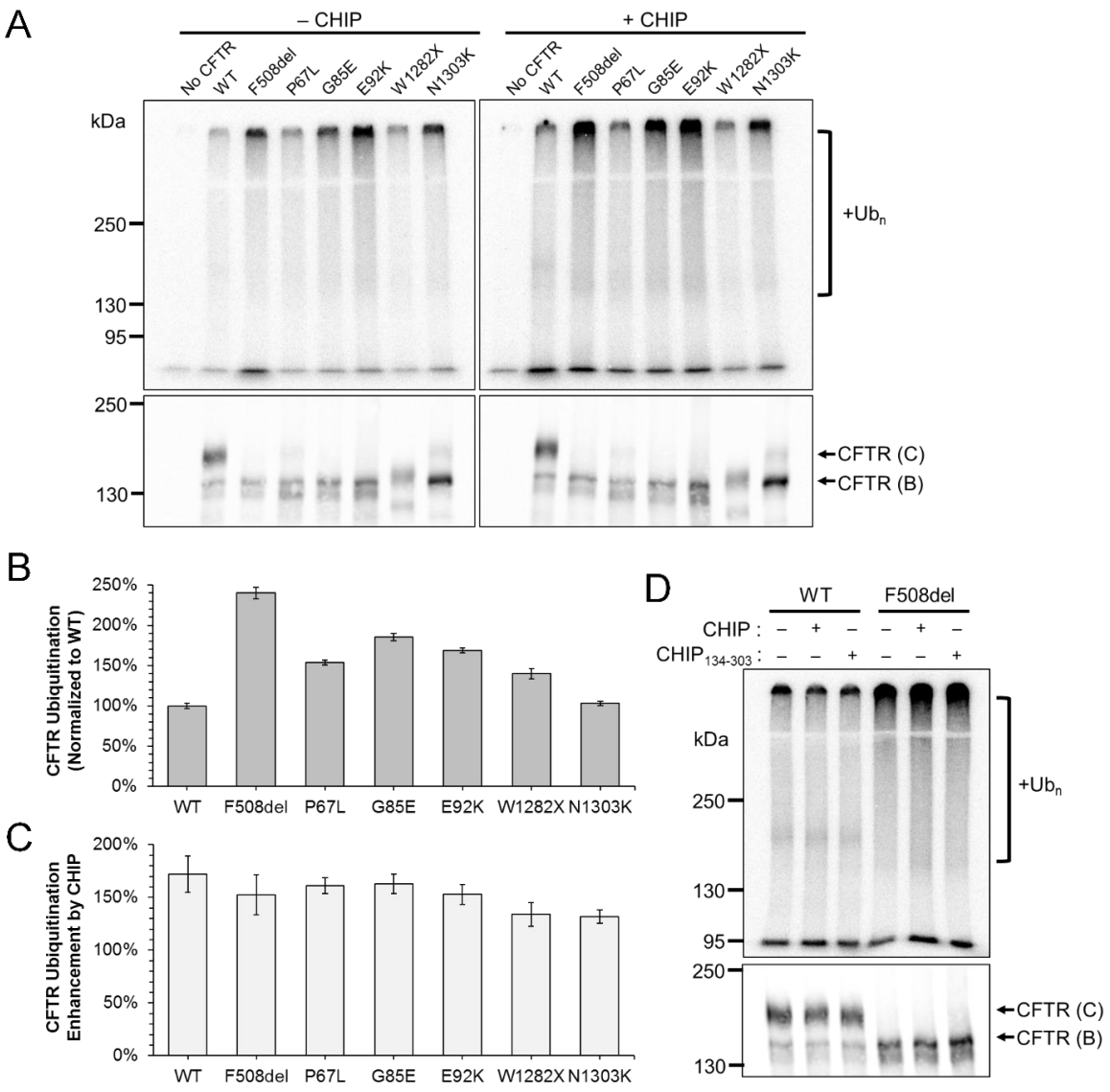

Figure 14. CHIP modestly enhances the ubiquitination of CFTR variants *in vitro*.

(A) Representative I-125 radiograph (top) and anti-CFTR western blot (bottom) of reactions with CFTR-containing microsomes from HEK293 cells. The variants were expressed from pCDNA3.1 prior to microsome isolation. All reactions contained His-Ube1 (E1), UbcH5b (E2), and ATP. Where indicated, reactions additionally contained His-CHIP. **(B)** Quantification of all reactions performed as in (A), indicating average ubiquitination adjusted for relative CFTR expression levels, which were normalized to wild-type (WT) CFTR. N=6; error bars depict standard errors of the mean. **(C)** Quantification of all reactions performed as in (A), indicating the average fold enhancement of CFTR ubiquitination between reactions containing the designated variant with CHIP compared to reactions without added

CHIP. N=6; error bars depict standard errors of the mean. **(D)** Representative I-125 radiograph (top) and anti-CFTR western blot (bottom) of reactions containing either wild-type or F508del CFTR, His-Ube1, UbcH5b, ATP, and either CHIP or TPR-less CHIP ($CHIP_{134-303}$) as indicated. While full length CHIP enhanced ubiquitination of both CFTR variants, reactions lacking CHIP were indistinguishable from reactions with TPR-less CHIP.

Given the relatively limited effect of CHIP on the ubiquitination of the CFTR variants, I hypothesized that by knocking down expression of endogenous CHIP prior to microsome preparation, I would be able to augment the effect of additional purified CHIP. I therefore treated HEK293 cells with CHIP siRNA, successfully knocking down CHIP by approximately 85% (Figure 15A). To my surprise however, microsomes prepared from these cells resisted the effect of additional CHIP, as reactions with and without added CHIP ubiquitinated the CFTR variants indistinguishably (Figure 15B). Possibly, the loss of CHIP results in remodeling of PQC pathways in cells, causing an upregulation in other factors—most notably other E3 ubiquitin ligases—that support CFTR ubiquitination.

To further assess the limited enhancement of purified CHIP upon CFTR ubiquitination, I sought to assess CHIP-supported ubiquitination independent of the contribution of other E3 ubiquitin ligases upon CFTR. To do so, I assayed enriched, solubilized wild-type CFTR (Hildebrandt et al., 2015) in place of microsomal CFTR. As anticipated, CHIP ubiquitinated wild-type CFTR in the presence of ATP, though this effect was partially abrogated when purified Hsp70 was added (Figures 16A,B; compare lanes 2 and 4). That CHIP ubiquitinated wild-type CFTR at all without purified Hsp70 (lane 2) suggests that the chaperone may co-purify with CFTR, or that CHIP has an inherent affinity for solubilized CFTR, which might be partially unfolded. Notably, CHIP has been suggested to exhibit endogenous chaperone-like activity (Kopp et al., 2017). Curiously, reactions without ATP also supported CHIP-dependent CFTR by

CHIP (lane 5). However, the CFTR sample assayed had been purified in a buffer containing ATP, which in future studies will need to be removed. Although preliminary, these data indicate that *in vitro* ubiquitination of CFTR primarily produces ubiquitinated species that fall between 150 and 250 kDa in size. Therefore, ubiquitinated species greater than 250 kDa produced during microsomal *in vitro* ubiquitination likely result at least in part from the activity of other E3 ubiquitin ligases.

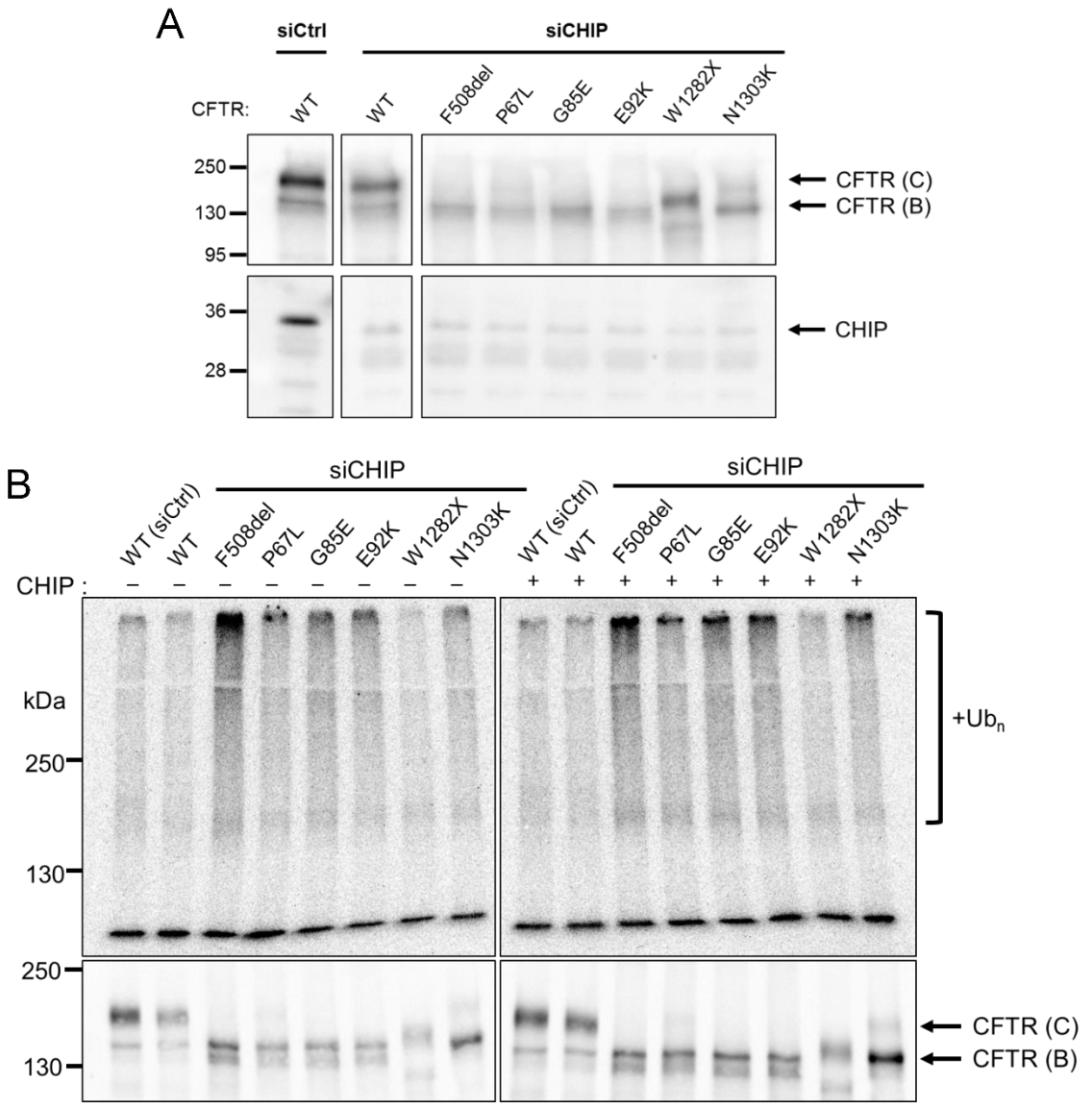

Figure 15. CHIP knockdown is unable to enhance the effect of added CHIP in *in vitro* ubiquitination reactions

(A) Anti-CFTR and anti-CHIP western blots of microsomes from HEK293 cells treated with either control siRNA (wild-type CFTR only) or siRNAs targeting CHIP transcripts. CHIP was knocked down ~85% in cells treated with CHIP siRNA. All western blots of each set were exposed concurrently. **(B)** Representative I-125 radiographs (top) and anti-CFTR western blots (bottom) depicting ubiquitination of CFTR variants in microsomes prepared from cells treated with either control or CHIP siRNA in (A). Between three experimental replicates, CFTR ubiquitination was not enhanced in reactions with added CHIP (right) compared to those without added CHIP (left).

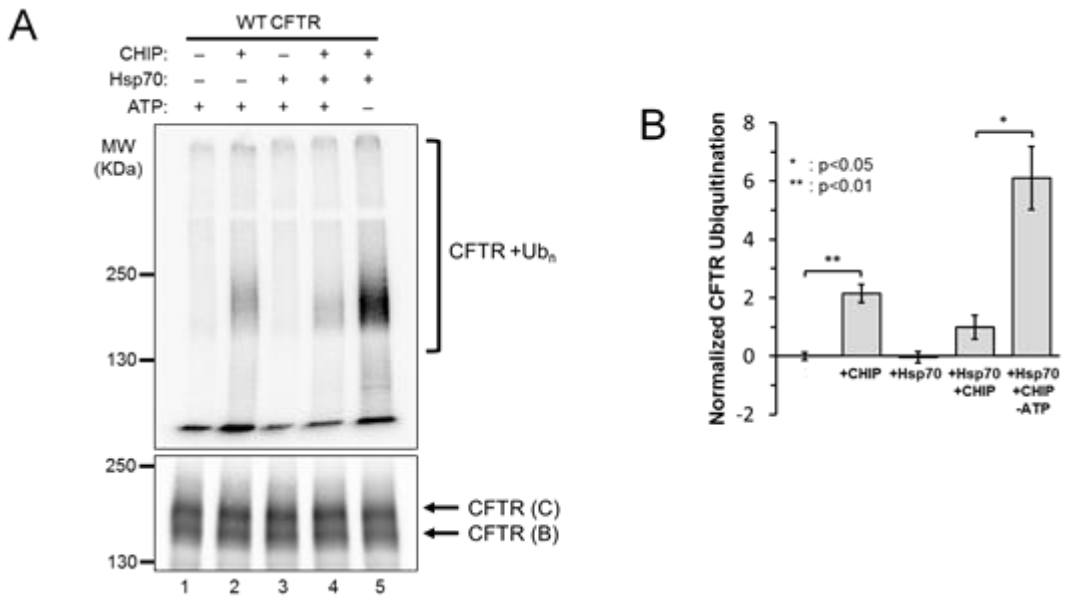

Figure 16. CHIP ubiquitinates enriched solubilized wild-type CFTR *in vitro*.

(A) I-125 radiograph (top) and anti-CFTR western blot (bottom) depicting *in vitro* ubiquitination of wild-type (WT) CFTR that was highly enriched from a stably expressing HEK293 cell line. **(B)** Quantification of reactions depicted in (A). n=3; error bars indicate standard error of the mean.

2.4 DISCUSSION

While there are abundant methods available to identify and study the contribution that E3 ubiquitin ligases make upon the turnover of substrates in the secretory pathway in cells, *in vitro* approaches are uniquely positioned to dissect the involvement of individual enzymes on these processes. Here I have presented two distinct *in vitro* ubiquitination assays for the study of ubiquitin ligases relevant to the degradation of CFTR by the ERAD pathway. For the first assay, I purified CHIP in conjunction with model substrates and other enzymes in order to scrutinize the activity of this ubiquitin ligase in a minimal system under a variety of conditions. For the second, I developed an *in vitro* ubiquitination assay utilizing radiolabeled ubiquitin and human ER-enriched microsomal membranes, adopting and optimizing this procedure from earlier yeast and human microsome-based assays that required yeast cytosol to support ubiquitination (Nakasone et al., 2017; Nakatsukasa and Brodsky, 2010). This assay represents an advancement over an earlier assay for CHIP-dependent CFTR ubiquitination, which utilized western blotting as a less sensitive means of detection and only recapitulated protein quality control events occurring at the cell periphery (Okiyoneda et al., 2010). After identifying an optimal cell line from which to source microsomal membranes and consequently optimizing the expression of CFTR in this cell line, I tested the degree to which a subset of distinct CF-causing CFTR variants are ubiquitinated by PQC factors *in vitro,* testing these variants in the presence and absence of added CHIP.

The data gathered using this assay indicate that disease-causing, class II CFTR variants differ in their susceptibility to E3 ubiquitin ligases. F508del CFTR was the most susceptible of

all variants tested, suggesting that this variant is perhaps the most catastrophically misfolded and thus especially predisposed to ubiquitination and degradation. This result is in-line with other studies examining a wide variety of CFTR2 alleles, which similarly suggested that F508del CFTR is one of the most poorly folded variants (Sosnay et al., 2013). In contrast, while a range of variants was tested along the lines of mutation position and pharmacological correction (Table 3), *in vitro* ubiquitination does not appear to correlate remarkably with either of these other characteristics. It is vital to note, however, that the number of variants tested in this study is relatively small. Nevertheless, it is notable that P67L, which is easily corrected (Sabusap et al., 2016), was ubiquitinated to an intermediate degree when wild-type and F508del CFTR are considered. In fact, most variants were similarly ubiquitinated, including G85E and E92K CFTR. That these variants, which are more challenging to correct and cause severe CF, are ubiquitinated to a similar degree as P67L is surprising. Earlier studies however suggested that these variants, especially G85E, which adds an unfavorably charged glutamate to the first transmembrane span of CFTR, primarily reduce integration between transmembrane spans and thus higher order TMDs (Patrick et al., 2011; Xiong et al., 1997). My findings therefore imply that all variants with disrupted transmembrane integration are ubiquitinated to a similar degree and while those with less obtrusive mutations (like P67L) are easily resolved by correctors, likely reducing ubiquitination, others with highly disruptive substitutions are more difficult to correct and remain aggressively ubiquitinated. Also curious, N1303K CFTR was ubiquitinated to the same degree as the wild-type protein. This could occur however due to the increased dependence upon autophagy, rather than ERAD, for the turnover of this variant (Liu et al., 2018b). Testing of a larger subset of class II variants will be necessary before broadly generalizable relationships emerge concerning *in vitro* ubiquitination and other variant characteristics.

That purified CHIP enhanced ubiquitination of all assayed variants to a similar degree is surprising (Figure 14C). Given that the ligase is thought to have the greatest activity upon fully translated CFTR—which is to say after translation of NBD2 (Younger et al., 2006)—one might expect that CFTR would be more extensively ubiquitinated due to mutations within this domain, yet W1282X CFTR, which bears a truncated NBD2, displayed a similar degree of enhanced ubiquitination with CHIP as F508del and other variants. This could occur if NBD1-NBD2 interactions for all tested variants are disrupted similarly to the way that this interaction is disrupted by F508del (Du and Lukacs, 2009; Hoelen et al., 2010; Sharma et al., 2001), regardless of the domain in which each mutation resides. While it is also true that wild-type CFTR displayed a similar enhancement in the presence of added CHIP, this might occur merely as a consequence of the diminished basal ubiquitination of wild-type CFTR by other E3 ubiquitin ligases, providing a greater opportunity for purified CHIP to polyubiquitinate it. Or rather, it might be true that complexes between CHIP and Hsc70 bind to and ubiquitinate CFTR irrespective of the strength of the NBD1-NBD2 interaction. Regardless, the overall modest effect of CHIP on the ubiquitination of all of the variants strongly suggests that the overwhelming majority of the ubiquitination signal observed *in vitro* occurs due to the activity of membrane-inserted, ER-localized E3 ubiquitin ligases that are also known to act upon CFTR: RMA1, RNF185, and gp78 (El Khouri et al., 2013; Morito et al., 2008; Younger et al., 2006). Additionally, the effect of exogenous CHIP on CFTR ubiquitination might have been muted due to the activity of other E3 ubiquitin ligases endogenously expressed by HEK293 cells as a consequence of their transformation, such as the adenoviral type 5 ubiquitin ligase E1B (Hung and Flint, 2017). To rule out this possibility, it would be valuable to contrast ubiquitination of CFTR by CHIP in HEK293 microsomes with those of another cell type.

Although *in vitro* ubiquitination of enriched, soluble wild-type CFTR produced confounding results concerning the role of Hsp70 in the assay (Figure 15), it is encouraging to note that purified CHIP successfully ubiquitinated this substrate, generating polyubiquitinated CFTR within a molecular weight range very similar to that observed with the microsome-based *in vitro* ubiquitination assays. If a subset of misfolding CFTR variants could be purified and assayed similarly, this approach would provide an especially straightforward way to test the susceptibility of these variants to CHIP, independent of the contributions otherwise made by other E3 ubiquitin ligases, as noted above.

In summary, these assays expand the set of tools available for the study of PQC in the secretory pathway, and most notably the early steps that lead to the selection of substrates for ERAD. The second of these two assays particularly provides the means to reconstitute active, physiologically relevant quality control pathways *in vitro* and to make precise measurements regarding the action of these pathways upon substrates of interest. More specifically, I've presented in this chapter how this assay captures early quality control events that occur with a set of disease-causing CFTR variants prior to their retrotranslocation and proteasomal degradation. In the future, this assay could be used to further explore the susceptibility of additional variants to ubiquitination machinery, to examine the role of additional PQC factors, to determine whether there are kinetic differences in the targeting of these variants for degradation, to recapitulate subsequent steps during ERAD (i.e., retrotranslocation and proteasome-mediated degradation), and perhaps even to determine if pharmacological correctors reduce the susceptibility of CFTR variants to ubiquitination. Moreover, this assay could also be used to similarly define the contribution of PQC factors in other protein conformational diseases that arise from misfolding in the ER.

3.0 FINAL DISCUSSION, CONCLUSIONS, AND FUTURE DIRECTIONS

In the following section I summarize how my research advances the study of CFTR PQC. I also elaborate upon the number of possible directions in which one could pursue this project, as there are still many pertinent questions about CFTR biogenesis that remain unanswered at this point, yet could be elucidated using the assays I have developed.

3.1 SIGNIFICANCE OF THIS STUDY

Previous studies of CFTR PQC have extensively utilized human tissue culture models to facilitate the identification of major quality control components that drive CFTR degradation. Several studies have recapitulated CFTR ubiquitination *in vitro* (Nakasone et al., 2017; Okiyoneda et al., 2010; Sato et al., 1998), though none had previously sought to specifically reconstitute ER PQC using a defined combination of enzymes required for the ubiquitination of a specific substrate. To this end, I established such an assay in order to compare ubiquitination between a set of disease-causing CFTR variants in a way that had never been tested previously. I also established a separate *in vitro* ubiquitination assay to more closely examine the activity of CHIP, an E3 ubiquitin ligase known to be involved in the ubiquitination and degradation of CFTR variants.

3.1.1 Major Conclusions

Class II CFTR variants contain mutations that impede the maturation of these channels beyond the ER (Veit et al., 2016). Variants belonging to this class purportedly misfold and are prematurely targeted for degradation by the ubiquitin proteasome system similar to the quintessential class II variant, F508del CFTR (Cheng et al., 1990; Qu et al., 1997; Ward et al., 1995). However, data directly comparing the susceptibility of each disease-causing variant to E3 ubiquitin ligases, key components of pro-degradative PQC machinery, remain surprisingly limited. Thus, I developed a pair of *in vitro* ubiquitination assays in order to better study the activity of these enzymes.

To conduct the first of these two assays, I over-expressed and enriched for human ubiquitination enzymes and model substrates required to reconstitute the activity of the cytosolic E3 ubiquitin ligase CHIP, which binds the Hsc70 molecular chaperones and contributes to ubiquitination of CFTR at both the ER and the cell periphery (Meacham et al., 2001; Okiyoneda et al., 2010; Younger et al., 2006; Younger et al., 2004). This minimal assay provided an ideal tool with which I could examine CHIP function. First, I used this assay to validate an *in silico* model for CHIP folding and activation, determining that the extreme C-terminus of CHIP is required for efficient enzymatic activation (see Appendix A) (Ye et al., 2017). I subsequently used the assay to verify the efficacy of putative CHIP inhibitors predicted by a novel drug discovery pipeline (see Appendix B) (Pabon et al., 2018). I separately shared this assay with collaborators to test if a post-translational modification would directly inhibit CHIP (see Appendix C) (Zaman et al., 2019). I then used this assay to investigate whether or not CHIP and upstream E1 and E2 enzymes could function with synthetically derived ubiquitin variants that contained unnatural properties. Indeed, CHIP *in vitro* ubiquitination provided a proof-of-

principle that some of these semi-synthetic peptides exhibited wild-type function (see Appendix D) (Werner et al., 2019).

To directly test the activity of E3 ubiquitin ligases upon misfolding, disease-causing CFTR variants in the second of my two assays, I prepared ER-enriched microsomes from HEK293 cell cultures transiently expressing variants of CFTR and combined the microsomes *in vitro* with isolated ubiquitination enzymes. After much optimization, I succeeded in developing an assay that reproducibly captured subtle differences in the degree to which a set of CFTR variants are ubiquitinated by endogenous E3 ubiquitin ligases. I concluded that F508del CFTR is ubiquitinated almost two and a half-fold greater than wild-type CFTR, while most other variants tested—P67L, G85E, E92K, W1282X, and N1303K—were ubiquitinated to intermediate degrees. Addition of CHIP to microsomal *in vitro* reactions enhanced ubiquitination of all variants to a similar, modest degree. In preliminary assays with enriched, solubilized wild-type CFTR, addition of CHIP stimulated ubiquitination to a similar degree as in the microsome-based assay, suggesting that the modest effect of CHIP on the ubiquitination of microsomal CFTR was not artifactual.

3.1.2 Limitations of this Study

While the *in vitro* ubiquitination assays I have described here offer new ways in which to examine the role of ubiquitination machinery in PQC, these assays have limitations and their results may rely on certain assumptions. In some cases the limitations of these assays may substantially affect the conclusions one can reasonably draw from the data.

First, regarding my CHIP *in vitro* ubiquitination assay (see section 2.3.1), it is essential to appreciate that while this assay can be used to tease apart the activity of CHIP under a wide

variety of conditions, it is designed to do so with only the minimum number of required components. While such a minimal design contributes greatly to the reproducibility and portability of this assay, by definition it also means that the assay fails to capture the true breadth of CHIP activity *in vivo*. Namely, CHIP rarely acts upon substrate proteins alone, but rather as part of broad, dynamic protein quality control complexes. Indeed, association of CHIP with chaperones, co-chaperones, either of two distinct E2 ubiquitin conjugating enzymes (UbcH5 and Ubc13-Uev1a), and deubiquitinating enzymes have all been shown to sharply modify its activity (Alberti et al., 2004; Demand et al., 2001; Murata et al., 2001; Narayan et al., 2015; Scaglione et al., 2011; Windheim et al., 2008; Younger et al., 2004; Zhang et al., 2005). These associations can either enhance or suppress activity of CHIP, adjust its substrate specificity, or change the type(s) of ubiquitin linkages that it appends to substrates.

Additionally, CHIP activity that is recapitulated by this assay could differ substantially from its endogenous activity as the model substrates I have used reflect only a narrow subset of its full substrate range. GST-Hsc70$_{395\text{-}646}$ and GST-AT-3 JD are both derived from endogenous substrates of CHIP, yet each of these substrates reflects a properly folded, cytosolic substrate. CHIP is intimately involved in the ubiquitination and turnover of active, properly folded molecular chaperones, such as Hsp/c70 (Kundrat and Regan, 2010; Qian et al., 2006), as well as the activation of AT-3 through chaperone-independent monoubiquitination (Scaglione et al., 2011). Alternate substrates, such as heat denatured luciferase, could perhaps be used to further model ubiquitination of misfolded CHIP substrates that require molecular chaperones for recognition (Murata et al., 2001). Even so, none of these substrates are likely to accurately recapitulate CHIP ubiquitination of membrane-inserted substrates, like CFTR. Thus, the study of substrates such as these is better suited to microsomal *in vitro* ubiquitination reactions.

Another limitation, especially when this assay is used to test the efficacy of putative CHIP inhibitors (see Appendices B-C) is that CHIP-dependent *in vitro* ubiquitination reactions rely on the addition of other enzymes, besides CHIP. Conceivably, an inhibitory compound could yield a false positive by interfering with the function of added E1 and/or E2 enzymes, rather than CHIP. Simply testing an alternate substrate would be insufficient to verify the specificity of such a compound, as these enzymes act upstream of CHIP. Therefore, when the assay is used in this way, it is imperative that additional experiments are used to corroborate any observed inhibitory effects. In the absence of compelling *in silico* data for the docking of these compounds to CHIP, one could assay if the compounds more robustly interfere with ubiquitination *in vitro* when pre-incubated with E1 and E2 enzymes than when pre-incubated with CHIP and substrate. Additionally, one could explore if an inhibitor of particular interest also interferes with ubiquitination of CHIP when combined with Ubc13-Uev1a and a client substrate instead of when it is combined with UbcH5. This assay would help determine if a compound specifically inhibits the activity of one of the two known E2/CHIP pairs (Windheim et al., 2008; Zhang et al., 2005).

With regard to the microsomal CFTR *in vitro* ubiquitination assay (see sections 2.3.2 and 2.3.3), one must be aware that this assay also has particular limitations, some of which affect how its results are interpreted. First and foremost, a key limitation of this assay is that CFTR-containing microsomes from HEK293 cell culture are "ER-enriched", which means that nuclei, a major contaminant of ER membranes, have been removed. In addition to ER membranes, these microsome preparations also likely contain membranes from the Golgi, endosomal network, and plasma membrane. Indeed, the presence of a maturely glycosylated species in my assays with select CFTR variants (Figures 14-15) confirms the presence of CFTR in post-ER membranes

(Chang et al., 1994; Cheng et al., 1990). The distribution of these CFTR variants between different organelles remains utterly unknown, as does the extent to which CFTR localized to these organelles is ubiquitinated *in vitro*. In principle, this could be addressed in part by first enriching for plasma membrane CFTR by performing a cycloheximide chase, such that any isolated CFTR would predominantly have exited the ER (Okiyoneda et al., 2010; Sharma et al., 2004) (also see section 3.2 below).

Furthermore, microsomal *in vitro* ubiquitination is limited because it is not comprised of defined components in the same way as the CHIP *in vitro* ubiquitination assay is. As noted previously (Figure 8), microsomal CFTR is readily ubiquitinated *in vitro* due to the plethora of endogenous PQC components present in and on microsomal membranes, including numerous molecular chaperones, co-chaperones, and E3 ubiquitin ligases that drive targeting of CFTR for ERAD (see section 1.2.2) (Estabrooks and Brodsky, 2020). As a result, it is difficult to disentangle the contribution made by any single quality control component from that of all the others. Determining the role that individual factors play in the ERAD of CFTR via this assay is only further exacerbated by the fact that microsome preparations do not exclusively contain ER-derived microsomes. As I have illustrated, knocking down an endogenous PQC component does not reliably accentuate the effect observed by adding the same purified component to reactions (Figure 15). In the case of CHIP, while knocking down other ER-localized E3 ubiquitin ligases (RMA1, RNF185, gp78) might clarify any selectivity that CHIP exhibits towards particular misfolded, disease-causing CFTR variants, this analysis would be surely confounded by a slew of compensatory cellular effects that would occur prior to microsome preparation, potentially shifting the interactomes for variants away from those that actually occur in cystic fibrosis patients.

In spite of these challenges, I have used this assay to detect differences in the susceptibility of a subset of disease-causing CFTR variants to ubiquitination by PQC factors (Figure 14A,B). While the aforementioned endogenous E3 ubiquitin ligases (in addition to endogenous CHIP) ubiquitinated each variant, producing copious high molecular weight ubiquitinated species (>250 kDa), the addition of purified CHIP only modestly enhanced ubiquitination of CFTR to relatively low molecular weight species (<200 kDa). Although it is tempting to conclude that the ubiquitin added by purified CHIP must be of limited functional consequence, this assay is not geared to determine the functional significance of polyubiquitin attached to CFTR, only to detect its relative presence; i.e., proteasome-dependent degradation has not been measured in this assay. As noted previously, ubiquitin chains are remarkably heterogeneous, with branched and mixed linkage chains being more common than once thought (Leto et al., 2019). While certain non-branching, monotypic linkages are canonically associated with particular proteolytic outcomes (Komander and Rape, 2012), the full scope of functions associated with various types of ubiquitin chains remains unknown.

3.2 FUTURE DIRECTIONS

As mentioned at the conclusion of section 2.4, there are ample possibilities for the ways in which these assays could be used further. I briefly describe potential future directions in the following section.

3.2.1 Short Term

First and foremost, the effect of ATP upon *in vitro* ubiquitination reactions with enriched, solubilized wild-type CFTR was perplexing yet repeatable (Figure 16A,B). In particular, it is unclear why reactions containing both an ATP regenerating system and soluble wild-type CFTR (which is stored in a buffer containing magnesium-ATP) would support substantially less ubiquitination than reactions without an ATP regenerating system (compare lanes 4 and 5). I will therefore repeat these assays, but first pretreat CFTR with apyrase to hydrolyze the ATP in the supplied buffer. Assuming depletion of ATP does not cause CFTR to become insoluble, I hypothesize that reactions lacking an ATP regenerating system will be inactive. Although reactions without additional purified Hsp70 are still likely to ubiquitinate CFTR due to the probable co-enrichment of the channel with the molecular chaperone (which could be confirmed by western blotting), these data would provide a convincing proof-of-principle that PQC of individual CFTR variants could be examined using a defined combination of E1, E2, and E3 enzymes in a similar manner as my CHIP *in vitro* ubiquitination assay with model substrates.

I hypothesized that misfolded, disease-causing CFTR variants would be ubiquitinated in my microsomal ubiquitination assay according to the degree to which they could be pharmacologically corrected and/or the mutated domain. However, no such relationship was observed among the seven variants I assayed. Assaying a broader set of variants might reveal a relationship between the extent of ubiquitination and an as-yet unknown property. More pressing perhaps is the need to assay a CFTR variant which causes disease, yet is not retained by ER PQC like the variants I have tested to date. I would therefore recommend preparing and assaying microsomes containing G551D CFTR. Given that this mutation only attenuates nucleotide binding of CFTR without impacting its assembly and maturation from the ER (Logan et al.,

1994; Qu et al., 1997), I would anticipate that *in vitro* it would be ubiquitinated to the same degree as wild-type CFTR, i.e. approximately two and a half-fold less than F508del. This result is essential in order to verify that the varying degrees of ubiquitination observed for tested variants so far is likely to be physiologically relevant.

In addition to the overall difference in ubiquitination observed for each variant, it is also possible that the kinetics of ubiquitin chain assembly differs between variants. Potentially, more catastrophically misfolded variants could be ubiquitinated at a faster rate than mildly misfolded variants. If this were true, then the most misfolded variants might be retrotranslocated and targeted to proteasomes more aggressively. To test this hypothesis I would conduct a time course with wild-type CFTR, F508del CFTR, and one variant that exhibits a more intermediate ubiquitination phenotype (e.g. E92K), and conduct assays over the timeframe I used previously (Figure 9C). Should F508del be ubiquitinated at the quickest rate, as I hypothesize, I would subsequently test the rate at which the remaining CFTR variants within my chosen set are ubiquitinated. In addition, the extent of retrotranslocation efficiency could also be assayed (see 3.2.2 below) (Doonan et al., 2019; Preston et al., 2018).

3.2.2 Long Term

Beyond the immediate future, microsomal *in vitro* ubiquitination of CFTR could be used to explore several long-term questions, some of which would require assay retooling. For instance, the assay could be used to assess the role of previously untested PQC factors in the selection of CFTR variants for degradation. Should these factors be cytosolic, they could be expressed and isolated from bacterial culture just as I have done with His-CHIP. Alternatively, ER-integral PQC factors could be overexpressed in HEK293 cells prior to microsome

preparation, and compared *in vitro* to reactions with microsomes lacking these factors. This strategy might produce a more robust difference in signal between reactions than seen after siRNA-mediated knockdown (Figure 15).

The assay could also be used to examine steps occurring downstream of CFTR ubiquitination. While ubiquitination is somewhat labile due to competition between deubiquitinating enzymes and E3 ubiquitin ligases (Zhang et al., 2013), only after retrotranslocation from the ER-membrane are substrates irreversibly committed to proteasomal degradation. Previous assays with yeast-derived microsomes have successfully recapitulated this critical step of ERAD, which could be supported by ensuring that the yeast AAA+ ATPase Cdc48 was active (Doonan et al., 2019; Guerriero et al., 2017; Preston et al., 2018). By adapting these methods to assays with HEK293 cell microsomes, whether by retrotranslocation via Cdc48 or the human homologue p97, one could test if more extensively ubiquitinated CFTR variants are also more readily retrotranslocated. An *in vitro* ubiquitination/retrotranslocation assay could also reveal if there is any functional significance of the modest amount of CHIP-dependent ubiquitination I observed (Figure 14A,C), by testing if ubiquitination actually results in a quantifiable enhancement in retrotranslocation.

Perhaps most intriguingly, the microsomal *in vitro* CFTR ubiquitination assay could be used as a tool to determine if pharmacological corrector compounds reduce the ubiquitination of CFTR variants. While these compounds are presumed exhibit this activity, and thus reduce targeting for ERAD by enhancing folding (Loo et al., 2013; Lopes-Pacheco et al., 2016; Ren et al., 2013), data that directly confirm this phenomenon are lacking. One could test this hypothesis by preparing microsomes from transiently transfected HEK293 cell cultures expressing select CFTR variants treated with corrector compounds, and comparing these *in vitro* to microsomes

prepared without corrector treatment. Should these efforts confirm that correctors indeed reduce CFTR ubiquitination, opportunities to use this assay expand even further. For example, due to the number of CF patients encoding "orphan" variants like P67L (Sabusap et al., 2016) for whom there are too few patients to conduct traditional clinical trials for corrector therapies, the FDA is currently considering *in vitro* data when determining which variants to recommend corrector-based therapeutics for (Ratner, 2017). Therefore, this assay could provide an additional line of evidence which could help match correctors therapies with the patients who need them most.

APPENDIX A: THE C-TERMINUS OF CHIP IS REQUIRED FOR FOLDING AND ENZYME ACTIVATION

This interdisciplinary project emerged from a collaboration with Dr. Carlos Camacho and Zhaofeng Ye at the University of Pittsburgh Department of Computational and Systems Biology. Our findings from this project were published in May 2017, appearing as a research article by Ye and colleagues in *Scientific Reports* (Ye et al., 2017).

A.1 INTRODUCTION

The lowest energy arrangements for protein multimers are typically symmetric, yet there are certain exceptions to this rule. While asymmetric homodimers are exceptionally rare in nature, the nuclear import factor Hikeshi and E3 ubiquitin ligase CHIP are two such examples (Song et al., 2015; Zhang et al., 2005). While the activities performed by each of these proteins has been thoroughly studied, how proteins like these are folded from monomers that are initially identical in conformation is far less understood.

To better understand the unique folding pathways that must occur to yield asymmetric homodimers, members of the Camacho Laboratory used full atom molecular dynamics simulations (MDS) to explore possible ways in which CHIP dimers could assemble. Previously published crystal structures of CHIP show that while zebrafish CHIP lacking its N-terminal TPR domains folds into a symmetric homodimer, complete mouse CHIP does not (Xu et al., 2006;

Zhang et al., 2005), indicating that the presence of this domain is in some way responsible for the asymmetry of CHIP. This asymmetric CHIP is comprised of two distinct "protomers". While the first is characterized by a straight central helix-helix domain and unbound TPR and U-box domains, the second is characterized by a bent helix-helix and tightly bound TPR and U-box domains. As the structure of CHIP monomers is unknown, the Camacho Laboratory explored how dimers could form by simulating assembly with either two "straight" monomers that are structurally identical to the first protomer, two "bent" monomers identical to the second protomer, or two "chimeric" protomers with the straight helix-helix of the first protomer, but the bound TPR and U-box domains of the second (Ye et al., 2017). In each case, the Camacho Laboratory also tested whether monomers dimerized by their helix-helix domains first, or by their U-box domains. Observing that all assemblies which initially dimerized by U-box domains produced sterically impossible conformations of CHIP, our collaborators concluded that dimerization must initially occur by helix-helix domains. Furthermore, they observed that only the assembly of chimeric monomers produced an asymmetric dimer in which the U-Box and TPR domains of one protomer were bound while those of the other were unbound.

Intriguingly, dimerization of these chimeric monomers forced together a positively charged sequence (KRKKR) at the C-terminal base of each monomer's helix-helix domain. This strain appeared to be relieved by "helix breaking" of one half, adopting the conformation of the "bent" protomer. Shortly thereafter, the extreme C-terminus of the "straight" protomer appeared to separate the U-box and TPR domain of the same protomer like a wedge, exposing the E2 binding site on the inner face of the U-box, which should render the enzyme active.

If these simulations accurately reflect actual events that occur during the assembly of CHIP dimers, then the C-terminus of CHIP should be required for its activity. To test if this is

the case, Dr. Patrick Needham of the Brodsky Laboratory cloned and purified a C-terminally truncated variant of human CHIP lacking its final six amino acids (GWVEDY). While this variant was substantially less soluble than wild-type CHIP and appeared poorly folded in both protease susceptibility assays and thermal unfolding assays, circular dichroism (CD) spectroscopy conducted by Dr. Saurav Misra revealed that it generally retained wild-type secondary structure (Ye et al., 2017). I therefore sought to test if this C-terminally truncated CHIP would ubiquitinate substrates *in vitro* as well as wild-type CHIP.

A.2 MATERIALS AND METHODS

CHIP *in vitro* ubiquitination assays were conducted as described in section 2.2.5, but with certain modifications. Reactions contained either 3 μM wild-type CHIP ($CHIP_{1-303}$) or 3 μM truncated CHIP ($CHIP_{1-297}$) and 10 μM GST-$Hsc70_{395-646}$ substrate protein. As initial assays with $CHIP_{1-297}$ predated the purification of His-Ube1 for *in vitro* use, 125 nM commercially purchased GST-Ube1 was used instead (Boston Biochem #E-306), in conjunction with 1 μM UbcH5b (Boston Biochem #E2-622). To accommodate the diminished solubility of C-terminally truncated CHIP, I conducted these *in vitro* ubiquitination assays at 20°C for 60 min. (instead of 37°C for 30 min.). Subsequent experiments with $CHIP_{6A}$, a variant in which the six C-terminal residues are mutated to alanine rather than truncated, were conducted using 75 nM His-Ube1 and 0.75 μM UbcH5b. These assays were also incubated at 20°C.

A.3 RESULTS AND DISCUSSION

In vitro reactions with both variants of CHIP revealed that while C-terminally truncated CHIP retained some activity of wild type, it was severely diminished (Figure 17A). While the truncated variant reliably produced small amounts of monoubiquitinated $Hsc70_{395-646}$ substrate, it produced only trace amounts of polyubiquitinated substrate. Moreover, C-terminally truncated CHIP also exhibited sharply reduced autoubiquitination compared to wild-type CHIP. Therefore, we concluded that these data were consistent with our hypothesis that the extreme C-terminus of CHIP is required for its unique mode of enzyme activation.

Since publication of these data, we have explored further if specific residues with the C-terminus are required to efficiently separate U-box and TPR domains during assembly/activation, or whether any C-terminal sequence is sufficient. Under my direction, undergraduate researcher Zexin Li cloned and purified two additional variants of CHIP: CHIP for which alanine is substituted for the six C-terminal amino acids ($CHIP_{6A}$) and CHIP for which only the bulky tryptophan and tyrosine residues within this span are substituted with alanine ($CHIP_{2A}$). Like C-terminally truncated CHIP, each of these new variants also had poor solubility compared to wild-type. While too little $CHIP_{2A}$ was purified for use in *in vitro* ubiquitination assays, sufficient quantities of $CHIP_{6A}$ were collected. Similar to C-terminally truncated CHIP, $CHIP_{6A}$ failed to substantially ubiquitinate either substrate proteins or itself, indicating that specific C-terminal residues are likely required to effectively wedge apart the U-box and TPR domains of CHIP (Figure 17B). Future studies concerning the activation of CHIP by its formation of an asymmetric homodimer will undoubtedly follow up on determining if ablation of the bulky, hydrophobic sides in its C-terminus is sufficient to abrogate activity. It further remains to be seen

if other cellular factors are involved in the activation of CHIP dimers, or if other asymmetric homodimers exist that assemble in similarly unique ways.

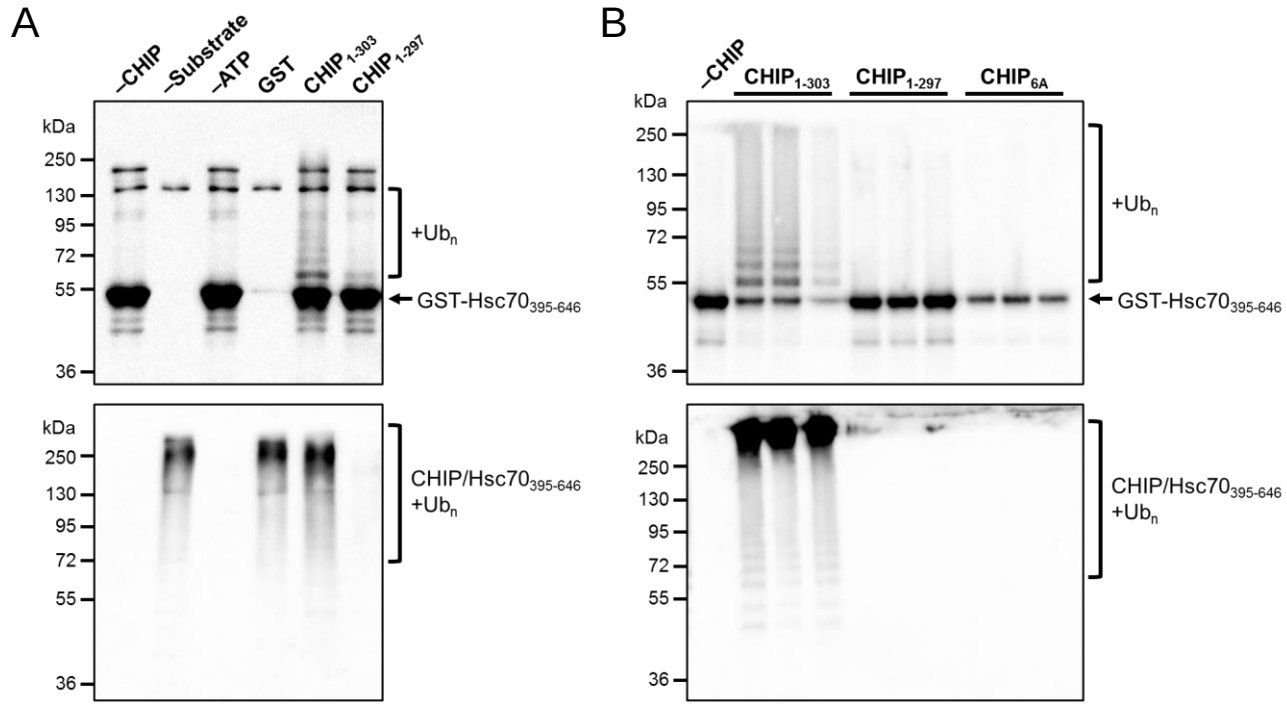

Figure 17. CHIP requires its C-terminus for activity.

(A) Representative anti-GST (top) and anti-ubiquitin (bottom) western blots depicting $Hsc70_{395-646}$ substrate ubiquitination and total ubiquitination, respectively. Reactions were conducted either without CHIP (-CHIP), with full length CHIP but without substrate (-Substrate), without ATP (-ATP), with GST in place of GST-$Hsc70_{395-646}$ (GST), with full length CHIP ($CHIP_{1-303}$), or with C-terminally truncated CHIP ($CHIP_{1-297}$). Reproduced from Figure 6E in (Ye et al., 2017) **(B)** Anti-GST and anti-ubiquitin western blots as in (A) for reactions containing no CHIP, $CHIP_{1-303}$, $CHIP_{1-297}$, or CHIP in which the six C-terminal residues are mutated to alanine instead of truncated ($CHIP_{6A}$).

APPENDIX B: CHIP INHIBITION PROVIDES PROOF-OF-PRINCIPLE FOR A NOVEL DRUG PREDICTION PIPELINE

As with the project described in Appendix A, this project also emerged through collaboration with the Camacho Laboratory at the University of Pittsburgh Department of Computational and Systems Biology, and comprises part of the dissertation research defended by graduate student Nicolas Pabon of the Camacho Laboratory. Our findings from this project have since been published in December 2018, appearing as a research article by Pabon and colleagues in *PloS Computational Biology* (Pabon et al., 2018).

B.1 INTRODUCTION

In silico screening of large chemical libraries is fundamental for the discovery of novel therapeutics that modulate protein interaction networks, however divergent approaches toward designing these screens has major implications for the quantity and quality of hits they identify. Ligand-based strategies, which seek to identify potential protein inhibitors by correlating the gene expression changes that occur in cell culture models when a protein target is knocked out with those that occur when cultures are treated with a small molecule are frequently used, yet face a variety of challenges that limit their usefulness. Most notably, the effects of small molecules in cell culture can be cell type specific, leading to both false positives and false negatives purely as a result of the cells type(s) considered. Furthermore, the expression profile

change observed when one target is knocked out is frequently similar to that observed when another target belonging to the same pathway is knocked out, leading to ambiguity over which of the two proteins a candidate inhibitor actually targets. Ligand-based strategies are also technically demanding, requiring a great deal of time and effort to rigorously collect the data sets upon which a screen can be designed. Alternatively, a structure-based strategy can be used by simulating the strength with which small molecules dock to potentially inhibitory sites in a target protein. While this approach excels at rapidly identifying novel drug-target interactions, it is severely limited by the amount of structural data available about the human proteome.

While each strategy faces its own advantages and limitations, members of the Camacho Laboratory predicted that by combining the two strategies, they would be better equipped to identify novel inhibitors than if they used either strategy alone. To test this hypothesis, a drug discovery pipeline was sought that initially searched for potential inhibitors of target proteins using publicly available data from the NIH Library of Integrated Cellular Signatures (LINCS) project, which contains gene expression profiles for over 20,000 small molecules and knockdown experiments (Subramanian et al., 2017). The Camacho group then filtered out false positives identified by this initial ligand-based screen by conducting a structure-based screen with the highest scoring hits in order to identify the subset of compounds that likely forms *bona fide* interactions with the target protein.

To test the pipeline, our collaborators screened for inhibitors of several disease-relevant proteins, including CHIP. While there are potentially multiple ways in which a small molecule might inhibit the activity of CHIP (see Appendix A), we specifically sought to find compounds that inhibited CHIP by binding to its N-terminal TPR domain. Of the output compounds suggested by the pipeline, we selected seven for further testing which varied widely by their

genetic rank, though not remarkably by their docking rank. I termed these compounds CI-2.1 through CI-2.7, where CI-2.1 held the highest genetic ranking. Fluorescence polarization (FP) assays conducted by Victoria Assimon and Dr. Jason Gestwicki at the University of California San Francisco showed that, indeed, CI-2.1 and CI-2.2 most effectively disrupted binding between CHIP and a peptide derived from the C-terminus of Hsp70, albeit at concentrations greater than 100 μM, while lower ranking compounds less effectively disrupted this interaction, if at all (Pabon et al., 2018). To further validate this drug discovery pipeline, I tested if these compounds would also prevent ubiquitination by CHIP *in vitro*.

B.2 MATERIALS AND METHODS

CHIP *in vitro* ubiquitination assays were generally conducted as described in section 2.2.5, but with modification to accommodate the addition of putative small molecule inhibitors of CHIP. Putative inhibitors were commercially purchased, dissolved in DMSO to create 10 mM stocks, aliquoted, and stored at -20°C until needed. *In vitro* ubiquitination assays with putative inhibitors were set up by incubating CHIP, compounds, additional DMSO, and additional buffer (50 mM HEPES, 50 mM NaCl pH 7.5) together on ice. After 20 min, substrate proteins were dispensed to reaction tubes (either GST-Hsc70$_{395\text{-}646}$ or GST-AT3 JD), followed by E1/E2/Ubiquitin/ATP master mix pre-incubated as described. Final reactions contained 125 nM His-Ube1, 1 μM UbcH5b, 200 μM ubiquitin, 3 μM CHIP, and 10 μM substrate protein. All reactions contained 5% DMSO, whether inhibitory compounds were added or not. Active reactions were incubated for 15 min at 37°C, before quenching by addition with 2X SDS Stop Buffer.

B.3 RESULTS AND DISCUSSION

LINCS compounds CI-2.1—CI-2.7 were initially tested in the presence of CHIP and $Hsc70_{395-646}$, up to 500 μM. In line with the data provided by FP assays, compounds CI-2.1 and CI-2.2 exhibited the most inhibitory effects, partially inhibiting CHIP at 300 μM while completely inhibiting its activity at 500 μM, while DMSO alone had no effect upon ubiquitination (Figure 18A,B). These concentrations at which CI-2.1 and CI-2.2 disrupted ubiquitination by CHIP are in line with those at which disruption of CHIP binding to Hsp70 peptide was observed by FP. In contrast, CI-2.6 and CI-2.7, which had no discernable effect upon FP, did not affect CHIP ubiquitiation at any concentration tested. Additionally, compound CI-2.3, which had a more intermediate effect by FP, also did not inhibit CHIP (Figure 18B).

To test the possibility that the effects observed with CI-2.1 and CI-2.2 were specific to reactions containing the $Hsc70_{395-646}$ substrate, I subsequently tested these compounds and one ineffective compound, CI-2.7, *in vitro* with an alternate substrate, a GST-tagged Josephin Domain of ataxin-3 (GST-AT3 JD). Unlike Hsc70 and Hsp70, which interact with the TPR domain of CHIP through their C-termini, ataxin-3 is a "non-canonical" substrate of CHIP which interacts independently of the CHIP TPR domain. Functionally, ataxin-3 is a deubiquitinating enzyme which must be mono-ubiquitinated by CHIP in order to be activated (Todi et al., 2010; Todi et al., 2009). Ataxin-3 in turn regulates the length of polyubiquitin chains CHIP attaches to itself and its substrates (Scaglione et al., 2011). Similar to reactions containing GST-$Hsc70_{395-646}$, GST-AT3 JD was monoubiquitinated in reactions containing either DMSO or CI-2.7, but not in the presence of 300 μM or more of CI-2.1 or CI-2.2 (Figure 18C). Therefore, I concluded that the effect of these compounds upon CHIP is not specific to whether is assayed with a canonical or non-canonical substrate.

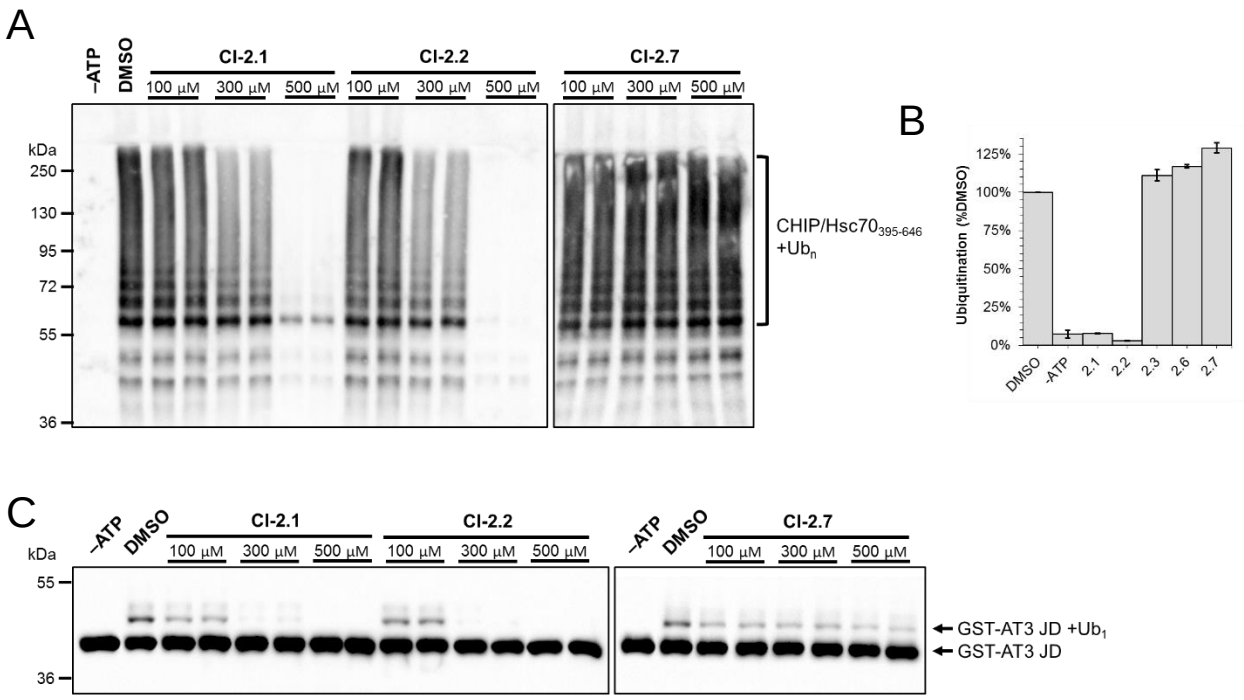

Figure 18. CHIP activity is inhibited by small molecular inhibitors.

(A) Representative anti-ubiquitin western blots depicting GST-Hsc70$_{395-646}$ substrate ubiquitination and CHIP autoubiquitination upon treatment with the indicated compounds at the denoted concentrations. Reactions were treated either with DMSO but without ATP (-ATP), with DMSO and ATP (DMSO), or with ATP and CI-2.1—CI-2.7. Reproduced from Figure S5 in (Pabon et al., 2018). **(B)** Quantitation of ubiquitination in (A). Error bars indicate standard error of the mean (SEM). 2.1, 2.2: N=4; all other compounds: n=2. Reproduced from Figure 5D in (Pabon et al., 2018). **(C)** Representative anti-GST western blots depicting GST-AT3 JD substrate ubiquitination. Reactions were conducted as in (A), but with GST-AT3 JD in place of GST-Hsc70$_{395-646}$ substrate. Reproduced from Figure S6 in (Pabon et al., 2018).

It is curious, however, that addition of these small molecules, which were screened for binding to the TPR domain of CHIP, would interfere with either the auto-ubiquitination of CHIP observed by anti-ubiquitin western blotting (Figure 18A) or with the ubiquitination of a non-canonical substrate (Figure 18C), as neither of these functions would seemingly require the TPR domain. It is possible that binding of a small molecular inhibitor to the TPR domain could

suppress the activity of CHIP even in these scenarios, as deletion of the TPR domain has been shown to partially, though not completely, reduce the activity of CHIP, implying that that the enzyme may exhibit a certain degree of allostery (Windheim et al., 2008). Similarly, binding between the TPR domain of CHIP and Hsp70 has been shown to reduce CHIP autoubiquitination in the presence of certain substrates (Narayan et al., 2015). Alternatively, it is possible that although these compounds were screened for docking to the CHIP TPR domain, they may bind with similar affinity to additional sites on CHIP dimers, thus reducing these activities. While CI-2.1 and CI-2.2 inhibit ubiquitination only at biologically unattainable concentrations, validation of these compounds as *bona fide* CHIP inhibitors provides support that this hybrid pipeline can identify novel inhibitors for target proteins from publicly available data. While neither of these compounds are amenable to further medicinal chemistry (CI-2.1 is the pH indicator phenolphthalein, while CI-2.2 is a putative Hsp90 inhibitor, CCT018159), further tuning of this pipeline could improve its ability to detect strongly binding small molecular inhibitors. Moving forward, this pipeline (or a later iteration) could be used to identify inhibitors that target other and perhaps more unique pockets of CHIP where a conformational change is required for the protein to function (see Appendix A).

APPENDIX C: S-NITROSYLATION INHIBITS CHIP FUNCTION

The project described in this appendix emerged from a collaboration between our laboratory and that of Dr. Khalequz Zaman at Case Western Reserve University, and was published in December 2019, appearing as a research article by Zaman and colleagues in the *American Journal of Respiratory Cell and Molecular Biology* (Zaman et al., 2019).

C.1 INTRODUCTION

In human bronchial epithelia, CHIP could potentially be inhibited to support CFTR trafficking and function in one of several ways, particularly if a folding corrector was also present. One way in which CHIP could be inhibited is by treatment with a small molecule inhibitor which specifically binds to CHIP and interferes with its ability to attach ubiquitin chains onto CFTR, as outlined in Appendix B. Alternately, CHIP could be targeted by a post-translational modification that reduces its activity. Similar to a small molecule inhibitor, such a modification could sterically impede binding of CHIP to molecular chaperones, such as Hsc70, which are required by CHIP to ubiquitinate CFTR (Meacham et al., 2001). However, unlike a small molecule inhibitor, an inhibitory post-translational modification would be covalently attached to CHIP, potentially extending its dwell time on CHIP. Such a therapy might be better tolerated by patients, with a diminished risk of deleterious off-target effects.

S-nitrosothiols (SNOs) are a class of signaling molecule capable of transferring one such potential post-translational modification onto target proteins. SNOs had been previously shown to improve the maturation and function of both wild-type and F508del CFTR (Andersson et al., 2002; Howard et al., 2003; Servetnyk et al., 2006; Zaman et al., 2001). Members of the Zaman Laboratory at Case Western Reserve University also found that CFTR biogenesis is improved by S-nitrosylation of cysteine sidechains on a variety of CFTR PQC components, including Hsc70, Hsp70, HOP, and Csp (Marozkina et al., 2010a; Zaman et al., 2006). As CHIP is also a known pro-degradative component of CFTR PQC and contains eight cysteines (Ballinger et al., 1999), the Zaman Laboratory predicted that it too could be S-nitrosylated, thus improving CFTR function. To test this hypothesis, they examined how treatment with S-nitrosoglutathione (GSNO) affected levels of CHIP and CFTR in CFBE cell culture. They demonstrated that GSNO reduced CHIP levels while increasing CFTR levels. They also predicted that GSNO would inhibit CHIP activity *in vitro*. To that end, I collaborated with the Zaman Laboratory and guided them in the use of the CHIP *in vitro* ubiquitination assay I had previously developed.

C.2 MATERIALS AND METHODS

His-Ube1, His-CHIP, and GST-Hsc70$_{395-646}$ substrate for CHIP *in vitro* ubiquitination assays were prepared as described (see sections 2.2.1, 2.2.2, and 2.2.4) and shipped to the Zaman Laboratory on dry ice along with 10X ATP Buffer, purchased UbcH5b (Boston Biochem #E2-622), and purchased ubiquitin (Boston Biochem #U-100H). Members of the Zaman Laboratory were instructed remotely in the use of these reagents to conduct CHIP *in vitro* ubiquitination assays (see section 2.2.5), with additional insight regarding how to conduct these assays in the

presence of putative inhibitors (see Appendix B). All CHIP *in vitro* ubiquitination assays conducted as part of this project were performed by members of the Zaman Laboratory.

C.3 RESULTS AND DISCUSSION

As predicted based on the initial observations in cell culture, addition of low micromolar GSNO to CHIP *in vitro* ubiquitination assays elicited a dose-dependent reduction in the degree of polyubiquitination observed (Figure 19). Additional nitric oxide analysis performed by the Zaman Laboratory indicated that incubating purified CHIP in the presence of either 5 µM or 10 µM GSNO for 4 hr resulted in a quantifiable increase in the attachment of NO to cysteines of CHIP (Zaman et al., 2019). We therefore concluded that the observed inhibition of CHIP activity is a direct result of its post-translational modification by GSNO.

How SNOs such as GSNO could be used to inhibit CHIP in CF patient tissues remains to be seen. Of note, these compounds were observed to be well tolerated (Snyder et al., 2002). As GSNO is depleted in patient tissues, it could have merit as a replacement therapy for respiratory function, similar to the way in which pancreatic enzymes are currently used to support digestive function in CF patients. Even so, it remains unclear just how much GSNO would be needed to sufficiently inhibit CHIP *in vivo* without broadly disturbing proteostasis, especially as key enzymes in the ubiquitination pathway also require solvent exposed cysteine residues to function. Further efforts to characterize SNOs will surely focus on better understanding the wide-ranging effects that these compounds have in order to better balance the potential benefits that these compounds could provide with any potential long-term risks.

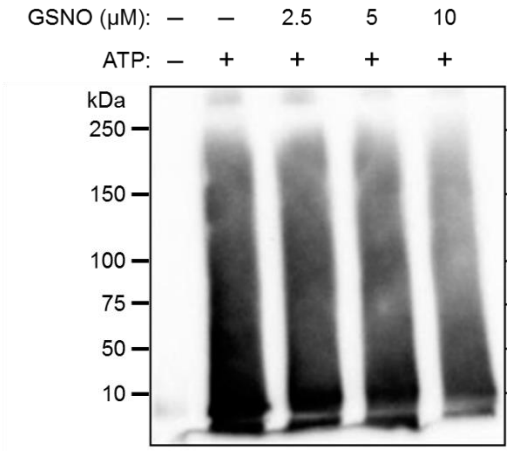

Figure 19. CHIP activity is inhibited by S-nitrosylation.

Anti-ubiquitin western blot indicating loss of CHIP activity with increasing concentrations of GSNO. Assays were conducted by the Zaman Laboratory at Case Western Reserve University with supplied reagents and methods either in the absence of ATP (-ATP), with ATP but in the absence of GSNO, or with both ATP and GSNO. Figure reproduced from Figure 5 in (Zaman et al., 2019).

APPENDIX D: CHIP FUNCTIONS WITH PARTIALLY UNNATURAL UBIQUITIN VARIANTS

This interdisciplinary project emerged out of a collaboration with Dr. Seth Horne and graduate student Halina Werner at the University of Pittsburgh Department of Chemistry. This project has since been completed and its findings published in September 2019, appearing as a research article by Werner and colleagues in *ChemBioChem* (Werner et al., 2019).

D.1 INTRODUCTION

One fundamental application of chemistry lies in the formulation and utilization of biologically active compounds that do not occur naturally. By their design, these synthetic compounds can either refine the properties of closely related natural products, such that they are better suited to their desired use, or confer altogether new activities, foreign to their intended biological setting. Early development of synthetic bioactive molecules focused almost exclusively upon their promising potential as antimicrobial agents, leading to the discovery of numerous medically valuable compounds, such as those containing sulfonamide functional groups (i.e. “sulfa drugs”) in the early 1930s. Ongoing interest led to the development of synthetic antibiotics and chemotherapeutics, which are designed to be either more effective, less toxic, less prone to resistance, or more cost-effective to mass produce than their natural counterparts (e.g. docetaxel and paclitaxel).

Yet small molecules such as these are typically restricted to just a narrow range of functions. While small molecule approaches have revolutionized treatment for many diseases (including cystic fibrosis, see section 1.3), alternate classes of compounds might better address certain conditions, such as those requiring the replacement of insufficient functions, or the addition of new ones. Among the most promising of these classes are peptide-based therapeutics. Indeed, to date over 250 distinct peptide therapies have received FDA approval for clinical use (http://crdd.osdd.net/raghava/thpdb/) (Usmani et al., 2017). Unlike small molecules, peptides are generally well tolerated and can encompass a myriad of functions. A single peptide can also combine activities in ways that would be challenging if not impossible for a small molecule to comprise, such as the ability to bind a target protein while also carrying an enzymatic function. Unfortunately, peptide-based therapies face many of their own challenges. Proteins and short peptides typically have poor circulatory half-lives, largely owing to their susceptibility to proteolysis. Polypeptides are also acutely sensitive to their surrounding environment and risk unfolding and becoming inactive outside of a specific temperature and pH range. Moreover, peptides can also elicit an immune response.

Just as synthetic features have improved the performance of small molecule therapeutics, so too could these improve the therapeutic benefit of peptides. By incorporating unnatural amino acids, a polypeptide could be redesigned to be less susceptible to proteolysis, to fold more stably, and/or to better evade the immune system. Perhaps most intriguingly, unnatural amino acids might even be used to bestow novel functions, never before captured by configurations of the 20 proteinogenic amino acids. For all these possibilities, the design principles upon which to create such semi-synthetic peptides remain poorly understood. Most critically, the extent to which a protein could be modified with unnatural residues while retaining its native activity and tertiary

structure is unclear. Our ability to test this question is exacerbated by difficulty in synthesizing functionally complex, partially synthetic peptides, as standard solid phase peptide synthesis is generally limited to polypeptides that are no more than ~50 residues in length. In spite of this challenge, members of the Horne Laboratory predicted that through native chemical ligation (NCL), two fragments of a protein could be synthesized separately and then modularly reattached to reconstitute the complete, active protein. To test this possibility, the Horne Laboratory sought to synthesize human ubiquitin, a 76 amino acid protein with varied and complex cellular functions, including its recognition and transferal between components of ubiquitination machinery, as described in section 1.2.2. As I have reconstituted these activities *in vitro*, I assayed ubiquitin derivatives prepared by the Horne Laboratory with varying degrees of synthetic content to determine if the variants could mimic the function of wild-type human ubiquitin.

D.2 MATERIALS AND METHODS

Leveraging their prior experience in designing stably folding polypeptides with unnatural backbone characteristics ("foldamers") (George and Horne, 2018), the Horne Laboratory conceptualized and synthesized a series of ubiquitin foldamers with variable synthetic content. Each foldamer contained an N-terminal and C-terminal fragment (Ub_{1-27} and Ub_{28-76}, respectively), which were independently synthesized and fused together by NCL. For each fragment, three different forms were designed: an unmodified, a "conservatively" modified, and an "ambitiously" modified form, characterized by increasing degrees of synthetic content. In this way, nine distinct ubiquitin foldamers were assembled by combining the fragments (Figure

20A). In eight of these foldamers, certain wild-type, L-α-residues were substituted with non-proteinogenic residues that primarily alter the protein backbone but in some cases also modify sidechains. These substitute residues included D-α-residues, N-Me-α-residues, β^3-residues, a C_α-Me-α-residue (α-aminoisobutyric acid; Aib), and a γ^{cyc}-residue (cis-3-aminocyclohexylcarboxylic acid; ACC) (Figure 20B). Only the foldamer containing an unmodified N-terminal fragment and an unmodified C-terminal fragment was free of synthetic content, save for the substitution of norleucine for methionine at Ub_1 (Figure 20C).

After circular dichroism (CD) spectroscopy confirmed that several semi-synthetic foldamers retained wild-type-like spectra (Werner et al., 2019), I tested if these foldamers would function with purified enzymes required for ubiquitination *in vitro*. These assays were generally conducted as described in section 2.2.5, though with minor modifications. First, many foldamers exhibited reduced aqueous solubility, limiting the concentration of stocks that could be prepared. Therefore, I added only 140 μM of each ubiquitin foldamer to *in vitro* assays with CHIP (instead of 200 μM; a 30% reduction). Second, as reactions with semi-synthetic ubiquitin foldamers might also proceed at a slower rate than reactions with wild-type ubiquitin (due to a diminished propensity of these foldamers to be recognized by ubiquitination enzymes as suitable substrates), I incubated reactions at 37°C for 60 min (rather than 30 min). Follow-up reactions with ubiquitin in which lysines 48 and/or 63 were mutated to arginine were conducted under these same conditions. Purified K48R, K63R, and K48R/K63R ubiquitin proteins were graciously provided by Dr. Philip Cole of Harvard Medical School.

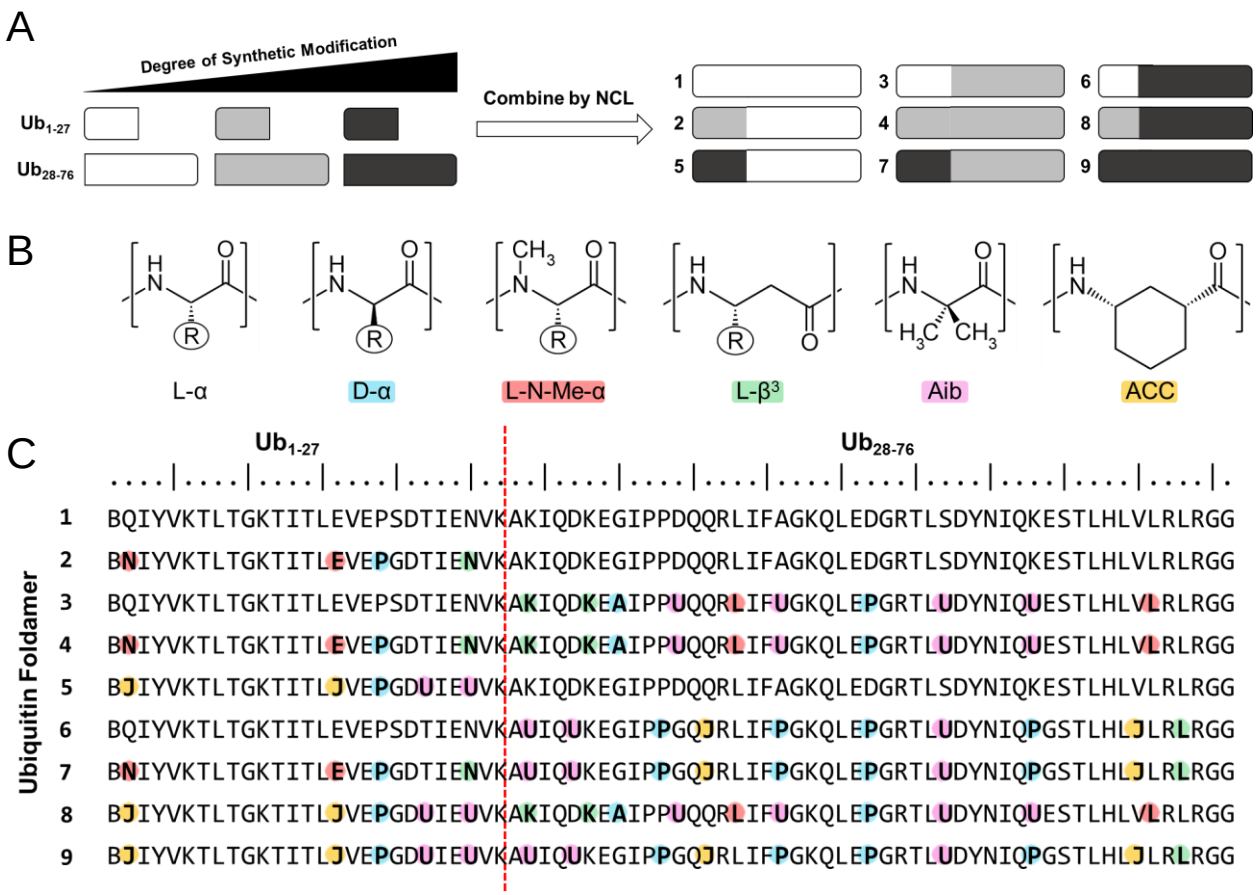

Figure 20. Design of semi-synthetic ubiquitin foldamers.

(A) Ubiquitin foldamers were synthesized via NCL by combining three versions of N-terminal ubiquitin fragments (Ub_{1-27}) with three versions of C-terminal ubiquitin fragments (Ub_{28-76}), resulting in nine distinct foldamers. **(B)** Representative structures of all non-proteinogenic amino acids used to synthesize partially synthetic ubiquitin foldamers. **(C)** Amino acid sequences of semi-synthetic ubiquitin foldamers. Bold characters indicate substituted residues; shading indicates substituted residue type based on color coding shown in (B). B=norleucine; U=Aib; J=ACC. Figure adapted from Figure 1 in (Werner et al., 2019).

D.3 RESULTS AND DISCUSSION

CHIP *in vitro* ubiquitination assays revealed that four of these nine semi-synthetic foldamers retain various degrees of activity when compared to wild-type ubiquitin (Figure 21A,B). Importantly, in reactions with foldamer 1, which contains no synthetic residues beyond the substitution of norleucine at Ub_1, GST-$Hsc70_{395-646}$ becomes polyubiquitinated nearly identically as when recombinant wild-type ubiquitin is used. This result signifies that ubiquitin moieties created by NCL can be successfully appended to E1 ubiquitin activating enzymes and then passed to E2 ubiquitin conjugating enzymes *en route* to substrates. Foldamer 2, which contains a conservatively modified N-terminus but unmodified C-terminus, could also polyubiquitinate substrates, although to a lesser degree. Foldamers 3 and 4, which contain conservatively modified C-termini fused to either an unmodified or a conservatively modified N-terminus, respectively, could also ubiquitinate substrates. However, the absence of polyubiquitinated substrates in reactions with these foldamers suggests that while these variants can successfully be appended onto substrates, they lack functional lysine sidechains to be efficiently appended onto a growing polyubiquitin chain. All remaining foldamers (5-9), which contain ambitiously modified N-termini and/or C-termini, failed to catalyze ubiquitination *in vitro*. While foldamer 9 partially appears as a high molecular weight species after incubation with CHIP, these likely reflect aggregated protein that could not be resolved by SDS-PAGE, as this foldamer rapidly precipitated when added to reactions.

As foldamers 3 and 4 differed from foldamer 2 by the substitution of K63 with Aib, I further explored whether removal of this lysine was responsible for the inability of these foldamers to polyubiquitinate substrates by conducting CHIP *in vitro* ubiquitination reactions with ubiquitin in which K48 and/or K63 were mutated to arginine. To my surprise, even in the

absence of both lysines, polyubiquitin was readily added to substrates by CHIP (Figure 21C). Therefore, the inability of foldamers 3 and 4 to polyubiquitinate substrates is more likely to be due to changes in the overall fold of these variants rather than the removal of any particular lysine required by CHIP for activity.

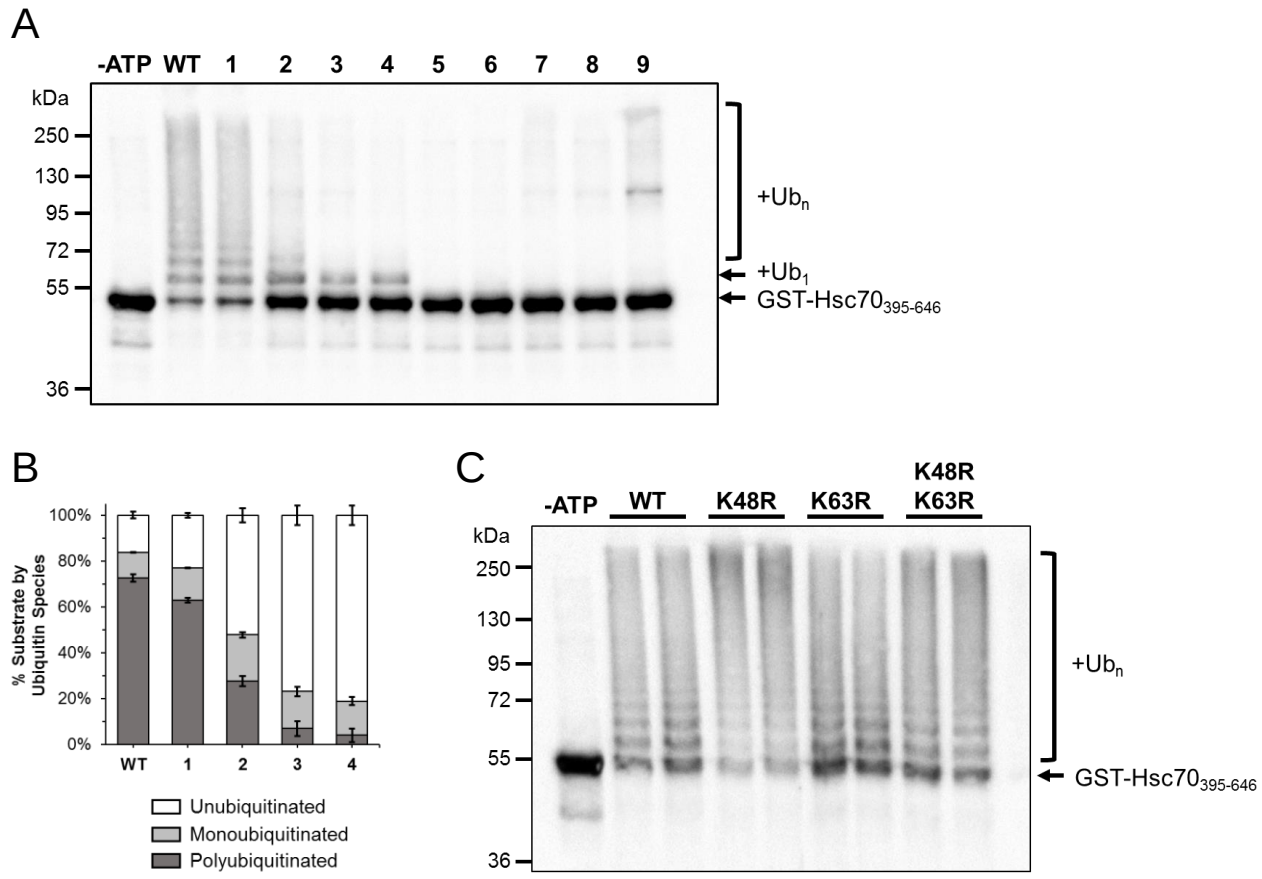

Figure 21. Ubiquitination by semi-synthetic ubiquitin foldamers *in vitro*.

(A) Representative anti-GST western blot depicting CHIP *in vitro* ubiquitination of GST-Hsc70$_{395-646}$ substrates by semi-synthetic ubiquitin foldamers. Reactions contained either wild-type human ubiquitin (WT) or a semi-synthetic foldamer (1-9) as indicated. Control reactions conducted without ATP (-ATP) contained wild-type ubiquitin. Figure reproduced from Figure 3 in (Werner et al., 2019). **(B)** Quantification of substrate ubiquitination observed with active ubiquitin. Error bars indicate standard error of the mean (n=3). **(C)** Representative anti-GST western blot depicting CHIP *in vitro* ubiquitination of GST-Hsc70$_{395-646}$ substrates as in (A), but with either wild-type ubiquitin, Ub$_{K48R}$, Ub$_{K63R}$, or Ub$_{K48R/K63R}$. Duplicate reactions shown for each ubiquitin variant are technical replicates.

To further explore the functionality of foldamers that exhibited activity with CHIP, Dr. Michael Preston, also in the Brodsky Laboratory, sought to determine if misfolded proteins ubiquitinated by these semi-synthetic variants could be extracted from ER membranes as if they had been ubiquitinated by wild-type ubiquitin during ERAD. Using a previously described *in vitro* ubiquitination assay consisting of ^{125}I-Ub and microsomes from *Saccharomyces cerevisiae* (Nakatsukasa et al., 2008), Dr. Preston observed that, like purified human ubiquitination enzymes, endogenous yeast enzymes could successfully attach foldamers 2 and 3 onto a protein known as Chimera A*, a chimeric misfolded protein derived from the yeast pheromone transporter, Ste6, albeit less efficiently than foldamer 1 (Werner et al., 2019). Furthermore, these ubiquitinated substrates were retrotranslocated from the ER membrane by the AAA-ATPase Cdc48 (homologous to human p97), just as an endogenous ERAD substrate would be (see section 1.2.2). Taken together, these data indicate that while no foldamer with synthetic content matched the activity of wild-type ubiquitin, the inclusion of non-proteinogenic residues does not preclude the ability of these foldamers interact with various components of ubiquitination machinery and successfully signal for the degradation of a misfolded substrate. While no foldamer containing either an ambitiously modified N-terminal or C-terminal fragment functioned *in vitro*, this could have occurred simply due to the inclusion of ACC residues, which were unique to these fragments. Future efforts to design functional, semi-synthetic peptides will therefore seek to elucidate which non-proteinogenic amino acids are best suited to the design of functional peptides, as well as the degree to which these peptides could contain synthetic content without disturbing their fold and function.

REFERENCES

1. Ahner, A., Gong, X., Schmidt, B.Z., Peters, K.W., Rabeh, W.M., Thibodeau, P.H., Lukacs, G.L., and Frizzell, R.A. (2013). Small heat shock proteins target mutant cystic fibrosis transmembrane conductance regulator for degradation via a small ubiquitin-like modifier-dependent pathway. Mol Biol Cell *24*, 74-84.

2. Ahner, A., Nakatsukasa, K., Zhang, H., Frizzell, R.A., and Brodsky, J.L. (2007). Small heat-shock proteins select deltaF508-CFTR for endoplasmic reticulum-associated degradation. Mol Biol Cell *18*, 806-814.

3. Alberti, S., Bohse, K., Arndt, V., Schmitz, A., and Hohfeld, J. (2004). The cochaperone HspBP1 inhibits the CHIP ubiquitin ligase and stimulates the maturation of the cystic fibrosis transmembrane conductance regulator. Mol Biol Cell *15*, 4003-4010.

4. Ameen, N., and Apodaca, G. (2007). Defective CFTR apical endocytosis and enterocyte brush border in myosin VI-deficient mice. Traffic *8*, 998-1006.

5. Anderson, D.H. (1938). Cystic Fibrosis of the Pancreas and its Relation to Celiac Disease: A Clinical and Pathologic Study. Am J Dis Child *56*, 344-399.

6. Anderson, D.H., and Hodges, R.G. (1946). Genetics of Cystic Fibrosis of the Pancreas With a Consideration of Etiology. Am J Dis Child *72*, 62-80.

7. Andersson, C., Gaston, B., and Roomans, G.M. (2002). S-Nitrosoglutathione induces functional DeltaF508-CFTR in airway epithelial cells. Biochem Biophys Res Commun *297*, 552-557.

8. Baaklini, I., Goncalves, C.C., Lukacs, G.L., and Young, J.C. (2020). Selective Binding of HSC70 and its Co-Chaperones to Structural Hotspots on CFTR. Sci Rep *10*, 4176.

9. Bagdany, M., Veit, G., Fukuda, R., Avramescu, R.G., Okiyoneda, T., Baaklini, I., Singh, J., Sovak, G., Xu, H., Apaja, P.M., *et al.* (2017). Chaperones rescue the energetic landscape of mutant CFTR at single molecule and in cell. Nat Commun *8*, 398.

10. Baldridge, R.D., and Rapoport, T.A. (2016). Autoubiquitination of the Hrd1 Ligase Triggers Protein Retrotranslocation in ERAD. Cell *166*, 394-407.

11. Ballar, P., Ors, A.U., Yang, H., and Fang, S. (2010). Differential regulation of CFTRDeltaF508 degradation by ubiquitin ligases gp78 and Hrd1. Int J Biochem Cell Biol *42*, 167-173.

12. Ballinger, C.A., Connell, P., Wu, Y., Hu, Z., Thompson, L.J., Yin, L.Y., and Patterson, C. (1999). Identification of CHIP, a novel tetratricopeptide repeat-containing protein that interacts with heat shock proteins and negatively regulates chaperone functions. Mol Cell Biol *19*, 4535-4545.

13. Bebök, Z., Collawn, J.F., Wakefield, J., Parker, W., Li, Y., Varga, K., Sorscher, E.J., and Clancy, J.P. (2005). Failure of cAMP agonists to activate rescued deltaF508 CFTR in CFBE41o- airway epithelial monolayers. J Physiol *569*, 601-615.

14. Bebök, Z., Mazzochi, C., King, S.A., Hong, J.S., and Sorscher, E.J. (1998). The mechanism underlying cystic fibrosis transmembrane conductance regulator transport from the endoplasmic reticulum to the proteasome includes Sec61beta and a cytosolic, deglycosylated intermediary. J Biol Chem *273*, 29873-29878.

15. Bergbower, E., Boinot, C., Sabirzhanova, I., Guggino, W., and Cebotaru, L. (2018). The CFTR-Associated Ligand Arrests the Trafficking of the Mutant DeltaF508 CFTR Channel in the ER Contributing to Cystic Fibrosis. Cell Physiol Biochem *45*, 639-655.

16. Bernardino, R.L., Jesus, T.T., Martins, A.D., Sousa, M., Barros, A., Cavaco, J.E., Socorro, S., Alves, M.G., and Oliveira, P.F. (2013). Molecular basis of bicarbonate membrane transport in the male reproductive tract. Curr Med Chem *20*, 4037-4049.

17. Bettencourt, C., de Yebenes, J.G., Lopez-Sendon, J.L., Shomroni, O., Zhang, X., Qian, S.B., Bakker, I.M., Heetveld, S., Ros, R., Quintans, B., *et al.* (2015). Clinical and Neuropathological Features of Spastic Ataxia in a Spanish Family with Novel Compound Heterozygous Mutations in STUB1. Cerebellum.

18. Bracher, A., and Verghese, J. (2015). The nucleotide exchange factors of Hsp70 molecular chaperones. Front Mol Biosci *2*, 10.

19. Bradbury, N.A., Cohn, J.A., Venglarik, C.J., and Bridges, R.J. (1994). Biochemical and biophysical identification of cystic fibrosis transmembrane conductance regulator chloride channels as components of endocytic clathrin-coated vesicles. J Biol Chem *269*, 8296-8302.

20. Brodsky, J.L. (2007). The protective and destructive roles played by molecular chaperones during ERAD (endoplasmic-reticulum-associated degradation). Biochem J *404*, 353-363.

21. Brown, C.R., Hong-Brown, L.Q., Biwersi, J., Verkman, A.S., and Welch, W.J. (1996). Chemical chaperones correct the mutant phenotype of the delta F508 cystic fibrosis transmembrane conductance regulator protein. Cell Stress Chaperones *1*, 117-125.

22. Brown, C.R., Hong-Brown, L.Q., and Welch, W.J. (1997). Correcting temperature-sensitive protein folding defects. J Clin Invest *99*, 1432-1444.

23. Buck, T.M., and Skach, W.R. (2005). Differential stability of biogenesis intermediates reveals a common pathway for aquaporin-1 topological maturation. J Biol Chem *280*, 261-269.

24. Buck, T.M., Wagner, J., Grund, S., and Skach, W.R. (2007). A novel tripartite motif involved in aquaporin topogenesis, monomer folding and tetramerization. Nat Struct Mol Biol *14*, 762-769.

25. Cantin, A.M., Hartl, D., Konstan, M.W., and Chmiel, J.F. (2015). Inflammation in cystic fibrosis lung disease: Pathogenesis and therapy. J Cyst Fibros *14*, 419-430.

26. Carvalho, A.F., Pinto, M.P., Grou, C.P., Vitorino, R., Domingues, P., Yamao, F., Sa-Miranda, C., and Azevedo, J.E. (2012). High-yield expression in Escherichia coli and purification of mouse ubiquitin-activating enzyme E1. Mol Biotechnol *51*, 254-261.

27. Carvalho, P., Stanley, A.M., and Rapoport, T.A. (2010). Retrotranslocation of a misfolded luminal ER protein by the ubiquitin-ligase Hrd1p. Cell *143*, 579-591.

28. Chang, X.B., Cui, L., Hou, Y.X., Jensen, T.J., Aleksandrov, A.A., Mengos, A., and Riordan, J.R. (1999). Removal of multiple arginine-framed trafficking signals overcomes misprocessing of delta F508 CFTR present in most patients with cystic fibrosis. Mol Cell *4*, 137-142.

29. Chang, X.B., Hou, Y.X., Jensen, T.J., and Riordan, J.R. (1994). Mapping of cystic fibrosis transmembrane conductance regulator membrane topology by glycosylation site insertion. J Biol Chem *269*, 18572-18575.

30. Chen, M., and Zhang, J.T. (1999). Topogenesis of cystic fibrosis transmembrane conductance regulator (CFTR): regulation by the amino terminal transmembrane sequences. Biochemistry *38*, 5471-5477.

31. Cheng, J., Cebotaru, V., Cebotaru, L., and Guggino, W.B. (2010). Syntaxin 6 and CAL mediate the degradation of the cystic fibrosis transmembrane conductance regulator. Mol Biol Cell *21*, 1178-1187.

32. Cheng, J., and Guggino, W. (2013). Ubiquitination and degradation of CFTR by the E3 ubiquitin ligase MARCH2 through its association with adaptor proteins CAL and STX6. PLoS One *8*, e68001.

33. Cheng, J., Wang, H., and Guggino, W.B. (2004). Modulation of mature cystic fibrosis transmembrane regulator protein by the PDZ domain protein CAL. J Biol Chem *279*, 1892-1898.

34. Cheng, S.H., Gregory, R.J., Marshall, J., Paul, S., Souza, D.W., White, G.A., O'Riordan, C.R., and Smith, A.E. (1990). Defective intracellular transport and processing of CFTR is the molecular basis of most cystic fibrosis. Cell *63*, 827-834.

35. Cheng, S.H., Rich, D.P., Marshall, J., Gregory, R.J., Welsh, M.J., and Smith, A.E. (1991). Phosphorylation of the R domain by cAMP-dependent protein kinase regulates the CFTR chloride channel. Cell *66*, 1027-1036.

36. Chiang, A.N., Valderramos, J.C., Balachandran, R., Chovatiya, R.J., Mead, B.P., Schneider, C., Bell, S.L., Klein, M.G., Huryn, D.M., Chen, X.S., *et al.* (2009). Select pyrimidinones inhibit the propagation of the malarial parasite, Plasmodium falciparum. Bioorg Med Chem *17*, 1527-1533.

37. Chillon, M., Casals, T., Mercier, B., Bassas, L., Lissens, W., Silber, S., Romey, M.C., Ruiz-Romero, J., Verlingue, C., and Claustres, M. (1995). Mutations in the cystic fibrosis gene in patients with congenital absence of the vas deferens. N Engl J Med *332*, 1475-1480.

38. Cholon, D.M., Quinney, N.L., Fulcher, M.L., Esther, C.R., Jr., Das, J., Dokholyan, N.V., Randell, S.H., Boucher, R.C., and Gentzsch, M. (2014). Potentiator ivacaftor abrogates pharmacological correction of DeltaF508 CFTR in cystic fibrosis. Sci Transl Med *6*, 246ra296.

39. Chung, W.J., Goeckeler-Fried, J.L., Havasi, V., Chiang, A., Rowe, S.M., Plyler, Z.E., Hong, J.S., Mazur, M., Piazza, G.A., Keeton, A.B., *et al.* (2016). Increasing the Endoplasmic Reticulum Pool of the F508del Allele of the Cystic Fibrosis Transmembrane Conductance Regulator Leads to Greater Folding Correction by Small Molecule Therapeutics. PLoS One *11*, e0163615.

40. Claessen, J.H., Mueller, B., Spooner, E., Pivorunas, V.L., and Ploegh, H.L. (2010). The transmembrane segment of a tail-anchored protein determines its degradative fate through dislocation from the endoplasmic reticulum. J Biol Chem *285*, 20732-20739.

41. Clancy, J.P., Cotton, C.U., Donaldson, S.H., Solomon, G.M., VanDevanter, D.R., Boyle, M.P., Gentzsch, M., Nick, J.A., Illek, B., Wallenburg, J.C., *et al.* (2019). CFTR modulator theratyping: Current status, gaps and future directions. J Cyst Fibros *18*, 22-34.

42. Collawn, J.F., Stangel, M., Kuhn, L.A., Esekogwu, V., Jing, S.Q., Trowbridge, I.S., and Tainer, J.A. (1990). Transferrin receptor internalization sequence YXRF implicates a tight turn as the structural recognition motif for endocytosis. Cell *63*, 1061-1072.

43. Cordoba, M., Rodriguez-Quiroga, S., Gatto, E.M., Alurralde, A., and Kauffman, M.A. (2014). Ataxia plus myoclonus in a 23-year-old patient due to STUB1 mutations. Neurology *83*, 287-288.

44. Cystic Fibrosis Foundation Patient Registry (2019). 2018 Annual Data Report (Bethesda, MD, USA: Cystic Fibrosis Foundation).

45. Dalemans, W., Barbry, P., Champigny, G., Jallat, S., Dott, K., Dreyer, D., Crystal, R.G., Pavirani, A., Lecocq, J.P., and Lazdunski, M. (1991). Altered chloride ion channel kinetics associated with the delta F508 cystic fibrosis mutation. Nature *354*, 526-528.

46. Davies, J.C., Wainwright, C.E., Canny, G.J., Chilvers, M.A., Howenstine, M.S., Munck, A., Mainz, J.G., Rodriguez, S., Li, H., Yen, K., *et al.* (2013). Efficacy and safety of ivacaftor in patients aged 6 to 11 years with cystic fibrosis with a G551D mutation. Am J Respir Crit Care Med *187*, 1219-1225.

47. Demand, J., Alberti, S., Patterson, C., and Hohfeld, J. (2001). Cooperation of a ubiquitin domain protein and an E3 ubiquitin ligase during chaperone/proteasome coupling. Curr Biol *11*, 1569-1577.

48. Denning, G.M., Anderson, M.P., Amara, J.F., Marshall, J., Smith, A.E., and Welsh, M.J. (1992). Processing of mutant cystic fibrosis transmembrane conductance regulator is temperature-sensitive. Nature *358*, 761-764.

49. Depondt, C., Donatello, S., Simonis, N., Rai, M., van Heurck, R., Abramowicz, M., D'Hooghe, M., and Pandolfo, M. (2014). Autosomal recessive cerebellar ataxia of adult onset due to STUB1 mutations. Neurology *82*, 1749-1750.

50. di Sant'Agnese, P.A., Darling, R.C., Perara, G.A., and Shea, A. (1953). Abnormal electrolyte composition of sweat in cystic fibrosis of the pancreas. AMA Am J Dis Child *86*, 618-619.

51. Doonan, L.M., Guerriero, C.J., Preston, G.M., Buck, T.M., Khazanov, N., Fisher, E.A., Senderowitz, H., and Brodsky, J.L. (2019). Hsp104 facilitates the endoplasmic-reticulum-associated degradation of disease-associated and aggregation-prone substrates. Protein Sci *28*, 1290-1306.

52. Du, K., and Lukacs, G.L. (2009). Cooperative assembly and misfolding of CFTR domains in vivo. Mol Biol Cell *20*, 1903-1915.

53. Eckford, P.D., Ramjeesingh, M., Molinski, S., Pasyk, S., Dekkers, J.F., Li, C., Ahmadi, S., Ip, W., Chung, T.E., Du, K., *et al.* (2014). VX-809 and related corrector compounds exhibit secondary activity stabilizing active F508del-CFTR after its partial rescue to the cell surface. Chem Biol *21*, 666-678.

54. Egan, M.E., Pearson, M., Weiner, S.A., Rajendran, V., Rubin, D., Glockner-Pagel, J., Canny, S., Du, K., Lukacs, G.L., and Caplan, M.J. (2004). Curcumin, a major constituent of turmeric, corrects cystic fibrosis defects. Science *304*, 600-602.

55. El Khouri, E., Le Pavec, G., Toledano, M.B., and Delaunay-Moisan, A. (2013). RNF185 is a novel E3 ligase of endoplasmic reticulum-associated degradation (ERAD) that targets cystic fibrosis transmembrane conductance regulator (CFTR). J Biol Chem *288*, 31177-31191.

56. Elborn, J.S. (2016). Cystic fibrosis. Lancet *388*, 2519-2531.

57. Estabrooks, S., and Brodsky, J.L. (2020). Regulation of CFTR Biogenesis by the Proteostatic Network and Pharmacological Modulators. Int J Mol Sci *21*.

58. Faggiano, S., Menon, R.P., Kelly, G.P., McCormick, J., Todi, S.V., Scaglione, K.M., Paulson, H.L., and Pastore, A. (2013). Enzymatic production of mono-ubiquitinated proteins for structural studies: The example of the Josephin domain of ataxin-3. FEBS Open Bio *3*, 453-458.

59. Farhan, H., Weiss, M., Tani, K., Kaufman, R.J., and Hauri, H.P. (2008). Adaptation of endoplasmic reticulum exit sites to acute and chronic increases in cargo load. EMBO J *27*, 2043-2054.

60. Farinha, C.M., and Amaral, M.D. (2005). Most F508del-CFTR is targeted to degradation at an early folding checkpoint and independently of calnexin. Mol Cell Biol *25*, 5242-5252.

61. Farinha, C.M., King-Underwood, J., Sousa, M., Correia, A.R., Henriques, B.J., Roxo-Rosa, M., Da Paula, A.C., Williams, J., Hirst, S., Gomes, C.M., *et al.* (2013). Revertants, low temperature, and correctors reveal the mechanism of F508del-CFTR rescue by VX-809 and suggest multiple agents for full correction. Chem Biol *20*, 943-955.

62. Farinha, C.M., Nogueira, P., Mendes, F., Penque, D., and Amaral, M.D. (2002). The human DnaJ homologue (Hdj)-1/heat-shock protein (Hsp) 40 co-chaperone is required for the in vivo stabilization of the cystic fibrosis transmembrane conductance regulator by Hsp70. Biochem J *366*, 797-806.

63. Farrell, P., Ferec, C., Macek, M., Frischer, T., Renner, S., Riss, K., Barton, D., Repetto, T., Tzetis, M., Giteau, K., *et al.* (2018). Estimating the age of p.(Phe508del) with family studies of geographically distinct European populations and the early spread of cystic fibrosis. Eur J Hum Genet *26*, 1832-1839.

64. Fay, J.F., Aleksandrov, L.A., Jensen, T.J., Cui, L.L., Kousouros, J.N., He, L., Aleksandrov, A.A., Gingerich, D.S., Riordan, J.R., and Chen, J.Z. (2018). Cryo-EM Visualization of an Active High Open Probability CFTR Anion Channel. Biochemistry *57*, 6234-6246.

65. Fisher, E.A., Lapierre, L.R., Junkins, R.D., and McLeod, R.S. (2008). The AAA-ATPase p97 facilitates degradation of apolipoprotein B by the ubiquitin-proteasome pathway. J Lipid Res *49*, 2149-2160.

66. Flume, P.A., Liou, T.G., Borowitz, D.S., Li, H., Yen, K., Ordonez, C.L., Geller, D.E., and VX 08-770-104 Study Group (2012). Ivacaftor in subjects with cystic fibrosis who are homozygous for the F508del-CFTR mutation. Chest *142*, 718-724.

67. Forloni, M., Liu, A.Y., and Wajapeyee, N. (2018). Creating Insertions or Deletions Using Overlap Extension Polymerase Chain Reaction (PCR) Mutagenesis. Cold Spring Harb Protoc *2018*.

68. Frayman, K.B., Armstrong, D.S., Grimwood, K., and Ranganathan, S.C. (2017). The airway microbiota in early cystic fibrosis lung disease. Pediatr Pulmonol *52*, 1384-1404.

69. Fromme, J.C., Orci, L., and Schekman, R. (2008). Coordination of COPII vesicle trafficking by Sec23. Trends Cell Biol *18*, 330-336.

70. Fu, L., Rab, A., Tang, L., Bebök, Z., Rowe, S.M., Bartoszewski, R., and Collawn, J.F. (2015). DeltaF508 CFTR surface stability is regulated by DAB2 and CHIP-mediated ubiquitination in post-endocytic compartments. PLoS One *10*, e0123131.

71. Fu, L., Rab, A., Tang, L.P., Rowe, S.M., Bebök, Z., and Collawn, J.F. (2012). Dab2 is a key regulator of endocytosis and post-endocytic trafficking of the cystic fibrosis transmembrane conductance regulator. Biochem J *441*, 633-643.

72. Fu, L., and Sztul, E. (2009). ER-associated complexes (ERACs) containing aggregated cystic fibrosis transmembrane conductance regulator (CFTR) are degraded by autophagy. Eur J Cell Biol *88*, 215-226.

73. Furukawa, B.S., and Flume, P.A. (2018). Nontuberculous Mycobacteria in Cystic Fibrosis. Semin Respir Crit Care Med *39*, 383-391.

74. Gabriel, S.E., Brigman, K.N., Koller, B.H., Boucher, R.C., and Stutts, M.J. (1994). Cystic fibrosis heterozygote resistance to cholera toxin in the cystic fibrosis mouse model. Science *266*, 107-109.

75. Gee, H.Y., Noh, S.H., Tang, B.L., Kim, K.H., and Lee, M.G. (2011). Rescue of DeltaF508-CFTR trafficking via a GRASP-dependent unconventional secretion pathway. Cell *146*, 746-760.

76. Gentzsch, M., Chang, X.B., Cui, L., Wu, Y., Ozols, V.V., Choudhury, A., Pagano, R.E., and Riordan, J.R. (2004). Endocytic trafficking routes of wild type and DeltaF508 cystic fibrosis transmembrane conductance regulator. Mol Biol Cell *15*, 2684-2696.

77. George, K.L., and Horne, W.S. (2018). Foldamer Tertiary Structure through Sequence-Guided Protein Backbone Alteration. Acc Chem Res *51*, 1220-1228.

78. Ghaemmaghami, S., Huh, W.K., Bower, K., Howson, R.W., Belle, A., Dephoure, N., O'Shea, E.K., and Weissman, J.S. (2003). Global analysis of protein expression in yeast. Nature *425*, 737-741.

79. Gilfillan, A., Warner, J.P., Kirk, J.M., Marshall, T., Greening, A., Ho, L.P., Hargreave, T., Stack, B., McIntyre, D., Davidson, R., *et al.* (1998). P67L: a cystic fibrosis allele with mild effects found at high frequency in the Scottish population. J Med Genet *35*, 122-125.

80. Gong, X., Ahner, A., Roldan, A., Lukacs, G.L., Thibodeau, P.H., and Frizzell, R.A. (2016). Non-native Conformers of Cystic Fibrosis Transmembrane Conductance

Regulator NBD1 Are Recognized by Hsp27 and Conjugated to SUMO-2 for Degradation. J Biol Chem *291*, 2004-2017.

81. Grosse-Onnebrink, J., Mellies, U., Olivier, M., Werner, C., and Stehling, F. (2017). Chest physiotherapy can affect the lung clearance index in cystic fibrosis patients. Pediatr Pulmonol *52*, 625-631.

82. Grove, D.E., Fan, C.Y., Ren, H.Y., and Cyr, D.M. (2011). The endoplasmic reticulum-associated Hsp40 DNAJB12 and Hsc70 cooperate to facilitate RMA1 E3-dependent degradation of nascent CFTRDeltaF508. Mol Biol Cell *22*, 301-314.

83. Grove, D.E., Rosser, M.F., Ren, H.Y., Naren, A.P., and Cyr, D.M. (2009). Mechanisms for rescue of correctable folding defects in CFTRDelta F508. Mol Biol Cell *20*, 4059-4069.

84. Guerriero, C.J., Reutter, K.R., Augustine, A.A., Preston, G.M., Weiberth, K.F., Mackie, T.D., Cleveland-Rubeor, H.C., Bethel, N.P., Callenberg, K.M., Nakatsukasa, K., *et al.* (2017). Transmembrane helix hydrophobicity is an energetic barrier during the retrotranslocation of integral membrane ERAD substrates. Mol Biol Cell *28*, 2076-2090.

85. Haggie, P.M., Kim, J.K., Lukacs, G.L., and Verkman, A.S. (2006). Tracking of quantum dot-labeled CFTR shows near immobilization by C-terminal PDZ interactions. Mol Biol Cell *17*, 4937-4945.

86. Haggie, P.M., Phuan, P.W., Tan, J.A., Xu, H., Avramescu, R.G., Perdomo, D., Zlock, L., Nielson, D.W., Finkbeiner, W.E., Lukacs, G.L., *et al.* (2016). Correctors and Potentiators Rescue Function of the Truncated W1282X-CFTR Translation Product. J Biol Chem *292*, 771-785.

87. Han, S.T., Rab, A., Pellicore, M.J., Davis, E.F., McCague, A.F., Evans, T.A., Joynt, A.T., Lu, Z., Cai, Z., Raraigh, K.S., *et al.* (2018). Residual function of cystic fibrosis mutants predicts response to small molecule CFTR modulators. JCI Insight *3*.

88. Hanrahan, J.W., Sato, Y., Carlile, G.W., Jansen, G., Young, J.C., and Thomas, D.Y. (2019). Cystic Fibrosis: Proteostatic correctors of CFTR trafficking and alternative therapeutic targets. Expert Opin Ther Targets *23*, 711-724.

89. Haq, I.J., Gray, M.A., Garnett, J.P., Ward, C., and Brodlie, M. (2016). Airway surface liquid homeostasis in cystic fibrosis: pathophysiology and therapeutic targets. Thorax *71*, 284-287.

90. Harada, K., Okiyoneda, T., Hashimoto, Y., Ueno, K., Nakamura, K., Yamahira, K., Sugahara, T., Shuto, T., Wada, I., Suico, M.A., *et al.* (2006). Calreticulin negatively regulates the cell surface expression of cystic fibrosis transmembrane conductance regulator. J Biol Chem *281*, 12841-12848.

91. Hayer, S.N., Deconinck, T., Bender, B., Smets, K., Zuchner, S., Reich, S., Schols, L., Schule, R., De Jonghe, P., Baets, J., *et al.* (2017). STUB1/CHIP mutations cause Gordon

Holmes syndrome as part of a widespread multisystemic neurodegeneration: evidence from four novel mutations. Orphanet J Rare Dis *12*, 31.

92. Hector, A., Kirn, T., Ralhan, A., Graepler-Mainka, U., Berenbrinker, S., Riethmueller, J., Hogardt, M., Wagner, M., Pfleger, A., Autenrieth, I., *et al.* (2016). Microbial colonization and lung function in adolescents with cystic fibrosis. J Cyst Fibros *15*, 340-349.

93. Heijerman, H.G.M., McKone, E.F., Downey, D.G., Van Braeckel, E., Rowe, S.M., Tullis, E., Mall, M.A., Welter, J.J., Ramsey, B.W., McKee, C.M., *et al.* (2019). Efficacy and safety of the elexacaftor plus tezacaftor plus ivacaftor combination regimen in people with cystic fibrosis homozygous for the F508del mutation: a double-blind, randomised, phase 3 trial. Lancet *394*, 1940-1948.

94. Heimdal, K., Sanchez-Guixe, M., Aukrust, I., Bollerslev, J., Bruland, O., Jablonski, G.E., Erichsen, A.K., Gude, E., Koht, J.A., Erdal, S., *et al.* (2014). STUB1 mutations in autosomal recessive ataxias - evidence for mutation-specific clinical heterogeneity. Orphanet J Rare Dis *9*, 146.

95. Hessa, T., Kim, H., Bihlmaier, K., Lundin, C., Boekel, J., Andersson, H., Nilsson, I., White, S.H., and von Heijne, G. (2005a). Recognition of transmembrane helices by the endoplasmic reticulum translocon. Nature *433*, 377-381.

96. Hessa, T., Meindl-Beinker, N.M., Bernsel, A., Kim, H., Sato, Y., Lerch-Bader, M., Nilsson, I., White, S.H., and von Heijne, G. (2007). Molecular code for transmembrane-helix recognition by the Sec61 translocon. Nature *450*, 1026-1030.

97. Hessa, T., White, S.H., and von Heijne, G. (2005b). Membrane insertion of a potassium-channel voltage sensor. Science *307*, 1427.

98. Hildebrandt, E., Mulky, A., Ding, H., Dai, Q., Aleksandrov, A.A., Bajrami, B., Diego, P.A., Wu, X., Ray, M., Naren, A.P., *et al.* (2015). A stable human-cell system overexpressing cystic fibrosis transmembrane conductance regulator recombinant protein at the cell surface. Mol Biotechnol *57*, 391-405.

99. Hoelen, H., Kleizen, B., Schmidt, A., Richardson, J., Charitou, P., Thomas, P.J., and Braakman, I. (2010). The primary folding defect and rescue of DeltaF508 CFTR emerge during translation of the mutant domain. PLoS One *5*, e15458.

100. Houck, S.A., and Cyr, D.M. (2012). Mechanisms for quality control of misfolded transmembrane proteins. Biochim Biophys Acta *1818*, 1108-1114.

101. Howard, M., Fischer, H., Roux, J., Santos, B.C., Gullans, S.R., Yancey, P.H., and Welch, W.J. (2003). Mammalian osmolytes and S-nitrosoglutathione promote Delta F508 cystic fibrosis transmembrane conductance regulator (CFTR) protein maturation and function. J Biol Chem *278*, 35159-35167.

102. Hung, G., and Flint, S.J. (2017). Normal human cell proteins that interact with the adenovirus type 5 E1B 55kDa protein. Virology *504*, 12-24.

103. Hutt, D.M., Roth, D.M., Chalfant, M.A., Youker, R.T., Matteson, J., Brodsky, J.L., and Balch, W.E. (2012). FK506 binding protein 8 peptidylprolyl isomerase activity manages a late stage of cystic fibrosis transmembrane conductance regulator (CFTR) folding and stability. J Biol Chem *287*, 21914-21925.

104. Hwang, T.C., Nagel, G., Nairn, A.C., and Gadsby, D.C. (1994). Regulation of the gating of cystic fibrosis transmembrane conductance regulator C1 channels by phosphorylation and ATP hydrolysis. Proc Natl Acad Sci U S A *91*, 4698-4702.

105. Hwang, T.C., Wang, F., Yang, I.C., and Reenstra, W.W. (1997). Genistein potentiates wild-type and delta F508-CFTR channel activity. Am J Physiol *273*, C988-C998.

106. Illek, B., Fischer, H., and Machen, T.E. (1996). Alternate stimulation of apical CFTR by genistein in epithelia. Am J Physiol *270*, C265-C275.

107. Illek, B., Fischer, H., Santos, G.F., Widdicombe, J.H., Machen, T.E., and Reenstra, W.W. (1995). cAMP-independent activation of CFTR Cl channels by the tyrosine kinase inhibitor genistein. Am J Physiol *268*, C886-C893.

108. Jensen, T.J., Loo, M.A., Pind, S., Williams, D.B., Goldberg, A.L., and Riordan, J.R. (1995). Multiple proteolytic systems, including the proteasome, contribute to CFTR processing. Cell *83*, 129-135.

109. Johnston, J.A., Ward, C.L., and Kopito, R.R. (1998). Aggresomes: a cellular response to misfolded proteins. J Cell Biol *143*, 1883-1898.

110. Joshi, D., Ehrhardt, A., Hong, J.S., and Sorscher, E.J. (2019). Cystic fibrosis precision therapeutics: Emerging considerations. Pediatr Pulmonol *54*, S13-S17.

111. Kabani, M., McLellan, C., Raynes, D.A., Guerriero, V., and Brodsky, J.L. (2002). HspBP1, a homologue of the yeast Fes1 and Sls1 proteins, is an Hsc70 nucleotide exchange factor. FEBS Lett *531*, 339-342.

112. Kamal, N., Surana, P., and Koh, C. (2018). Liver disease in patients with cystic fibrosis. Curr Opin Gastroenterol *34*, 146-151.

113. Keating, D., Marigowda, G., Burr, L., Daines, C., Mall, M.A., McKone, E.F., Ramsey, B.W., Rowe, S.M., Sass, L.A., Tullis, E., *et al.* (2018). VX-445-Tezacaftor-Ivacaftor in Patients with Cystic Fibrosis and One or Two Phe508del Alleles. N Engl J Med *379*, 1612-1620.

114. Kelly, J.W. (2019). Pharmacologic Approaches for Adapting Proteostasis in the Secretory Pathway to Ameliorate Protein Conformational Diseases. Cold Spring Harb Perspect Biol, a034108.

115. Kelsey, R., Manderson Koivula, F.N., McClenaghan, N.H., and Kelly, C. (2019). Cystic Fibrosis-Related Diabetes: Pathophysiology and Therapeutic Challenges. Clin Med Insights Endocrinol Diabetes *12*, 1-7.

116. Kerem, B.S., Zielenski, J., Markiewicz, D., Bozon, D., Gazit, E., Yahav, J., Kennedy, D., Riordan, J.R., Collins, F.S., and Rommens, J.M. (1990). Identification of mutations in regions corresponding to the two putative nucleotide (ATP)-binding folds of the cystic fibrosis gene. Proc Natl Acad Sci U S A *87*, 8447-8451.

117. Kim Chiaw, P., Eckford, P.D., and Bear, C.E. (2011). Insights into the mechanisms underlying CFTR channel activity, the molecular basis for cystic fibrosis and strategies for therapy. Essays Biochem *50*, 233-248.

118. Kim, J., Noh, S.H., Piao, H., Kim, D.H., Kim, K., Cha, J.S., Chung, W.Y., Cho, H.S., Kim, J.Y., and Lee, M.G. (2016). Monomerization and ER Relocalization of GRASP Is a Requisite for Unconventional Secretion of CFTR. Traffic *17*, 733-753.

119. Kleizen, B., van Vlijmen, T., de Jonge, H.R., and Braakman, I. (2005). Folding of CFTR is predominantly cotranslational. Mol Cell *20*, 277-287.

120. Komander, D., and Rape, M. (2012). The Ubiquitin Code. Annu Rev Biochem *81*, 203-229.

121. Kopp, Y., Lang, W.H., Schuster, T.B., Martinez-Limon, A., Hofbauer, H.F., Ernst, R., Calloni, G., and Vabulas, R.M. (2017). CHIP as a membrane-shuttling proteostasis sensor. Elife *6*.

122. Koulov, A.V., LaPointe, P., Lu, B., Razvi, A., Coppinger, J., Dong, M.Q., Matteson, J., Laister, R., Arrowsmith, C., Yates, J.R., 3rd, *et al.* (2010). Biological and structural basis for Aha1 regulation of Hsp90 ATPase activity in maintaining proteostasis in the human disease cystic fibrosis. Mol Biol Cell *21*, 871-884.

123. Kumari, V., Desai, S., and Ameen, N.A. (2017). AP2 alpha modulates cystic fibrosis transmembrane conductance regulator function in the human intestine. J Cyst Fibros *16*, 327-334.

124. Kundrat, L., and Regan, L. (2010). Identification of residues on Hsp70 and Hsp90 ubiquitinated by the cochaperone CHIP. J Mol Biol *395*, 587-594.

125. Labbadia, J., and Morimoto, R.I. (2015). The biology of proteostasis in aging and disease. Annu Rev Biochem *84*, 435-464.

126. Lee, S., Henderson, M.J., Schiffhauer, E., Despanie, J., Henry, K., Kang, P.W., Walker, D., McClure, M.L., Wilson, L., Sorscher, E.J., *et al.* (2014). Interference with ubiquitination in CFTR modifies stability of core glycosylated and cell surface pools. Mol Cell Biol *34*, 2554-2565.

127. LeGrys, V.A., Moon, T.C., Laux, J., Rock, M.J., and Accurso, F. (2018). Analytical and biological variation in repeated sweat chloride concentrations in clinical trials for CFTR modulator therapy. J Cyst Fibros *17*, 43-49.

128. Leto, D.E., Morgens, D.W., Zhang, L., Walczak, C.P., Elias, J.E., Bassik, M.C., and Kopito, R.R. (2019). Genome-wide CRISPR Analysis Identifies Substrate-Specific Conjugation Modules in ER-Associated Degradation. Mol Cell *73*, 377-389.

129. Li, W., Bengtson, M.H., Ulbrich, A., Matsuda, A., Reddy, V.A., Orth, A., Chanda, S.K., Batalov, S., and Joazeiro, C.A. (2008). Genome-wide and functional annotation of human E3 ubiquitin ligases identifies MULAN, a mitochondrial E3 that regulates the organelle's dynamics and signaling. PLoS One *3*, e1487.

130. Liu, C., Lou, W., Yang, J.C., Liu, L., Armstrong, C.M., Lombard, A.P., Zhao, R., Noel, O.D.V., Tepper, C.G., Chen, H.W., *et al.* (2018a). Proteostasis by STUB1/HSP70 complex controls sensitivity to androgen receptor targeted therapy in advanced prostate cancer. Nat Commun *9*, 4700.

131. Liu, F., Zhang, Z., Csanady, L., Gadsby, D.C., and Chen, J. (2017). Molecular Structure of the Human CFTR Ion Channel. Cell *169*, 85-95.

132. Liu, F., Zhang, Z., Levit, A., Levring, J., Touhara, K.K., Shoichet, B.K., and Chen, J. (2019). Structural identification of a hotspot on CFTR for potentiation. Science *364*, 1184-1188.

133. Liu, Q., Sabirzhanova, I., Yanda, M.K., Bergbower, E.A.S., Boinot, C., Guggino, W.B., and Cebotaru, L. (2018b). Rescue of CFTR NBD2 mutants N1303K and S1235R is influenced by the functioning of the autophagosome. J Cyst Fibros *17*, 582-594.

134. Locher, K.P. (2016). Mechanistic diversity in ATP-binding cassette (ABC) transporters. Nat Struct Mol Biol *23*, 487-493.

135. Logan, J., Hiestand, D., Daram, P., Huang, Z., Muccio, D.D., Hartman, J., Haley, B., Cook, W.J., and Sorscher, E.J. (1994). Cystic fibrosis transmembrane conductance regulator mutations that disrupt nucleotide binding. J Clin Invest *94*, 228-236.

136. Loo, M.A., Jensen, T.J., Cui, L., Hou, Y., Chang, X.B., and Riordan, J.R. (1998). Perturbation of Hsp90 interaction with nascent CFTR prevents its maturation and accelerates its degradation by the proteasome. EMBO J *17*, 6879-6887.

137. Loo, T.W., Bartlett, M.C., and Clarke, D.M. (2013). Corrector VX-809 stabilizes the first transmembrane domain of CFTR. Biochem Pharmacol *86*, 612-619.

138. Lopes-Pacheco, M., Boinot, C., Sabirzhanova, I., Rapino, D., and Cebotaru, L. (2017). Combination of Correctors Rescues CFTR Transmembrane-Domain Mutants by Mitigating their Interactions with Proteostasis. Cell Physiol Biochem *41*, 2194-2210.

139. Lopes-Pacheco, M., Sabirzhanova, I., Rapino, D., Morales, M.M., Guggino, W.B., and Cebotaru, L. (2016). Correctors rescue CFTR mutations in nucleotide-binding domain 1 (NBD1) by modulating proteostasis. Chembiochem.

140. Loureiro, C.A., Matos, A.M., Dias-Alves, A., Pereira, J.F., Uliyakina, I., Barros, P., Amaral, M.D., and Matos, P. (2015). A molecular switch in the scaffold NHERF1 enables misfolded CFTR to evade the peripheral quality control checkpoint. Sci Signal *8*, ra48.

141. Luan, H., Mohapatra, B., Bielecki, T.A., Mushtaq, I., Mirza, S., Jennings, T.A., Clubb, R.J., An, W., Ahmed, D., El-Ansari, R., *et al.* (2018). Loss of the Nuclear Pool of Ubiquitin Ligase CHIP/STUB1 in Breast Cancer Unleashes the MZF1-Cathepsin Pro-oncogenic Program. Cancer Res *78*, 2524-2535.

142. Luciani, A., Villella, V.R., Esposito, S., Brunetti-Pierri, N., Medina, D., Settembre, C., Gavina, M., Pulze, L., Giardino, I., Pettoello-Mantovani, M., *et al.* (2010). Defective CFTR induces aggresome formation and lung inflammation in cystic fibrosis through ROS-mediated autophagy inhibition. Nat Cell Biol *12*, 863-875.

143. Lukacs, G.L., Chang, X.B., Bear, C., Kartner, N., Mohamed, A., Riordan, J.R., and Grinstein, S. (1993). The delta F508 mutation decreases the stability of cystic fibrosis transmembrane conductance regulator in the plasma membrane. Determination of functional half-lives on transfected cells. J Biol Chem *268*, 21592-21598.

144. Lukacs, G.L., Mohamed, A., Kartner, N., Chang, X.B., Riordan, J.R., and Grinstein, S. (1994). Conformational maturation of CFTR but not its mutant counterpart (delta F508) occurs in the endoplasmic reticulum and requires ATP. EMBO J *13*, 6076-6086.

145. Lukacs, G.L., Segal, G., Kartner, N., Grinstein, S., and Zhang, F. (1997). Constitutive internalization of cystic fibrosis transmembrane conductance regulator occurs via clathrin-dependent endocytosis and is regulated by protein phosphorylation. Biochem J *328 (Pt 2)*, 353-361.

146. Ma, T., Vetrivel, L., Yang, H., Pedemonte, N., Zegarra-Moran, O., Galietta, L.J., and Verkman, A.S. (2002). High-affinity activators of cystic fibrosis transmembrane conductance regulator (CFTR) chloride conductance identified by high-throughput screening. J Biol Chem *277*, 37235-37241.

147. Madrigal, S.C., McNeil, Z., Sanchez-Hodge, R., Shi, C.H., Patterson, C., Scaglione, K.M., and Schisler, J.C. (2019). Changes in protein function underlie the disease spectrum in patients with CHIP mutations. J Biol Chem *294*, 19236-19245.

148. Maqbool, A., and Pauwels, A. (2017). Cystic Fibrosis and gastroesophageal reflux disease. J Cyst Fibros *16*, S2-S13.

149. Marozkina, N.V., Yemen, S., Borowitz, M., Liu, L., Plapp, M., Sun, F., Islam, R., Erdmann-Gilmore, P., Townsend, R.R., Lichti, C.F., *et al.* (2010a). Hsp 70/Hsp 90 organizing protein as a nitrosylation target in cystic fibrosis therapy. Proc Natl Acad Sci U S A *107*, 11393-11398.

150. Marozkina, N.V., Yemen, S., Borowitz, M., Liu, L., Plapp, M., Sun, F., Islam, R., Erdmann-Gilmore, P., Townsend, R.R., Lichti, C.F., *et al.* (2010b). Hsp 70/Hsp 90

organizing protein as a nitrosylation target in cystic fibrosis therapy. Proc Natl Acad Sci U S A *107*, 11393-11398.

151. Matsumura, Y., David, L.L., and Skach, W.R. (2011). Role of Hsc70 binding cycle in CFTR folding and endoplasmic reticulum-associated degradation. Mol Biol Cell *22*, 2797-2809.

152. McIlwaine, M., Button, B., and Nevitt, S.J. (2019). Positive expiratory pressure physiotherapy for airway clearance in people with cystic fibrosis. Cochrane Database Syst Rev *2019*.

153. Meacham, G.C., Lu, Z., King, S., Sorscher, E., Tousson, A., and Cyr, D.M. (1999). The Hdj-2/Hsc70 chaperone pair facilitates early steps in CFTR biogenesis. EMBO J *18*, 1492-1505.

154. Meacham, G.C., Patterson, C., Zhang, W., Younger, J.M., and Cyr, D.M. (2001). The Hsc70 co-chaperone CHIP targets immature CFTR for proteasomal degradation. Nat Cell Biol *3*, 100-105.

155. Mehnert, M., Sommer, T., and Jarosch, E. (2014). Der1 promotes movement of misfolded proteins through the endoplasmic reticulum membrane. Nat Cell Biol *16*, 77-86.

156. Mehnert, M., Sommermeyer, F., Berger, M., Kumar Lakshmipathy, S., Gauss, R., Aebi, M., Jarosch, E., and Sommer, T. (2015). The interplay of Hrd3 and the molecular chaperone system ensures efficient degradation of malfolded secretory proteins. Mol Biol Cell *26*, 185-194.

157. Mendoza, J.L., Schmidt, A., Li, Q., Nuvaga, E., Barrett, T., Bridges, R.J., Feranchak, A.P., Brautigam, C.A., and Thomas, P.J. (2012). Requirements for efficient correction of DeltaF508 CFTR revealed by analyses of evolved sequences. Cell *148*, 164-174.

158. Middleton, P.G., Mall, M.A., Drevinek, P., Lands, L.C., McKone, E.F., Polineni, D., Ramsey, B.W., Taylor-Cousar, J.L., Tullis, E., Vermeulen, F., *et al.* (2019). Elexacaftor-Tezacaftor-Ivacaftor for Cystic Fibrosis with a Single Phe508del Allele. N Engl J Med *381*, 1809-1819.

159. Mogayzel, P.J., Jr., Naureckas, E.T., Robinson, K.A., Brady, C., Guill, M., Lahiri, T., Lubsch, L., Matsui, J., Oermann, C.M., Ratjen, F., *et al.* (2014). Cystic Fibrosis Foundation pulmonary guideline. pharmacologic approaches to prevention and eradication of initial Pseudomonas aeruginosa infection. Ann Am Thorac Soc *11*, 1640-1650.

160. Mogk, A., Ruger-Herreros, C., and Bukau, B. (2019). Cellular Functions and Mechanisms of Action of Small Heat Shock Proteins. Annu Rev Microbiol *73*, 89-110.

161. Moheet, A., and Moran, A. (2018). Pharmacological management of cystic fibrosis related diabetes. Expert Rev Clin Pharmacol *11*, 185-191.

162. Moran, O. (2014). On the structural organization of the intracellular domains of CFTR. Int J Biochem Cell Biol *52*, 7-14.

163. Morito, D., Hirao, K., Oda, Y., Hosokawa, N., Tokunaga, F., Cyr, D.M., Tanaka, K., Iwai, K., and Nagata, K. (2008). Gp78 cooperates with RMA1 in endoplasmic reticulum-associated degradation of CFTRDeltaF508. Mol Biol Cell *19*, 1328-1336.

164. Mornon, J.P., Lehn, P., and Callebaut, I. (2008). Atomic model of human cystic fibrosis transmembrane conductance regulator: membrane-spanning domains and coupling interfaces. Cell Mol Life Sci *65*, 2594-2612.

165. Murata, S., Minami, Y., Minami, M., Chiba, T., and Tanaka, K. (2001). CHIP is a chaperone-dependent E3 ligase that ubiquitylates unfolded protein. EMBO Rep *2*, 1133-1138.

166. Nakasone, M.A., Lewis, T.A., Walker, O., Thakur, A., Mansour, W., Castaneda, C.A., Goeckeler-Fried, J.L., Parlati, F., Chou, T.F., Hayat, O., *et al.* (2017). Structural Basis for the Inhibitory Effects of Ubistatins in the Ubiquitin-Proteasome Pathway. Structure *25*, 1839-1855 e1811.

167. Nakatsukasa, K., and Brodsky, J.L. (2010). in vitro reconstitution of the selection, ubiquitination, and membrane extraction of a polytopic ERAD substrate. Methods Mol Biol *619*, 365-376.

168. Nakatsukasa, K., Huyer, G., Michaelis, S., and Brodsky, J.L. (2008). Dissecting the ER-associated degradation of a misfolded polytopic membrane protein. Cell *132*, 101-112.

169. Narayan, V., Landre, V., Ning, J., Hernychova, L., Muller, P., Verma, C., Walkinshaw, M.D., Blackburn, E.A., and Ball, K.L. (2015). Protein-Protein Interactions Modulate the Docking-Dependent E3-Ubiquitin Ligase Activity of Carboxy-Terminus of Hsc70-Interacting Protein (CHIP). Mol Cell Proteomics *14*, 2973-2987.

170. Needham, P.G., Guerriero, C.J., and Brodsky, J.L. (2019). Chaperoning Endoplasmic Reticulum-Associated Degradation (ERAD) and Protein Conformational Diseases. Cold Spring Harb Perspect Biol *11*.

171. Nikolay, R., Wiederkehr, T., Rist, W., Kramer, G., Mayer, M.P., and Bukau, B. (2004). Dimerization of the human E3 ligase CHIP via a coiled-coil domain is essential for its activity. J Biol Chem *279*, 2673-2678.

172. O'Donnell, B.M., Mackie, T.D., Subramanya, A.R., and Brodsky, J.L. (2017). Endoplasmic reticulum-associated degradation of the renal potassium channel, ROMK, leads to type II Bartter syndrome. J Biol Chem *292*, 12813-12827.

173. Oberdorf, J., Carlson, E.J., and Skach, W.R. (2001). Redundancy of mammalian proteasome beta subunit function during endoplasmic reticulum associated degradation. Biochemistry *40*, 13397-13405.

174. Oberdorf, J., Pitonzo, D., and Skach, W.R. (2005). An energy-dependent maturation step is required for release of the cystic fibrosis transmembrane conductance regulator from early endoplasmic reticulum biosynthetic machinery. J Biol Chem *280*, 38193-38202.

175. Ojemalm, K., Halling, K.K., Nilsson, I., and von Heijne, G. (2012). Orientational preferences of neighboring helices can drive ER insertion of a marginally hydrophobic transmembrane helix. Mol Cell *45*, 529-540.

176. Okazuka, K., and Ishida, T. (2018). Proteasome inhibitors for multiple myeloma. Jpn J Clin Oncol *48*, 785-793.

177. Okiyoneda, T., Barriere, H., Bagdany, M., Rabeh, W.M., Du, K., Hohfeld, J., Young, J.C., and Lukacs, G.L. (2010). Peripheral protein quality control removes unfolded CFTR from the plasma membrane. Science *329*, 805-810.

178. Okiyoneda, T., Niibori, A., Harada, K., Kohno, T., Michalak, M., Duszyk, M., Wada, I., Ikawa, M., Shuto, T., Suico, M.A., *et al.* (2008). Role of calnexin in the ER quality control and productive folding of CFTR; differential effect of calnexin knockout on wild-type and DeltaF508 CFTR. Biochim Biophys Acta *1783*, 1585-1594.

179. Okiyoneda, T., Veit, G., Dekkers, J.F., Bagdany, M., Soya, N., Xu, H., Roldan, A., Verkman, A.S., Kurth, M., Simon, A., *et al.* (2013). Mechanism-based corrector combination restores DeltaF508-CFTR folding and function. Nat Chem Biol *9*, 444-454.

180. Okiyoneda, T., Veit, G., Sakai, R., Aki, M., Fujihara, T., Higashi, M., Susuki-Miyata, S., Miyata, M., Fukuda, N., Yoshida, A., *et al.* (2018). Chaperone-Independent Peripheral Quality Control of CFTR by RFFL E3 Ligase. Dev Cell *44*, 694-708.

181. Ostedgaard, L.S., Rogers, C.S., Dong, Q., Randak, C.O., Vermeer, D.W., Rokhlina, T., Karp, P.H., and Welsh, M.J. (2007). Processing and function of CFTR-DeltaF508 are species-dependent. Proc Natl Acad Sci U S A *104*, 15370-15375.

182. Pabon, N.A., Xia, Y., Estabrooks, S.K., Ye, Z., Herbrand, A.K., Suss, E., Biondi, R.M., Assimon, V.A., Gestwicki, J.E., Brodsky, J.L., *et al.* (2018). Predicting protein targets for drug-like compounds using transcriptomics. PLoS Comput Biol *14*, e1006651.

183. Page, R.C., Pruneda, J.N., Amick, J., Klevit, R.E., and Misra, S. (2012). Structural insights into the conformation and oligomerization of E2~ubiquitin conjugates. Biochemistry *51*, 4175-4187.

184. Pankow, S., Bamberger, C., Calzolari, D., Martinez-Bartolome, S., Lavallee-Adam, M., Balch, W.E., and Yates, J.R., 3rd (2015). F508 CFTR interactome remodelling promotes rescue of cystic fibrosis. Nature *528*, 510-516.

185. Patrick, A.E., Karamyshev, A.L., Millen, L., and Thomas, P.J. (2011). Alteration of CFTR transmembrane span integration by disease-causing mutations. Mol Biol Cell *22*, 4461-4471.

186. Pedemonte, N., Lukacs, G.L., Du, K., Caci, E., Zegarra-Moran, O., Galietta, L.J., and Verkman, A.S. (2005). Small-molecule correctors of defective DeltaF508-CFTR cellular processing identified by high-throughput screening. J Clin Invest *115*, 2564-2571.

187. Peter, K., Varga, K., Bebök, Z., McNicholas-Bevensee, C.M., Schwiebert, L., Sorscher, E.J., Schwiebert, E.M., and Collawn, J.F. (2002). Ablation of internalization signals in the carboxyl-terminal tail of the cystic fibrosis transmembrane conductance regulator enhances cell surface expression. J Biol Chem *277*, 49952-49957.

188. Pezzulo, A.A., Tang, X.X., Hoegger, M.J., Abou Alaiwa, M.H., Ramachandran, S., Moninger, T.O., Karp, P.H., Wohlford-Lenane, C.L., Haagsman, H.P., van Eijk, M., *et al.* (2012). Reduced airway surface pH impairs bacterial killing in the porcine cystic fibrosis lung. Nature *487*, 109-113.

189. Piao, H., Kim, J., Noh, S.H., Kweon, H.S., Kim, J.Y., and Lee, M.G. (2017). Sec16A is critical for both conventional and unconventional secretion of CFTR. Sci Rep *7*, 39887.

190. Pind, S., Riordan, J.R., and Williams, D.B. (1994). Participation of the endoplasmic reticulum chaperone calnexin (p88, IP90) in the biogenesis of the cystic fibrosis transmembrane conductance regulator. J Biol Chem *269*, 12784-12788.

191. Pitonzo, D., Yang, Z., Matsumura, Y., Johnson, A.E., and Skach, W.R. (2009). Sequence-specific retention and regulated integration of a nascent membrane protein by the endoplasmic reticulum Sec61 translocon. Mol Biol Cell *20*, 685-698.

192. Preston, G.M., and Brodsky, J.L. (2017). The evolving role of ubiquitin modification in endoplasmic reticulum-associated degradation. Biochem J *474*, 445-469.

193. Preston, G.M., Guerriero, C.J., Metzger, M.B., Michaelis, S., and Brodsky, J.L. (2018). Substrate Insolubility Dictates Hsp104-Dependent Endoplasmic-Reticulum-Associated Degradation. Mol Cell *70*, 242-253 e246.

194. Qian, S.B., McDonough, H., Boellmann, F., Cyr, D.M., and Patterson, C. (2006). CHIP-mediated stress recovery by sequential ubiquitination of substrates and Hsp70. Nature *440*, 551-555.

195. Qu, B.H., Strickland, E.H., and Thomas, P.J. (1997). Localization and suppression of a kinetic defect in cystic fibrosis transmembrane conductance regulator folding. J Biol Chem *272*, 15739-15744.

196. Qu, D., Teckman, J.H., Omura, S., and Perlmutter, D.H. (1996). Degradation of a mutant secretory protein, alpha1-antitrypsin Z, in the endoplasmic reticulum requires proteasome activity. J Biol Chem *271*, 22791-22795.

197. Quittner, A.L., Goldbeck, L., Abbott, J., Duff, A., Lambrecht, P., Sole, A., Tibosch, M.M., Bergsten Brucefors, A., Yuksel, H., Catastini, P., *et al.* (2014). Prevalence of depression and anxiety in patients with cystic fibrosis and parent caregivers: results of

The International Depression Epidemiological Study across nine countries. Thorax *69*, 1090-1097.

198. Rabeh, W.M., Bossard, F., Xu, H., Okiyoneda, T., Bagdany, M., Mulvihill, C.M., Du, K., di Bernardo, S., Liu, Y., Konermann, L., *et al.* (2012). Correction of both NBD1 energetics and domain interface is required to restore DeltaF508 CFTR folding and function. Cell *148*, 150-163.

199. Ram, S.J., and Kirk, K.L. (1989). Cl- permeability of human sweat duct cells monitored with fluorescence-digital imaging microscopy: evidence for reduced plasma membrane Cl- permeability in cystic fibrosis. Proc Natl Acad Sci U S A *86*, 10166-10170.

200. Ramsey, B.W., Davies, J., McElvaney, N.G., Tullis, E., Bell, S.C., Drevinek, P., Griese, M., McKone, E.F., Wainwright, C.E., Konstan, M.W., *et al.* (2011). A CFTR potentiator in patients with cystic fibrosis and the G551D mutation. N Engl J Med *365*, 1663-1672.

201. Rapino, D., Sabirzhanova, I., Lopes-Pacheco, M., Grover, R., Guggino, W.B., and Cebotaru, L. (2015). Rescue of NBD2 mutants N1303K and S1235R of CFTR by small-molecule correctors and transcomplementation. PLoS One *10*, e0119796.

202. Rapoport, T.A., Li, L., and Park, E. (2017). Structural and Mechanistic Insights into Protein Translocation. Annu Rev Cell Dev Biol *33*, 369-390.

203. Ratjen, F., Hug, C., Marigowda, G., Tian, S., Huang, X., Stanojevic, S., Milla, C.E., Robinson, P.D., Waltz, D., Davies, J.C., *et al.* (2017). Efficacy and safety of lumacaftor and ivacaftor in patients aged 6-11 years with cystic fibrosis homozygous for F508del-CFTR: a randomised, placebo-controlled phase 3 trial. Lancet Respir Med *5*, 557-567.

204. Ratner, M. (2017). FDA deems in vitro data on mutations sufficient to expand cystic fibrosis drug label. Nat Biotechnol *35*, 606.

205. Ren, H.Y., Grove, D.E., De La Rosa, O., Houck, S.A., Sopha, P., Van Goor, F., Hoffman, B.J., and Cyr, D.M. (2013). VX-809 corrects folding defects in cystic fibrosis transmembrane conductance regulator protein through action on membrane-spanning domain 1. Mol Biol Cell *24*, 3016-3024.

206. Richardson, P.G., Sonneveld, P., Schuster, M.W., Irwin, D., Stadtmauer, E.A., Facon, T., Harousseau, J.L., Ben-Yehuda, D., Lonial, S., Goldschmidt, H., *et al.* (2005). Bortezomib or high-dose dexamethasone for relapsed multiple myeloma. N Engl J Med *352*, 2487-2498.

207. Richly, H., Rape, M., Braun, S., Rumpf, S., Hoege, C., and Jentsch, S. (2005). A series of ubiquitin binding factors connects CDC48/p97 to substrate multiubiquitylation and proteasomal targeting. Cell *120*, 73-84.

208. Riordan, J.R., Rommens, J.M., Kerem, B., Alon, N., Rozmahel, R., Grzelczak, Z., Zielenski, J., Lok, S., Plavsic, N., and Chou, J.L. (1989). Identification of the cystic

fibrosis gene: cloning and characterization of complementary DNA. Science *245*, 1066-1073.

209. Rosen, B.H., Evans, T.I.A., Moll, S.R., Gray, J.S., Liang, B., Sun, X., Zhang, Y., Jensen-Cody, C.W., Swatek, A.M., Zhou, W., *et al.* (2018). Infection is Not Required for Mucoinflammatory Lung Disease in CFTR-knockout Ferrets. Am J Respir Crit Care Med *197*, 1308-1318.

210. Rosenbaum, J.C., Fredrickson, E.K., Oeser, M.L., Garrett-Engele, C.M., Locke, M.N., Richardson, L.A., Nelson, Z.W., Hetrick, E.D., Milac, T.I., Gottschling, D.E., *et al.* (2011). Disorder targets misorder in nuclear quality control degradation: a disordered ubiquitin ligase directly recognizes its misfolded substrates. Mol Cell *41*, 93-106.

211. Rosser, M.F., Grove, D.E., Chen, L., and Cyr, D.M. (2008). Assembly and misassembly of cystic fibrosis transmembrane conductance regulator: folding defects caused by deletion of F508 occur before and after the calnexin-dependent association of membrane spanning domain (MSD) 1 and MSD2. Mol Biol Cell *19*, 4570-4579.

212. Rubenstein, R.C., Egan, M.E., and Zeitlin, P.L. (1997). In vitro pharmacologic restoration of CFTR-mediated chloride transport with sodium 4-phenylbutyrate in cystic fibrosis epithelial cells containing delta F508-CFTR. J Clin Invest *100*, 2457-2465.

213. Rubenstein, R.C., and Zeitlin, P.L. (1998). A pilot clinical trial of oral sodium 4-phenylbutyrate (Buphenyl) in deltaF508-homozygous cystic fibrosis patients: partial restoration of nasal epithelial CFTR function. Am J Respir Crit Care Med *157*, 484-490.

214. Rubenstein, R.C., and Zeitlin, P.L. (2000). Sodium 4-phenylbutyrate downregulates Hsc70: implications for intracellular trafficking of DeltaF508-CFTR. Am J Physiol Cell Physiol *278*, C259-C267.

215. Ruggiano, A., Foresti, O., and Carvalho, P. (2014). Quality control: ER-associated degradation: protein quality control and beyond. J Cell Biol *204*, 869-879.

216. Sabusap, C.M., Wang, W., McNicholas, C.M., Chung, W.J., Fu, L., Wen, H., Mazur, M., Kirk, K.L., Collawn, J.F., Hong, J.S., *et al.* (2016). Analysis of cystic fibrosis-associated P67L CFTR illustrates barriers to personalized therapeutics for orphan diseases. JCI Insight *1*.

217. Sato, S., Ward, C.L., and Kopito, R.R. (1998). Cotranslational ubiquitination of cystic fibrosis transmembrane conductance regulator in vitro. J Biol Chem *273*, 7189-7192.

218. Sato, S., Ward, C.L., Krouse, M.E., Wine, J.J., and Kopito, R.R. (1996). Glycerol reverses the misfolding phenotype of the most common cystic fibrosis mutation. J Biol Chem *271*, 635-638.

219. Sawicki, G.S., McKone, E.F., Pasta, D.J., Millar, S.J., Wagener, J.S., Johnson, C.A., and Konstan, M.W. (2015). Sustained Benefit from ivacaftor demonstrated by combining

clinical trial and cystic fibrosis patient registry data. Am J Respir Crit Care Med *192*, 836-842.

220. Saxena, A., Banasavadi-Siddegowda, Y.K., Fan, Y., Bhattacharya, S., Roy, G., Giovannucci, D.R., Frizzell, R.A., and Wang, X. (2012). Human heat shock protein 105/110 kDa (Hsp105/110) regulates biogenesis and quality control of misfolded cystic fibrosis transmembrane conductance regulator at multiple levels. J Biol Chem *287*, 19158-19170.

221. Scaglione, K.M., Zavodszky, E., Todi, S.V., Patury, S., Xu, P., Rodriguez-Lebron, E., Fischer, S., Konen, J., Djarmati, A., Peng, J., *et al.* (2011). Ube2w and ataxin-3 coordinately regulate the ubiquitin ligase CHIP. Mol Cell *43*, 599-612.

222. Schmidt, B.Z., Watts, R.J., Aridor, M., and Frizzell, R.A. (2009). Cysteine string protein promotes proteasomal degradation of the cystic fibrosis transmembrane conductance regulator (CFTR) by increasing its interaction with the C terminus of Hsp70-interacting protein and promoting CFTR ubiquitylation. J Biol Chem *284*, 4168-4178.

223. Scott-Ward, T.S., and Amaral, M.D. (2009). Deletion of Phe508 in the first nucleotide-binding domain of the cystic fibrosis transmembrane conductance regulator increases its affinity for the heat shock cognate 70 chaperone. FEBS J *276*, 7097-7109.

224. Servetnyk, Z., Krjukova, J., Gaston, B., Zaman, K., Hjelte, L., Roomans, G.M., and Dragomir, A. (2006). Activation of chloride transport in CF airway epithelial cell lines and primary CF nasal epithelial cells by S-nitrosoglutathione. Respir Res *7*, 124.

225. Shah, V.S., Meyerholz, D.K., Tang, X.X., Reznikov, L., Abou Alaiwa, M., Ernst, S.E., Karp, P.H., Wohlford-Lenane, C.L., Heilmann, K.P., Leidinger, M.R., *et al.* (2016). Airway acidification initiates host defense abnormalities in cystic fibrosis mice. Science *351*, 503-507.

226. Shang, Y., He, J., Wang, Y., Feng, Q., Zhang, Y., Guo, J., Li, J., Li, S., Wang, Y., Yan, G., *et al.* (2017). CHIP/Stub1 regulates the Warburg effect by promoting degradation of PKM2 in ovarian carcinoma. Oncogene *36*, 4191-4200.

227. Sharma, M., Benharouga, M., Hu, W., and Lukacs, G.L. (2001). Conformational and temperature-sensitive stability defects of the delta F508 cystic fibrosis transmembrane conductance regulator in post-endoplasmic reticulum compartments. J Biol Chem *276*, 8942-8950.

228. Sharma, M., Pampinella, F., Nemes, C., Benharouga, M., So, J., Du, K., Bache, K.G., Papsin, B., Zerangue, N., Stenmark, H., *et al.* (2004). Misfolding diverts CFTR from recycling to degradation: quality control at early endosomes. J Cell Biol *164*, 923-933.

229. Sheppard, D.N., Ostedgaard, L.S., Winter, M.C., and Welsh, M.J. (1995). Mechanism of dysfunction of two nucleotide binding domain mutations in cystic fibrosis transmembrane conductance regulator that are associated with pancreatic sufficiency. EMBO J *14*, 876-883.

230. Sheppard, D.N., and Welsh, M.J. (1999). Structure and function of the CFTR chloride channel. Physiol Rev *79*, S23-S45.

231. Shi, C.H., Schisler, J.C., Rubel, C.E., Tan, S., Song, B., McDonough, H., Xu, L., Portbury, A.L., Mao, C.Y., True, C., *et al.* (2014). Ataxia and hypogonadism caused by the loss of ubiquitin ligase activity of the U box protein CHIP. Hum Mol Genet *23*, 1013-1024.

232. Shi, Y., Wang, J., Li, J.D., Ren, H., Guan, W., He, M., Yan, W., Zhou, Y., Hu, Z., Zhang, J., *et al.* (2013). Identification of CHIP as a novel causative gene for autosomal recessive cerebellar ataxia. PLoS One *8*, e81884.

233. Shurtleff, M.J., Itzhak, D.N., Hussmann, J.A., Schirle Oakdale, N.T., Costa, E.A., Jonikas, M., Weibezahn, J., Popova, K.D., Jan, C.H., Sinitcyn, P., *et al.* (2018). The ER membrane protein complex interacts cotranslationally to enable biogenesis of multipass membrane proteins. Elife *7*.

234. Singh, V.K., and Schwarzenberg, S.J. (2017). Pancreatic insufficiency in Cystic Fibrosis. J Cyst Fibros *16*, S70-S78.

235. Smith, B.A., Georgiopoulos, A.M., and Quittner, A.L. (2016). Maintaining mental health and function for the long run in cystic fibrosis. Pediatr Pulmonol *51*, S71-S78.

236. Snyder, A.H., McPherson, M.E., Hunt, J.F., Johnson, M., Stamler, J.S., and Gaston, B. (2002). Acute effects of aerosolized S-nitrosoglutathione in cystic fibrosis. Am J Respir Crit Care Med *165*, 922-926.

237. Song, J., Kose, S., Watanabe, A., Son, S.Y., Choi, S., Hong, H., Yamashita, E., Park, I.Y., Imamoto, N., and Lee, S.J. (2015). Structural and functional analysis of Hikeshi, a new nuclear transport receptor of Hsp70s. Acta Crystallogr D Biol Crystallogr *71*, 473-483.

238. Sosnay, P.R., Siklosi, K.R., Van Goor, F., Kaniecki, K., Yu, H., Sharma, N., Ramalho, A.S., Amaral, M.D., Dorfman, R., Zielenski, J., *et al.* (2013). Defining the disease liability of variants in the cystic fibrosis transmembrane conductance regulator gene. Nat Genet *45*, 1160-1167.

239. Staub, O., Gautschi, I., Ishikawa, T., Breitschopf, K., Ciechanover, A., Schild, L., and Rotin, D. (1997). Regulation of stability and function of the epithelial Na+ channel (ENaC) by ubiquitination. EMBO J *16*, 6325-6336.

240. Strickland, E., Qu, B.H., Millen, L., and Thomas, P.J. (1997). The molecular chaperone Hsc70 assists the in vitro folding of the N-terminal nucleotide-binding domain of the cystic fibrosis transmembrane conductance regulator. J Biol Chem *272*, 25421-25424.

241. Subramanian, A., Narayan, R., Corsello, S.M., Peck, D.D., Natoli, T.E., Lu, X., Gould, J., Davis, J.F., Tubelli, A.A., Asiedu, J.K., *et al.* (2017). A Next Generation Connectivity Map: L1000 Platform and the First 1,000,000 Profiles. Cell *171*, 1437-1452 e1417.

242. Sun, C., Li, H.L., Chen, H.R., Shi, M.L., Liu, Q.H., Pan, Z.Q., Bai, J., and Zheng, J.N. (2015). Decreased expression of CHIP leads to increased angiogenesis via VEGF-VEGFR2 pathway and poor prognosis in human renal cell carcinoma. Sci Rep *5*, 9774.

243. Sun, F., Zhang, R., Gong, X., Geng, X., Drain, P.F., and Frizzell, R.A. (2006). Derlin-1 promotes the efficient degradation of the cystic fibrosis transmembrane conductance regulator (CFTR) and CFTR folding mutants. J Biol Chem *281*, 36856-36863.

244. Swiatecka-Urban, A., Boyd, C., Coutermarsh, B., Karlson, K.H., Barnaby, R., Aschenbrenner, L., Langford, G.M., Hasson, T., and Stanton, B.A. (2004). Myosin VI regulates endocytosis of the cystic fibrosis transmembrane conductance regulator. J Biol Chem *279*, 38025-38031.

245. Synofzik, M., Schule, R., Schulze, M., Gburek-Augustat, J., Schweizer, R., Schirmacher, A., Krageloh-Mann, I., Gonzalez, M., Young, P., Zuchner, S., *et al.* (2014). Phenotype and frequency of STUB1 mutations: next-generation screenings in Caucasian ataxia and spastic paraplegia cohorts. Orphanet J Rare Dis *9*, 57.

246. Szczesniak, R., Heltshe, S.L., Stanojevic, S., and Mayer-Hamblett, N. (2017). Use of FEV1 in cystic fibrosis epidemiologic studies and clinical trials: A statistical perspective for the clinical researcher. J Cyst Fibros *16*, 318-326.

247. Tang, D.E., Dai, Y., Lin, L.W., Xu, Y., Liu, D.Z., Hong, X.P., Jiang, H.W., and Xu, S.H. (2019). STUB1 suppresseses tumorigenesis and chemoresistance through antagonizing YAP1 signaling. Cancer Sci *110*, 3145-3156.

248. Tannous, A., Pisoni, G.B., Hebert, D.N., and Molinari, M. (2015). N-linked sugar-regulated protein folding and quality control in the ER. Semin Cell Dev Biol *41*, 79-89.

249. Thomas, P.J., Shenbagamurthi, P., Sondek, J., Hullihen, J.M., and Pedersen, P.L. (1992). The cystic fibrosis transmembrane conductance regulator. Effects of the most common cystic fibrosis-causing mutation on the secondary structure and stability of a synthetic peptide. J Biol Chem *267*, 5727-5730.

250. Todi, S.V., Scaglione, K.M., Blount, J.R., Basrur, V., Conlon, K.P., Pastore, A., Elenitoba-Johnson, K., and Paulson, H.L. (2010). Activity and cellular functions of the deubiquitinating enzyme and polyglutamine disease protein ataxin-3 are regulated by ubiquitination at lysine 117. J Biol Chem *285*, 39303-39313.

251. Todi, S.V., Winborn, B.J., Scaglione, K.M., Blount, J.R., Travis, S.M., and Paulson, H.L. (2009). Ubiquitination directly enhances activity of the deubiquitinating enzyme ataxin-3. EMBO J *28*, 372-382.

252. Tomati, V., Sondo, E., Armirotti, A., Caci, E., Pesce, E., Marini, M., Gianotti, A., Ju Jeon, Y., Cilli, M., Pistorio, A., *et al.* (2015). Genetic Inhibition Of The Ubiquitin Ligase Rnf5 Attenuates Phenotypes Associated To F508del Cystic Fibrosis Mutation. Sci Rep *5*, 12138.

253. Usmani, S.S., Bedi, G., Samuel, J.S., Singh, S., Kalra, S., Kumar, P., Ahuja, A.A., Sharma, M., Gautam, A., and Raghava, G.P.S. (2017). THPdb: Database of FDA-approved peptide and protein therapeutics. PLoS One *12*, e0181748.

254. Valentine, C.D., Lukacs, G.L., Verkman, A.S., and Haggie, P.M. (2012). Reduced PDZ interactions of rescued DeltaF508CFTR increases its cell surface mobility. J Biol Chem *287*, 43630-43638.

255. Van Goor, F., Hadida, S., Grootenhuis, P.D., Burton, B., Cao, D., Neuberger, T., Turnbull, A., Singh, A., Joubran, J., Hazlewood, A., *et al.* (2009). Rescue of CF airway epithelial cell function in vitro by a CFTR potentiator, VX-770. Proc Natl Acad Sci U S A *106*, 18825-18830.

256. Van Goor, F., Hadida, S., Grootenhuis, P.D., Burton, B., Stack, J.H., Straley, K.S., Decker, C.J., Miller, M., McCartney, J., Olson, E.R., *et al.* (2011). Correction of the F508del-CFTR protein processing defect in vitro by the investigational drug VX-809. Proc Natl Acad Sci U S A *108*, 18843-18848.

257. Van Goor, F., Straley, K.S., Cao, D., Gonzalez, J., Hadida, S., Hazlewood, A., Joubran, J., Knapp, T., Makings, L.R., Miller, M., *et al.* (2006). Rescue of DeltaF508-CFTR trafficking and gating in human cystic fibrosis airway primary cultures by small molecules. Am J Physiol Lung Cell Mol Physiol *290*, L1117-L1130.

258. Van Goor, F., Yu, H., Burton, B., and Hoffman, B.J. (2014). Effect of ivacaftor on CFTR forms with missense mutations associated with defects in protein processing or function. J Cyst Fibros *13*, 29-36.

259. Varga, K., Jurkuvenaite, A., Wakefield, J., Hong, J.S., Guimbellot, J.S., Venglarik, C.J., Niraj, A., Mazur, M., Sorscher, E.J., Collawn, J.F., *et al.* (2004). Efficient intracellular processing of the endogenous cystic fibrosis transmembrane conductance regulator in epithelial cell lines. J Biol Chem *279*, 22578-22584.

260. Varshavsky, A. (2012). The ubiquitin system, an immense realm. Annu Rev Biochem *81*, 167-176.

261. Veit, G., Avramescu, R.G., Chiang, A.N., Houck, S.A., Cai, Z., Peters, K.W., Hong, J.S., Pollard, H.B., Guggino, W.B., Balch, W.E., *et al.* (2016). From CFTR biology toward combinatorial pharmacotherapy: expanded classification of cystic fibrosis mutations. Mol Biol Cell *27*, 424-433.

262. Veit, G., Avramescu, R.G., Perdomo, D., Phuan, P.W., Bagdany, M., Apaja, P.M., Borot, F., Szollosi, D., Wu, Y.S., Finkbeiner, W.E., *et al.* (2014). Some gating potentiators, including VX-770, diminish DeltaF508-CFTR functional expression. Sci Transl Med *6*, 246ra297.

263. Venter, J.C., Adams, M.D., Myers, E.W., Li, P.W., Mural, R.J., Sutton, G.G., Smith, H.O., Yandell, M., Evans, C.A., Holt, R.A., *et al.* (2001). The sequence of the human genome. Science *291*, 1304-1351.

264. Verkman, A.S., Song, Y., and Thiagarajah, J.R. (2003). Role of airway surface liquid and submucosal glands in cystic fibrosis lung disease. Am J Physiol Cell Physiol *284*, C2-C15.

265. Wahlman, J., DeMartino, G.N., Skach, W.R., Bulleid, N.J., Brodsky, J.L., and Johnson, A.E. (2007). Real-time fluorescence detection of ERAD substrate retrotranslocation in a mammalian in vitro system. Cell *129*, 943-955.

266. Wainwright, C.E., Elborn, J.S., Ramsey, B.W., Marigowda, G., Huang, X., Cipolli, M., Colombo, C., Davies, J.C., De Boeck, K., Flume, P.A., *et al.* (2015). Lumacaftor-Ivacaftor in Patients with Cystic Fibrosis Homozygous for Phe508del CFTR. N Engl J Med *373*, 220-231.

267. Wang, B., Heath-Engel, H., Zhang, D., Nguyen, N., Thomas, D.Y., Hanrahan, J.W., and Shore, G.C. (2008). BAP31 interacts with Sec61 translocons and promotes retrotranslocation of CFTRDeltaF508 via the derlin-1 complex. Cell *133*, 1080-1092.

268. Wang, T., Yang, J., Xu, J., Li, J., Cao, Z., Zhou, L., You, L., Shu, H., Lu, Z., Li, H., *et al.* (2014). CHIP is a novel tumor suppressor in pancreatic cancer through targeting EGFR. Oncotarget *5*, 1969-1986.

269. Wang, W., Okeyo, G.O., Tao, B., Hong, J.S., and Kirk, K.L. (2011). Thermally unstable gating of the most common cystic fibrosis mutant channel (DeltaF508): "rescue" by suppressor mutations in nucleotide binding domain 1 and by constitutive mutations in the cytosolic loops. J Biol Chem *286*, 41937-41948.

270. Wang, X., Matteson, J., An, Y., Moyer, B., Yoo, J.S., Bannykh, S., Wilson, I.A., Riordan, J.R., and Balch, W.E. (2004). COPII-dependent export of cystic fibrosis transmembrane conductance regulator from the ER uses a di-acidic exit code. J Cell Biol *167*, 65-74.

271. Wang, X., Venable, J., LaPointe, P., Hutt, D.M., Koulov, A.V., Coppinger, J., Gurkan, C., Kellner, W., Matteson, J., Plutner, H., *et al.* (2006). Hsp90 cochaperone Aha1 downregulation rescues misfolding of CFTR in cystic fibrosis. Cell *127*, 803-815.

272. Ward, C.L., and Kopito, R.R. (1994). Intracellular turnover of cystic fibrosis transmembrane conductance regulator. Inefficient processing and rapid degradation of wild-type and mutant proteins. J Biol Chem *269*, 25710-25718.

273. Ward, C.L., Omura, S., and Kopito, R.R. (1995). Degradation of CFTR by the ubiquitin-proteasome pathway. Cell *83*, 121-127.

274. Weixel, K., and Bradbury, N.A. (2002). Analysis of CFTR endocytosis by cell surface biotinylation. Methods Mol Med *70*, 323-340.

275. Weixel, K.M., and Bradbury, N.A. (2000). The carboxyl terminus of the cystic fibrosis transmembrane conductance regulator binds to AP-2 clathrin adaptors. J Biol Chem *275*, 3655-3660.

276. Welch, W.J. (2004). Role of quality control pathways in human diseases involving protein misfolding. Semin Cell Dev Biol *15*, 31-38.

277. Wellhauser, L., Kim Chiaw, P., Pasyk, S., Li, C., Ramjeesingh, M., and Bear, C.E. (2009). A small-molecule modulator interacts directly with deltaPhe508-CFTR to modify its ATPase activity and conformational stability. Mol Pharmacol *75*, 1430-1438.

278. Welsh, M.J., and Smith, A.E. (1993). Molecular mechanisms of CFTR chloride channel dysfunction in cystic fibrosis. Cell *73*, 1251-1254.

279. Werner, H.M., Estabrooks, S.K., Preston, G.M., Brodsky, J.L., and Horne, W.S. (2019). Exploring the Functional Consequences of Protein Backbone Alteration in Ubiquitin through Native Chemical Ligation. Chembiochem *20*, 2346-2350.

280. Windheim, M., Peggie, M., and Cohen, P. (2008). Two different classes of E2 ubiquitin-conjugating enzymes are required for the mono-ubiquitination of proteins and elongation by polyubiquitin chains with a specific topology. Biochem J *409*, 723-729.

281. Wolde, M., Fellows, A., Cheng, J., Kivenson, A., Coutermarsh, B., Talebian, L., Karlson, K., Piserchio, A., Mierke, D.F., Stanton, B.A., *et al.* (2007). Targeting CAL as a negative regulator of DeltaF508-CFTR cell-surface expression: an RNA interference and structure-based mutagenetic approach. J Biol Chem *282*, 8099-8109.

282. Xiong, X., Bragin, A., Widdicombe, J.H., Cohn, J., and Skach, W.R. (1997). Structural cues involved in endoplasmic reticulum degradation of G85E and G91R mutant cystic fibrosis transmembrane conductance regulator. J Clin Invest *100*, 1079-1088.

283. Xiong, X., Chong, E., and Skach, W.R. (1999). Evidence that endoplasmic reticulum (ER)-associated degradation of cystic fibrosis transmembrane conductance regulator is linked to retrograde translocation from the ER membrane. J Biol Chem *274*, 2616-2624.

284. Xu, Z., Devlin, K.I., Ford, M.G., Nix, J.C., Qin, J., and Misra, S. (2006). Structure and interactions of the helical and U-box domains of CHIP, the C terminus of HSP70 interacting protein. Biochemistry *45*, 4749-4759.

285. Xu, Z., Kohli, E., Devlin, K.I., Bold, M., Nix, J.C., and Misra, S. (2008). Interactions between the quality control ubiquitin ligase CHIP and ubiquitin conjugating enzymes. BMC Struct Biol *8*, 26.

286. Yamamoto, Y.H., Kimura, T., Momohara, S., Takeuchi, M., Tani, T., Kimata, Y., Kadokura, H., and Kohno, K. (2010). A novel ER J-protein DNAJB12 accelerates ER-associated degradation of membrane proteins including CFTR. Cell Struct Funct *35*, 107-116.

287. Yang, H., Shelat, A.A., Guy, R.K., Gopinath, V.S., Ma, T., Du, K., Lukacs, G.L., Taddei, A., Folli, C., Pedemonte, N., *et al.* (2003). Nanomolar affinity small molecule correctors of defective Delta F508-CFTR chloride channel gating. J Biol Chem *278*, 35079-35085.

288. Yang, Y., Janich, S., Cohn, J.A., and Wilson, J.M. (1993). The common variant of cystic fibrosis transmembrane conductance regulator is recognized by hsp70 and degraded in a pre-Golgi nonlysosomal compartment. Proc Natl Acad Sci U S A *90*, 9480-9484.

289. Yang, Y., Kitagaki, J., Dai, R.M., Tsai, Y.C., Lorick, K.L., Ludwig, R.L., Pierre, S.A., Jensen, J.P., Davydov, I.V., Oberoi, P., *et al.* (2007). Inhibitors of ubiquitin-activating enzyme (E1), a new class of potential cancer therapeutics. Cancer Res *67*, 9472-9481.

290. Ye, Z., Needham, P.G., Estabrooks, S.K., Whitaker, S.K., Garcia, B.L., Misra, S., Brodsky, J.L., and Camacho, C.J. (2017). Symmetry breaking during homodimeric assembly activates an E3 ubiquitin ligase. Sci Rep *7*, 1789.

291. Yoo, J.S., Moyer, B.D., Bannykh, S., Yoo, H.M., Riordan, J.R., and Balch, W.E. (2002). Non-conventional trafficking of the cystic fibrosis transmembrane conductance regulator through the early secretory pathway. J Biol Chem *277*, 11401-11409.

292. Youker, R.T., Walsh, P., Beilharz, T., Lithgow, T., and Brodsky, J.L. (2004). Distinct roles for the Hsp40 and Hsp90 molecular chaperones during cystic fibrosis transmembrane conductance regulator degradation in yeast. Mol Biol Cell *15*, 4787-4797.

293. Younger, J.M., Chen, L., Ren, H.Y., Rosser, M.F., Turnbull, E.L., Fan, C.Y., Patterson, C., and Cyr, D.M. (2006). Sequential quality-control checkpoints triage misfolded cystic fibrosis transmembrane conductance regulator. Cell *126*, 571-582.

294. Younger, J.M., Ren, H.Y., Chen, L., Fan, C.Y., Fields, A., Patterson, C., and Cyr, D.M. (2004). A foldable CFTRΔF508 biogenic intermediate accumulates upon inhibition of the Hsc70-CHIP E3 ubiquitin ligase. J Cell Biol *167*, 1075-1085.

295. Yu, H., Burton, B., Huang, C.J., Worley, J., Cao, D., Johnson, J.P., Jr., Urrutia, A., Joubran, J., Seepersaud, S., Sussky, K., *et al.* (2012). Ivacaftor potentiation of multiple CFTR channels with gating mutations. J Cyst Fibros *11*, 237-245.

296. Zaman, K., Carraro, S., Doherty, J., Henderson, E.M., Lendermon, E., Liu, L., Verghese, G., Zigler, M., Ross, M., Park, E., *et al.* (2006). S-nitrosylating agents: a novel class of compounds that increase cystic fibrosis transmembrane conductance regulator expression and maturation in epithelial cells. Mol Pharmacol *70*, 1435-1442.

297. Zaman, K., Knight, J., Hussain, F., Cao, R., Estabrooks, S.K., Altawallbeh, G., Holloway, K., Jafri, A., Sawczak, V., Li, Y., *et al.* (2019). S-Nitrosylation of CHIP Enhances F508Del-CFTR Maturation. Am J Respir Cell Mol Biol *61*, 765-775.

298. Zaman, K., McPherson, M., Vaughan, J., Hunt, J., Mendes, F., Gaston, B., and Palmer, L.A. (2001). S-nitrosoglutathione increases cystic fibrosis transmembrane regulator maturation. Biochem Biophys Res Commun *284*, 65-70.

299. Zaman, K., Sawczak, V., Zaidi, A., Butler, M., Bennett, D., Getsy, P., Zeinomar, M., Greenberg, Z., Forbes, M., Rehman, S., *et al.* (2016). Augmentation of CFTR maturation by S-nitrosoglutathione reductase. Am J Physiol Lung Cell Mol Physiol *310*, L263-L270.

300. Zeitlin, P.L., Diener-West, M., Rubenstein, R.C., Boyle, M.P., Lee, C.K., and Brass-Ernst, L. (2002). Evidence of CFTR function in cystic fibrosis after systemic administration of 4-phenylbutyrate. Mol Ther *6*, 119-126.

301. Zhang, F., Kartner, N., and Lukacs, G.L. (1998). Limited proteolysis as a probe for arrested conformational maturation of delta F508 CFTR. Nat Struct Biol *5*, 180-183.

302. Zhang, H., Amick, J., Chakravarti, R., Santarriaga, S., Schlanger, S., McGlone, C., Dare, M., Nix, J.C., Scaglione, K.M., Stuehr, D.J., *et al.* (2015). A bipartite interaction between Hsp70 and CHIP regulates ubiquitination of chaperoned client proteins. Structure *23*, 472-482.

303. Zhang, H., Peters, K.W., Sun, F., Marino, C.R., Lang, J., Burgoyne, R.D., and Frizzell, R.A. (2002). Cysteine string protein interacts with and modulates the maturation of the cystic fibrosis transmembrane conductance regulator. J Biol Chem *277*, 28948-28958.

304. Zhang, H., Schmidt, B.Z., Sun, F., Condliffe, S.B., Butterworth, M.B., Youker, R.T., Brodsky, J.L., Aridor, M., and Frizzell, R.A. (2006). Cysteine string protein monitors late steps in cystic fibrosis transmembrane conductance regulator biogenesis. J Biol Chem *281*, 11312-11321.

305. Zhang, L., Sato, Y., Hessa, T., von Heijne, G., Lee, J.K., Kodama, I., Sakaguchi, M., and Uozumi, N. (2007). Contribution of hydrophobic and electrostatic interactions to the membrane integration of the Shaker K+ channel voltage sensor domain. Proc Natl Acad Sci U S A *104*, 8263-8268.

306. Zhang, M., Windheim, M., Roe, S.M., Peggie, M., Cohen, P., Prodromou, C., and Pearl, L.H. (2005). Chaperoned ubiquitylation--crystal structures of the CHIP U box E3 ubiquitin ligase and a CHIP-Ubc13-Uev1a complex. Mol Cell *20*, 525-538.

307. Zhang, Z., and Chen, J. (2016). Atomic Structure of the Cystic Fibrosis Transmembrane Conductance Regulator. Cell *167*, 1586-1597.

308. Zhang, Z., Liu, F., and Chen, J. (2018). Molecular structure of the ATP-bound, phosphorylated human CFTR. Proc Natl Acad Sci U S A *115*, 12757-12762.

309. Zhang, Z.R., Bonifacino, J.S., and Hegde, R.S. (2013). Deubiquitinases sharpen substrate discrimination during membrane protein degradation from the ER. Cell *154*, 609-622.

310. Zhao, Y., Cushing, P.R., Smithson, D.C., Pellegrini, M., Pletnev, A.A., Al-Ayyoubi, S., Grassetti, A.V., Gerber, S.A., Guy, R.K., and Madden, D.R. (2018). Cysteine modifiers suggest an allosteric inhibitory site on the CAL PDZ domain. Biosci Rep *38*, BSR20180231.

311. Zhou, Z., Gong, Q., Epstein, M.L., and January, C.T. (1998). HERG channel dysfunction in human long QT syndrome. Intracellular transport and functional defects. J Biol Chem *273*, 21061-21066.